# Rip Density and Dynamics along the New Zealand Coastline

A thesis presented in partial fulfilment of the requirements
for the degree of Master in Science in Geography

Massey University
Palmerston North
New Zealand

**Sarah Rose Flavall**
**2000**

# ABSTRACT

Rip currents are the most obvious component of the nearshore cell circulation system. The aim of this research was to investigate the applicability to the New Zealand coastal setting of a rip density scaling hypothesis, based on regional wave climate as proposed by Short and Brander (1999). Leading on from this investigation was a second aim to explore the relationship between rip velocities, rip density and surf zone morphology. Rip morphometrics were assessed for the entire New Zealand coastline through the use of aerial photographs. It was intended that four case study sites be investigated in more detail: The Gap, Castlepoint; Taranaki; Piha; and Tairua, but due to prevailing low wave energy, only two sites were examined.

Seventy-one beaches were examined around the New Zealand coast. Aerial photographs were examined and the following features were measured: rip spacing ($Y_s$); rip length ($L_r$); rip width ($W_r$); surf zone width ($X_s$); length of beach sampled ($L_b$); total beach length ($L_{bt}$); and beach type (Wright and Short, 1984; Short and Aagaard, 1993).

It was found that the scaling relationship for rip density suggested by Short and Brander (1999) of 2.5 between West Coast Swell (WCS) and East Coast Swell beaches is incorrect for New Zealand. The use of significant wave height as a rip spacing predictor produced no relationship, while the utilisation of mean sediment size as a rip spacing predictor produced the best relationship, with an $R^2$ value of 0.61 (p-value $<0.01$). Furthermore, although sediment size produced the best outcome, sediment fall velocity, which is used in a variety of morphodynamic models, had no statistically significant relationship. This relationship warrants further investigation. Finally, Muriwai beach, which is indicated by Short and Brander (1999) to be a representative New Zealand WCS example, is in fact, a highly atypical WCS beach. Therefore, the use of this beach as the sole New Zealand example is problematic in Short and Brander's (1999) investigation.

The exploration into rip current velocities at the Gap, Castlepoint provided some useful insights into rip velocities for beaches in a transitional state. Periodic velocities

of between $3ms^{-1}$ and $4ms^{-1}$ were recorded on four occasions at this site. However, Short (1985) states that rip velocities in mega-rips can approach $3ms^{-1}$. The outcome from this research suggests that there is a strong need to gain further quantitative measurements of rip currents both in transitional and cellular (i.e. mega-rips) states.

The rip currents that were investigated at the Taranaki beaches of Fitzroy and Oakura were examples of unsteady, episodic rip currents. Rip current trajectories demonstrated marked differences between rips in different surf zone types. Fitzroy, in a transverse bar and rip state, produced rip currents that exited through the surf zone. Oakura, a double bar, inner bar rhythmic bar and beach state, produced rip currents that were inhibited from exiting the surf zone by the outer bar. A circulatory flow was observed, which may have been produced through a combination of onshore directed wave energy and return flow from the rip current.

## ACKNOWLEDGEMENTS

This thesis could not have been carried out without the help of many people. There are four people in particular that I would like to thank. As my supervisor, Associate Professor Patrick Hesp gave me the opportunity to pursue my studies in coastal geomorphology. I thank him for his time, patience and friendship throughout this year. Secondly, thanks to Richard Poole for all his assistance with the fieldwork at Castlepoint, Taranaki and Tairua, and for the work carried out on the Surfer program. Kane Chapman was exceptional as the human rip float during the Taranaki and Tairua experiments (even if he did go blue from the cold), risking life and limb in the name of science. Thanks is also given to Kane for his help in the final stages of this thesis with scanning and manipulation of diagrams. Finally, thanks to Brian Harrison, who accompanied me on numerous excursions to Wellington and to fieldwork sites, who put up with a year of 'rip spotting' whenever we went past a beach, and who let me monopolise the computer.

There are a large number of people who need to be thanked. Thankyou to Nigel Donovan, Georgina McPherson, Sarah Nelson, Gilbert Flavall and the Piha Surf Life Saving Club for accommodation on the numerous travels around New Zealand. Also thanks to my parents, Jenny and Farquhar Flavall, for their support and supply stop-off point during fieldwork. The staff at the NIWA library in Wellington were particularly helpful during the early stages of the literature review. Thank you to Frank O'Leary of the Land Information (archives) for the use of their aerial photograph collection. Thanks also to Dr Mike Shepherd for advice and Tim O'Dea for his work with surveying and the surfer program at Castlepoint, and help throughout this thesis. Thanks to Karin Bryan at NIWA for her assistance and advice with regard to Cam-Era, Tairua and the provision of diagrams.

The fieldwork would have been practically impossible without the help of the following people. At Castlepoint, thanks is given to the class of 145.329, Coastal Dynamics and Management for all their assistance. Sarah Nelson, Helen Marr, Rosemary Marr, Andrew Flynn, Kane Chapman, Richard Poole and Brian Harrison braved the cold winter winds to measure rip velocities at Taranaki. Emma Bermingham, Elizabeth Flavall, Chris Hermanns, Kane Chapman and Richard Poole helped to search for rip currents (although there were none to be found) at Tairua.

Finally thanks to Phillipa Ringrose, Wayne Harrison, Emma Bermingham and Dr David Thomas for taking the time to read and correct various chapters of this dissertation.

# TABLE OF CONTENTS

## CHAPTER FOUR: BEACH TYPES, SEDIMENT CHARACTERISTICS, WAVE CLIMATE, RIP DENSITY AND MORPHOMETRY



## CHAPTER FIVE: THE GAP, CASTLEPOINT: THE EFFECT OF TOPOGRAPHIC CONTROL ON SURF ZONE AND RIP CHARACTERISTICS

## CHAPTER SIX: RIP CURRENTS AT THE MODERATE TO HIGH ENERGY TARANAKI COASTLINE



## CHAPTER SEVEN: CONCLUSION

# LIST OF FIGURES

## CHAPTER ONE



## CHAPTER TWO



## CHAPTER THREE



## CHAPTER FOUR

## CHAPTER FIVE

## CHAPTER SIX



## LIST OF TABLES

# CHAPTER ONE: INTRODUCTION

*"It [a rip current] is a sort of river, a stream showing on the surface deep and powerful, easily perceptible, running with the velocity of a mill race. So swift and powerful is it that a motorboat could not stem its sweeping current. It will carry brick, large rocks and even chunks of lead far out to sea. The most powerful swimmer will find himself helpless as a babe in its rushing grasp."*

M.P.Hite.

*Science* (1925), in Komar (1998).

Rip currents are the most obvious component of the nearshore cell circulation system Shepard *et al*., 1941). They are characterised by weak to strong, and narrow to wide rip currents flowing seawards through topographic depressions in a bar (Aagaard and Masselink, 1999). Although numerous qualitative investigations have been carried out, little quantitative data is available, due, in large part to the logistical problems inherent with the undertaking of field research on rip currents.

The following investigation is based primarily on a paper produced by Short and Brander (1999), which suggests that rip density (the number of rip currents per kilometre of coastline) and other additional morphometric parameters, gathered from beaches from around the world, can be categorised into groups based on their respective regional wave climate, as proposed by Davies (1980). The New Zealand coastline can be placed into two of the five wave climates as identified by Davies, namely West Coast Swell (WCS) and East Coast Swell (ECS). However, only one example from New Zealand, Muriwai Beach, was used in Short and Brander's investigation.

## 1.1 AIMS

The following aims for this study were defined:

1. To investigate the applicability of Short and Brander's (1999) rip density hypothesis in the New Zealand coastal setting.

2. To examine a range of parameters that could be used to predict rip spacing for a variety of beaches in New Zealand
3. To investigate the relationship between rip velocities, rip density and surf zone morphology.

## 1.2 OBJECTIVES

The aims defined above were translated into the following objectives:

1. Analyse aerial photographs from around the entire New Zealand coastline to establish a database to analyse rip morphometric parameters.
2. Assess the validity of Short and Brander's scaling factors for the New Zealand coast.
3. Assess the applicability of the use of Muriwai beach as a 'classic' west coast swell example in Short and Brander's (1999) investigation.
4. Compare rip spacing with a range of other sediment, wave climate and surf zone parameters to establish the 'best' predictor for rip spacing.
5. Assess the use of beach state (Wright and Short, 1984; Short and Aagaard, 1993) as a means to predict rip spacing.
6. Obtain quantitative measurements of rip velocity, rip density, rip and surf zone morphology, and additional sediment and wave climate data from a variety of beaches around the North Island of New Zealand.

## 1.3 STUDY AREA

In contrast to the majority of investigations carried out at this level, which focus on a very specific investigation of a single site, this research will look at the entire New Zealand coastline, with four sites examined in closer detail.

On a global scale, New Zealand can be divided up into two wave climates; West Coast Swell (WCS) on the west coast of New Zealand and East Coast Swell (ECS) on the eastern coast (Davies, 1980). The New Zealand wave climate can be further divided up into Western, Southern, Eastern and Northern based systems (Pickrill and

Mitchell, 1979). Topography and sedimentology can also play an important role in many locations.

The west coast of New Zealand is characterised by a high-energy coastal system. Beaches tend to be intermediate state pocket beaches, such as Piha Beach, or long, wide, multi-barred dissipative beaches. The west coast is typified by an open sand system, with large inland dune fields, 100 metre high coastal cliffs of erodible Pleistocene sands in some places, river mouths and large tidal deltas. Ocean swells from the Tasman Sea and the Southern Ocean result in a highly energetic wave climate. The sediment of the west coast of the North Island is characterised by dense titanomagnetite sands.

In contrast, the east coast is characterised by a more benign wave climate, with occasional tropical cyclones. Beach states range from intermediate states to reflective, with small pocket beaches nestled in between headlands being the dominant beach form, although there are a few large embayments. This results in a more disconnected sand system, as compared with the west coast. The east coast sediment is characterised by quartzo-feldspathic sands (Shepherd and Hesp, in press).

## 1.4 Case Studies

This study attempted to look at four sites in more detail to delve further into some of the outcomes from the initial investigation into rip currents found in Chapter Four. Each investigation intended to incorporate further exploration of rip current velocity and its relationship with rip spacing, rip and surf zone morphology, and beach length.

### 1.4.1 The Gap, Castlepoint

The Gap at Castlepoint was investigated due to the major topographic controls exerted on this small embayment. The Gap is located on the east coast of the North Island (Figure 1.1), approximately 27 kilometres by road from the township of Masterton, in the Wairarapa. At the time of investigation, this system was characterised by a major rip current flowing from south to north, which removed the majority of water out of the embayment.

### 1.4.2 Piha Beach

Piha Beach is located on the west coast of Auckland (Figure 1.1). It is a high energy, mesotidal beach renowned for its prominent and highly dangerous rip currents. The mean wave height for Piha is 1.46 (O'Dea and Hesp, 2000) with a southwest swell dominating the system. The mean sediment size is 2.59 phi and is dominated by iron sands.

### 1.4.3 Taranaki

Two beaches were investigated along the Taranaki coastline: Fitzroy Beach and Oakura Beach (Figure 1.1). The Taranaki coastline is a high-energy wave environment, with exposure to waves approaching from the southwest though to the north and dominated by a long period swell from the west (McComb *et al.,* 1997).

Fitzroy is a moderate to high-energy mesotidal beach. The bathymetry of this beach is complex with predominant reef and channel structures of inter-bedded lahar deposits (McComb *et al.,* 1997). The substrate is intermittently overlain with sand, gravels and boulders (Arron and Mitchell, 1984), which were observed to control the morphology and location of the rip currents to some extent during the investigation. During the investigation wave height was approximately one metre, with a transverse bar and rip state present.

Oakura is located south of New Plymouth. This beach is again of moderate to high energy. During the experiment the wave height was 1.6 metres high, with a two bar system: rhythmic bar and beach inner bar; and longshore bar and trough outer bar.

Both beaches have an average wave height of 1.5 metres and wave period of 10 seconds (O'Dea and Hesp, 2000). The sediment composition for both beaches is high in iron sands, with a mean grain size for Fitzroy and Oakura of 2.27 and 0.99 phi respectively (Hesp and O'Dea, 1999).

### 1.4.4 Tairua Beach

Tairua Beach is located on the eastern side of the Coromandel Peninsula (Figure 1.1). It is a mesotidal, embayed beach which experiences moderate controls from topographic features, namely the prominent headlands of Paku Hill to the south and

Pumpkin Hill to the north. The wave climate is of medium energy, which results in a steep beach face and a coarse sand mean grain size (Flint, 1998) of 0.93 (Hesp and O'Dea, 1999). The average wave height ranges between 0.5 and 1.0 metres (O'Dea and Hesp, 1999; Bogle *et al.*, 1999).

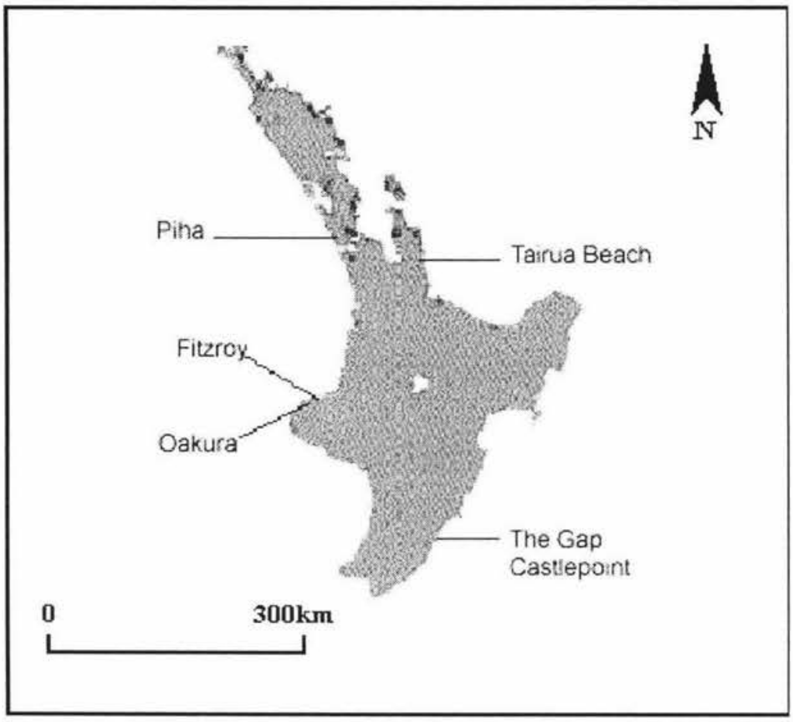


Figure 1.1 Location map of the case study sites.

## 1.5 PROBLEMS WITH THE FIELDWORK

The study of rip currents is renowned for the logistical difficulties that are encountered when fieldwork is attempted. Of the four beaches where it was attempted to gain data on rip currents, only two, Taranaki and The Gap, Castlepoint, provided any useful data. The following outlines the difficulties found at the other two sites.

### 1.5.1 Tairua Beach

Tairua was chosen as a site for three reasons: (a) it is an example of an east coast beach which is relatively renowned for its rip current activity; (b) it is monitored by NIWA through a Cam-Era station which can be observed via the internet; and (c) accommodation was easily available.

The NIWA web site was observed on an almost daily basis for approximately four months. Although rips were evident at times, strong rip systems were not observed to be the norm during this monitoring period. The ability to carry out field investigations was further hampered by time restrictions and the ability to gather at least four additional assistants for a minimum of three days to carry out the experiments.

One expedition to Tairua was carried out on the $27^{th}$ to the $30^{th}$ of September, 2000. Although topographical surveying, dye and rip float techniques were attempted, it was apparent that by the time we arrived at Tairua Beach the system had become dominated by a longshore current pattern and no accurate data was collected.

### 1.5.2 Piha Beach

Piha Beach is renowned in New Zealand for the dominant rip currents that occur in this particular beach system. It was assumed, although wrongly in this case, that rips would be evident at almost any time at this beach, due to its high energy and the degree to which the topography of this beach limits dissipative beach types.

Unfortunately, the day which was chosen to investigate the Piha rip system turned out to be a period when the rip currents were inactive, with particularly low wave energy conditions (1.5 metre wave height) for the entire upper west coast region.

One particular area of interest from this excursion however, was the nature of the surf zone morphology. A visual assessment of Piha Beach determined that there were three rip channels evident, with topographically controlled rip channels at either end of the beach and a third rip channel exiting the surf zone in an oblique manner in the middle of the beach. Nevertheless, investigation of the rips, particularly the middle rip, proved that the rip current was, in fact, inactive. A relict rip channel was evident from the lack of breaking waves in the area and mega ripples, however the rip current was dormant. This in itself may have interesting implications, particularly in the long term Cam-Era monitoring of rip current dynamics.

# CHAPTER TWO: LITERATURE REVIEW

## 2.1 RIP CURRENTS: AN INTRODUCTION

Rip currents are the most evident component of the nearshore cell circulation (Shepard *et al.*, 1941; Shepard and Inman, 1950, 1951; Dolan, 1971; Komar, 1971; Davis and Fox, 1972; Sonu, 1972; Davidson-Arnott and Greenwood, 1974; Goldsmith *et al.*, 1982).

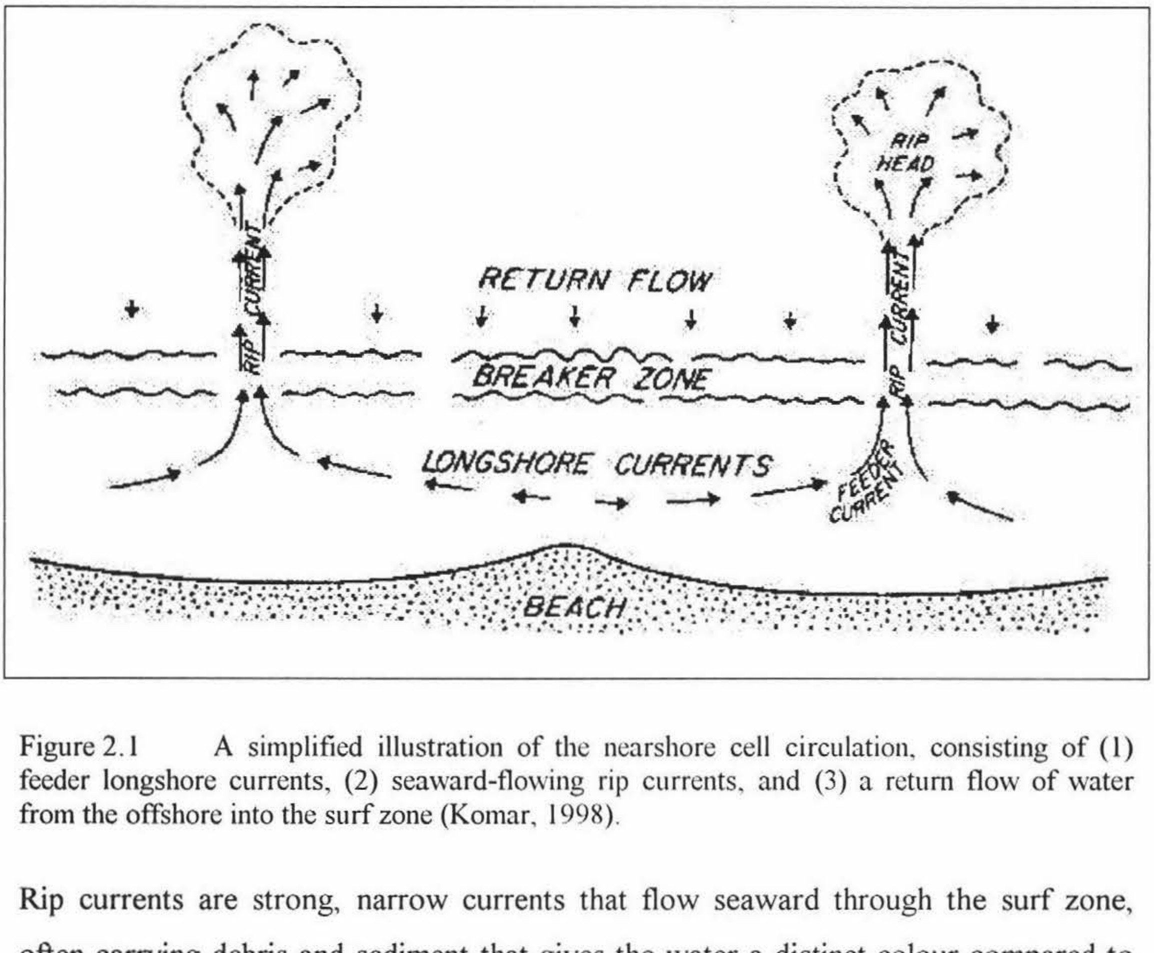


Figure 2.1 A simplified illustration of the nearshore cell circulation, consisting of (1) feeder longshore currents, (2) seaward-flowing rip currents, and (3) a return flow of water from the offshore into the surf zone (Komar, 1998).

Rip currents are strong, narrow currents that flow seaward through the surf zone, often carrying debris and sediment that gives the water a distinct colour compared to the adjacent clear water (Komar, 1998). Rips occur in areas of horizontal flow convergence in the surf zone. As depicted in Figure 2.1, the rip current consists of two converging feeder currents, the rip neck which occupies the rip channel across the bar, and the rip head (Aagaard and Masselink, 1999).

The rip current pulsates as a confined jet-like flow across the surf-zone (Short, 1985), with the largest velocities occurring in the rip neck (Aagaard and Masselink, 1999) as shown in Figure 2.2. Velocities in the rip channel frequently pulse at low frequencies, from 30 seconds to several minutes (McKenzie, 1958; Chappell and Wright, 1978) as a response to infragravity waves and/or wave groups (Aagaard and Masselink, 1999). Some distance seaward, flows expand and decelerate, usually producing a series of vortices that compose the rip head (Short, 1985).

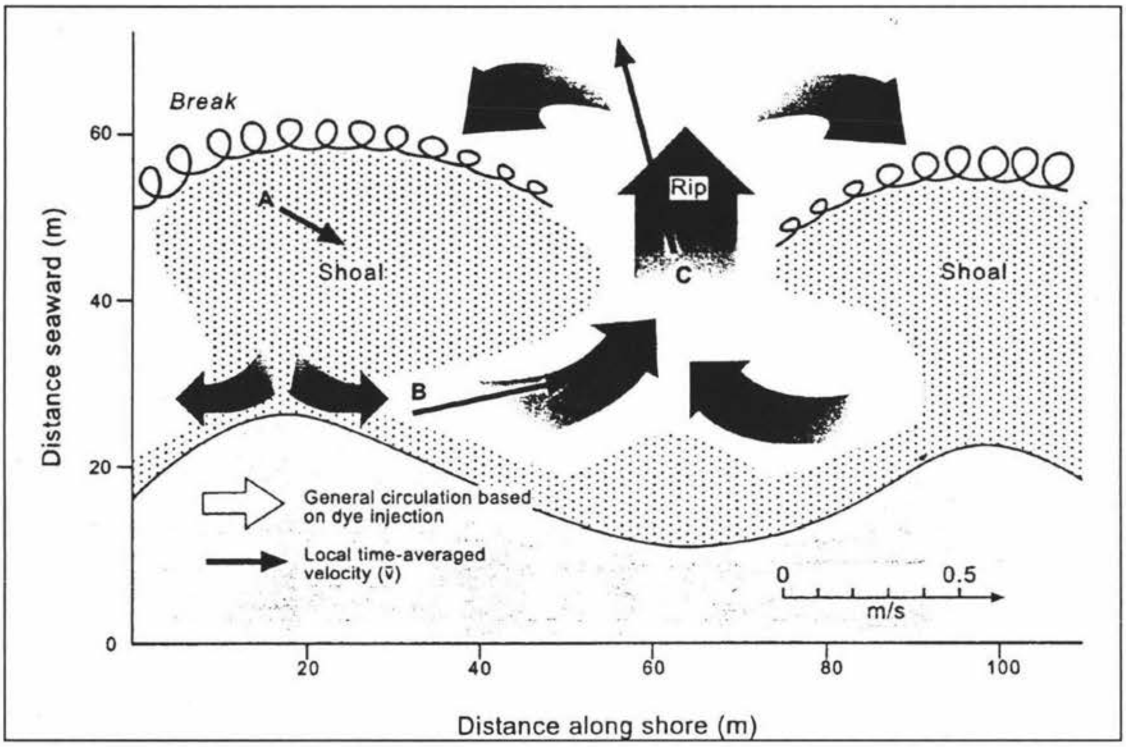


Figure 2.2 Rip circulation observed and recorded in a transverse bar and rip system (modified from Wright and Short (1984) by Short (1999)).

The idealised circulation cell form is a rip orientated perpendicular to the shoreline, with longshore currents feeding the rip neck from both sides (Figure 2.3a). However, rip currents often occur at oblique angles, cutting through the surf zone, with longshore feeder currents on either side varying both in longshore extent and in intensity (Komar, 1998) (Figure 2.3b).

Rips do not occur on all beaches or beach types. They are absent from reflective beaches that are dominated by shore-normal swash oscillations. Rips are also rare on fully dissipative beaches, where surf zones are controlled by low-frequency surf beat in which circulation is segregated vertically rather than horizontally (Wright *et al.*, 1982a; Short, 1985). Rips are characteristic of the intermediate beach types, those dominated by cellular surf zone circulation and rhythmic topography (Wright and Short, 1983).

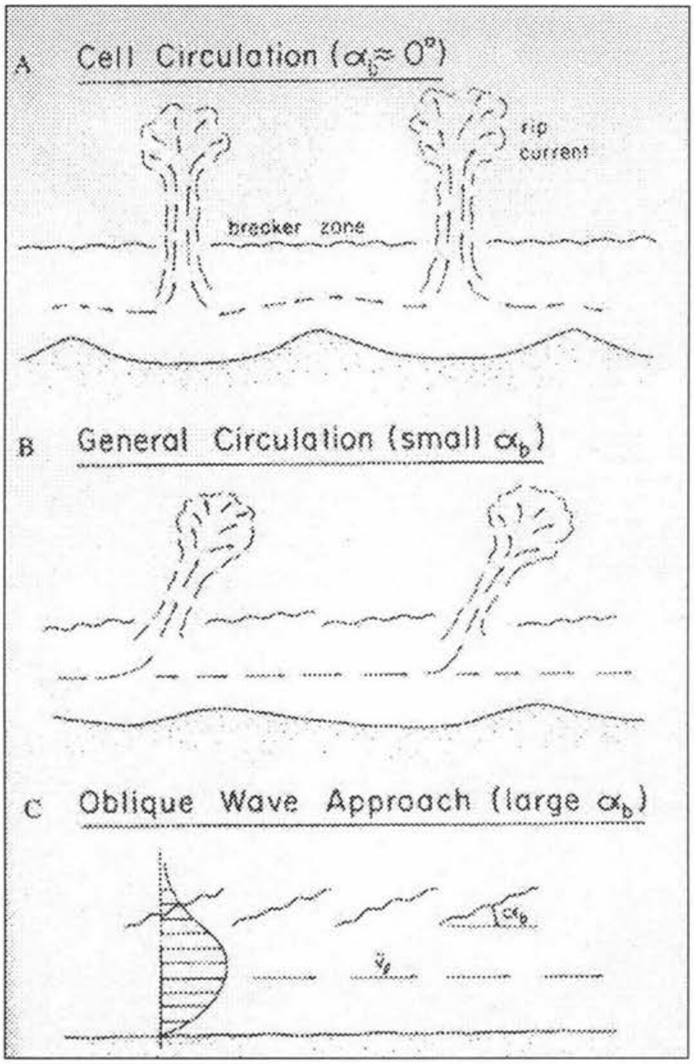


Figure 2.3 Nearshore current patterns, which depend in large part on the angle of wave breaking ($\alpha_b$). Cell circulation tends to develop when wave crests are parallel to the shore, whereas a large angle of wave breaking generates longshore currents (Komar, 1998).

The first scientific investigation into rip currents began with Shepherd *et al.* (1941), who discussed the nature of rip currents and the important role that offshore topography has in controlling the position of rip currents. The first comprehensive series of field measurements of the complete cell circulation were carried out by Shepard and Inman (1950a, 1950b). They recognised that offshore topography and its effects on wave refraction may govern the position of rip currents. However, circulation cells with rip currents can also exist on long straight beaches with regular bottom topography. McKenzie (1958) described commonly occurring rip currents along the southeast Australian coast and demonstrated that a given group of incident waves arriving at the beach form a characteristic pattern of longshore currents and rip currents. Growth in rip current interest has continued since these initial investigations.

## 2.2 RIP CURRENT GENERATION MECHANISMS

A major area of research into rip currents is concentrated on the mechanisms by which they are generated. Initial explanations as to the occurrence of rip currents were based on the existence of an onshore mass transport of water associated with waves. However, this explanation of cell circulation was never particularly successful in field measurements (eg Putman, Munk and Traylor, 1949), although it is theoretically possible. A more successful explanation for cell circulation generation is based upon wave induced variations in wave heights along shore, known as *Radiation Stress*.

The concept of *Radiation Stress*, as a means to describe some of the non-linear properties of surface gravity waves, was introduced by Longuet-Higgins and Stewart (1964). Radiation stress is defined as the 'excess flow of momentum due to the presence of waves' (Longuet-Higgins and Stewart, 1964 pp. 531). The circulation patterns are driven by longshore variations in the radiation stress in the surf zone as shown in Figure 2.4. Radiation stress generates set-ups and set-downs, which result in an elevation of the mean water level in the surf and swash zones, and its depression within and just outside the breaker zone (Trenhaile, 1997).

Researchers have suggested numerous rip current generation mechanisms. These can be divided up into three categories (Ranasinghe *et al.*, 1999): (a) wave-boundary interaction mechanisms; (b) wave-wave interaction mechanisms; and (c) instability mechanisms.

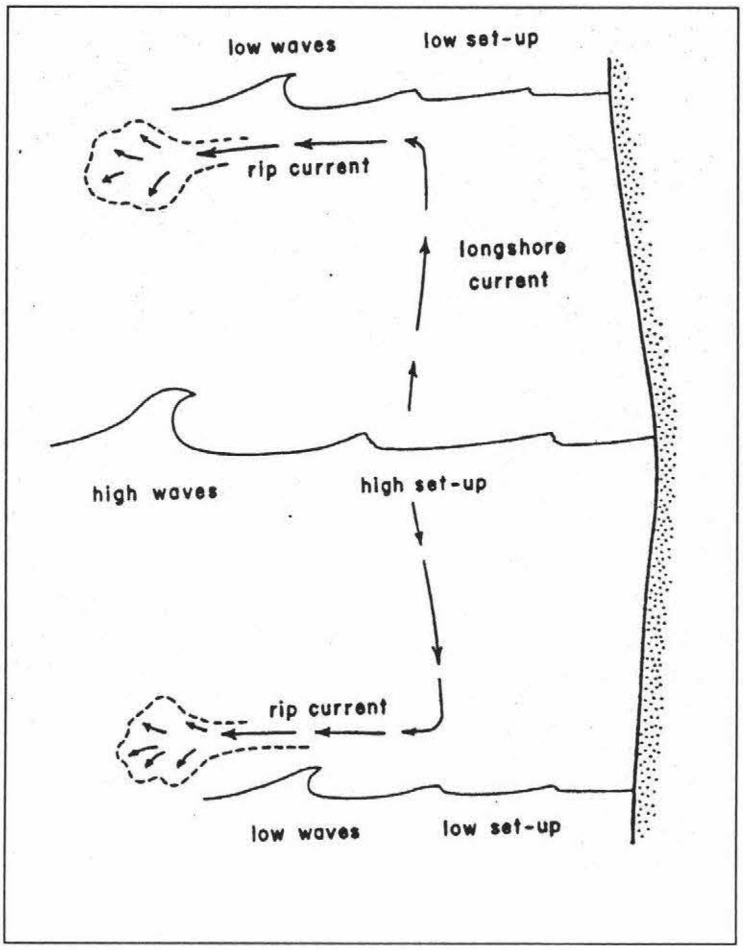


Figure 2.4 Illustration of cell circulation generation by a longshore variation in wave heights, producing a parallel variation in the elevation of the set-up within the surf zone Komar (1998).

### 2.2.1 Wave Boundary Interaction Mechanisms

Wave boundary interaction mechanisms include wave refraction and diffraction (Gourley, 1974, 1976; Sasaki, 1975; Mei and Lui, 1977). Wave refraction over non-uniform bathymetry concentrates the wave rays in one area of the beach, producing alongshore gradients with lower waves and set-up in the lee of a headland or breakwater, which in turn generate longshore currents flowing inward toward the sheltered region. Therefore, the position of rip currents and the overall cell circulation may be controlled by offshore topography (Shepard and Inman, 1950a, 1950b), headlands, breakers and jetties.

### 2.2.2 Wave-Wave Interaction Mechanisms

Two wave-wave interaction mechanisms have been proposed. The first example involves longshore standing waves as a mechanism that can explain the common regularity in alongshore rip current channel spacing (Bowen, 1969; Bowen and Inman, 1969; Holman and Bowen, 1982). Regular longshore variations in wave height and set-up can be produced by resonant interaction of incident waves with edge waves trapped by refraction between a shoaling beach and a caustic (Holman, 1983; Schaffer and Jonsson, 1992). For cell circulation to be generated the edge waves must be synchronous, that is, they must have the same period as the incident waves so they can be systematically in phase and out of phase along the length of shore.

Synchronous edge waves produce variations in breaker heights, with alternative high and low breakers. Rip currents develop where the breaking waves are lowest, at every other antinode, and therefore at intervals along the beach equal to the edge wavelength ($L_e$):

$$L_e = (g/2\pi)T_e^2\sin[(2n + 1)\ \beta]$$

where $T_e$ is the edge wave period, equal to the incoming waves, and n is an integer wave mode number (0,1,2,3...) that defines the number of shore-normal zero-crossings of the mean water level (Trenhaile, 1997). Thus, a regular pattern of rip currents and cell circulation is produced (Figure 2.5).

Gruszczynski *et al.* (1993) suggested that edge waves are the major agent in the formation of rip currents either directly (Bowen and Guza, 1978; Holman and Bowen, 1984) or indirectly, due to the formation of rhythmic topography, which induces nearshore circulation (Noda, 1974). Huntley and Short (1992) have also hypothesised that the tendency for larger rip current spacings to occur with larger wave heights, is the result of edge wave dimensions which are in some way being constrained by surf zone width.

However, the model proposed by Bowen and Inman (1969b); on which the reliance on edge wave control is based, requires the presence of synchronous edge waves, which are believed to be restricted to steep, reflective beaches (Guza and Inman, 1975; Bowen and Guza, 1978). There has also been a lack of field evidence to substantiate this model (Komar, 1998).

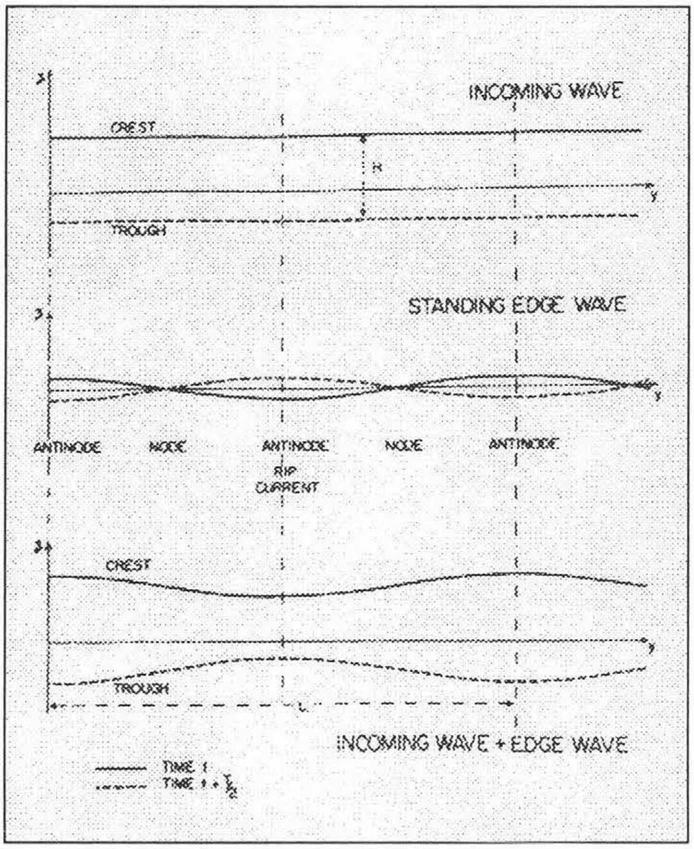


Figure 2.5 A longshore variation in observed wave height is produced through the addition of an incoming ocean wave and a standing edge wave at the breaker position. The net height is greatest where the edge wave and incoming wave are in phase and lowest where they are 180° out of phase (Komar, 1998).

A second wave-wave interaction mechanism was proposed by Dalrymple (1975). Rip currents may be created by intersecting wave trains of the same frequency, periodically reinforcing and cancelling each other out as they propagate towards the shore. Rip currents develop in the surf zone where lines of cancellation, or nodal lines, intersect the beach. Suitable wave trains could be formed by reflectance, different storm systems, wave diffraction caused by islands, or refraction over a submarine shoal (Dalrymple, 1975). Refraction of incident waves around pre-existing rip currents could also facilitate the growth of cell circulation systems (Trenhaile, 1997).

### 2.2.3 Instability Mechanisms

A final explanation is concerned with the effect of a small initial disturbance to an otherwise constant longshore wave set-up (Hino, 1974). Others have also suggested that rip currents can be produced by hydrodynamic instability in the surf zone (Iwata, 1976; Dalrymple and Lozano, 1978; Miller and Barcillon, 1978).

Although these mechanisms have been validated to some extent through laboratory experiments and/or sparse field data, it is apparent that the generation of cell circulation could occur from one or a combination of the above mechanisms (Komar, 1998). In particular, work by Ranasinghe *et al.* (1999) indicates, "rip current generation cannot be directly attributed to any one of the rip generation models described in the literature... rips are generated through a combination of wave-wave interactions, instability, and wave boundary interaction mechanisms" (Ranasinghe *et al.*, 1999, pp. 1000-1001).

## 2.3 MORPHODYNAMIC MODELS

Rip circulation and associated topographical features are prominent elements of surf zone circulation and beach type models (Hom-ma and Sonu, 1962; Sonu, 1974; Short, 1979; Wright and Short, 1983,1984; Goldsmith *et al.*, 1982; Sasaki, 1983; Bowman and Goldsmith, 1983; Sunamura, 1989; Aagaard, 1990; Lippmann and Holman, 1990; Short 1992; Short and Aagaard, 1993).

Figure 2.6 provides a useful synthesis of the single bar models suggested by Short (1979b), Wright and Short (1984), Sunamura (1989) and Lippmann and Holman (1990). A particularly constructive model is the widely accepted Wright and Short (1984) six-stage single bar model, where rip currents play a major role in intermediate beach type morphology. It identified both the morphological characteristics and processes associated with each beach state. Beach type is determined by the use of the dimensionless fall velocity parameter, Ω (Gourlay, 1968) where:

$$\Omega = H_b/w_s T$$

where $H_b$ is breaker wave height in metres, $w_s$ is sediment fall velocity ($ms^{-1}$) and T is wave period (s). Short and Wright (1984) proposed that beaches would be reflective when $\Omega < 1$, intermediate when $1 < \Omega < 6$, and dissipative when $\Omega > 6$ (Wright and Short, 1984).

Rip currents primarily occur on intermediate state beaches, and are most prominent in the transverse bar and rip, and rhythmic bar and beach types. Weak rip currents are present in the longshore bar-trough and ridge-runnel/low tide terrace types, while the dissipative and reflective beach states generally possess no rip currents, at least in the single bar surf zones.

Sunamura (1988) proposed a beach change model based on erosional (dissipative) and accretionary (reflective) extremes, with linkages achieved through erosional and accretionary sequences. The dimensionless parameter K* was introduced where:

$$K^* = H_b^2/gT^2D$$

where D is mean grain diameter (mm).

Lippman and Holman (1990) proposed an eight stage single bar model which utilises a sequential classification system based on four independent criteria. While it essentially verified the Short and Wright model, it identified two modes of intermediate bar types based on rhythmic and non-rhythmic longshore spacings of bars and rips.

### 2.3.1 Multi-bar Models

Morphodynamic models are not limited to single bar beach states. Short and Aagaard (1993) developed a multi-bar morphodynamic beach model (Figure 2.7). They suggest the approximate characteristics of a beach, its bar number and type(s) can be estimated by using the bar parameter B* where:

$$B^* = x_s/g \tan \beta \, T_i^2$$

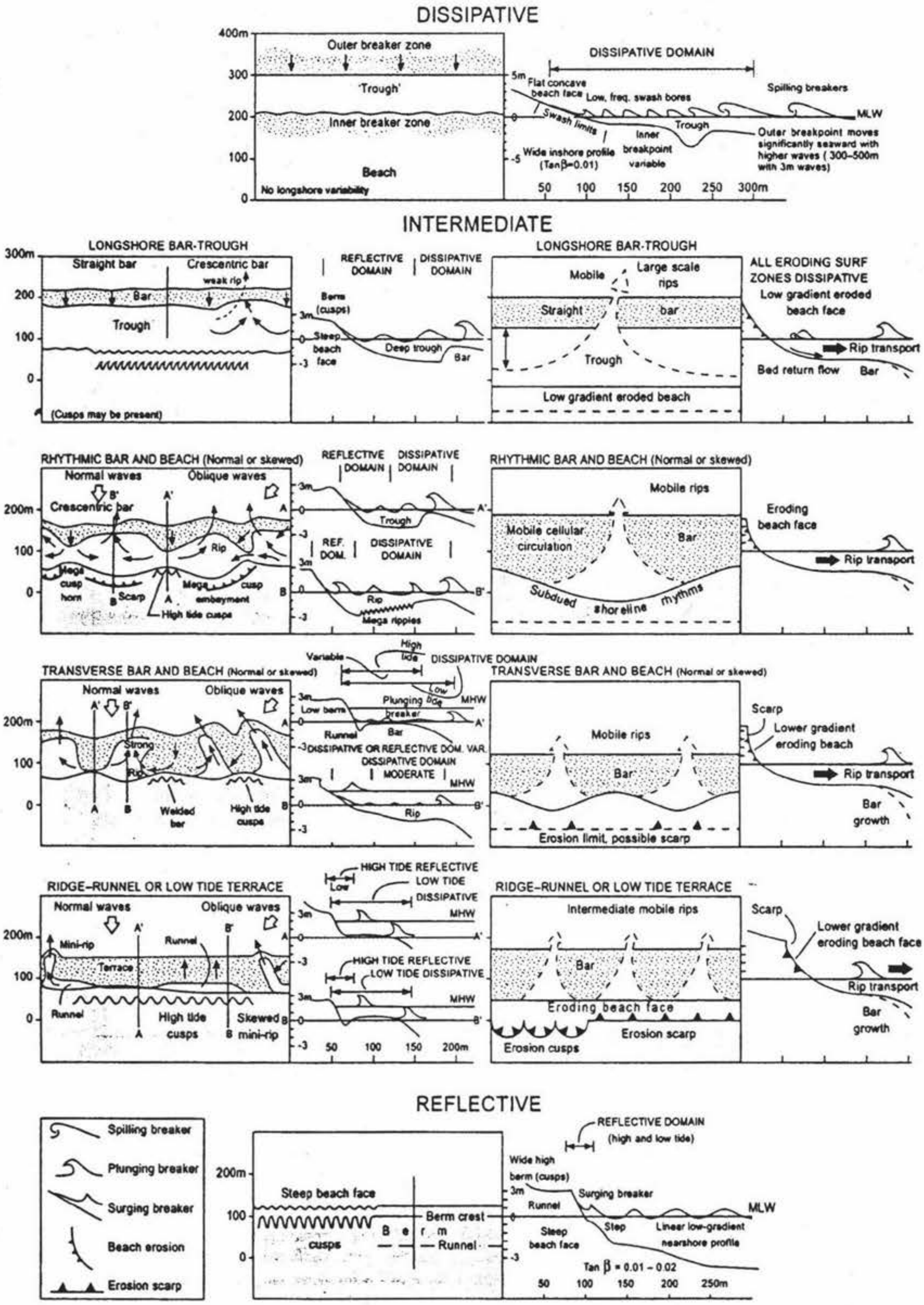

Figure 2.6 Three-dimensional sequence of wave-dominated beach changes for accretionary (left) and erosional (right) wave conditions, based on Short (1979b), Wright and Short (1984), Sunamura (1988) and Lippmann and Holman (1990) (from Short, 1999).

where $x_s$ is nearshore width, $\beta$ is gradient, and $T_i$ is the incident wave period. The bar parameter predicts increasing bar number with decreasing gradient (finer sediments) and wave period, and increasing profile width.

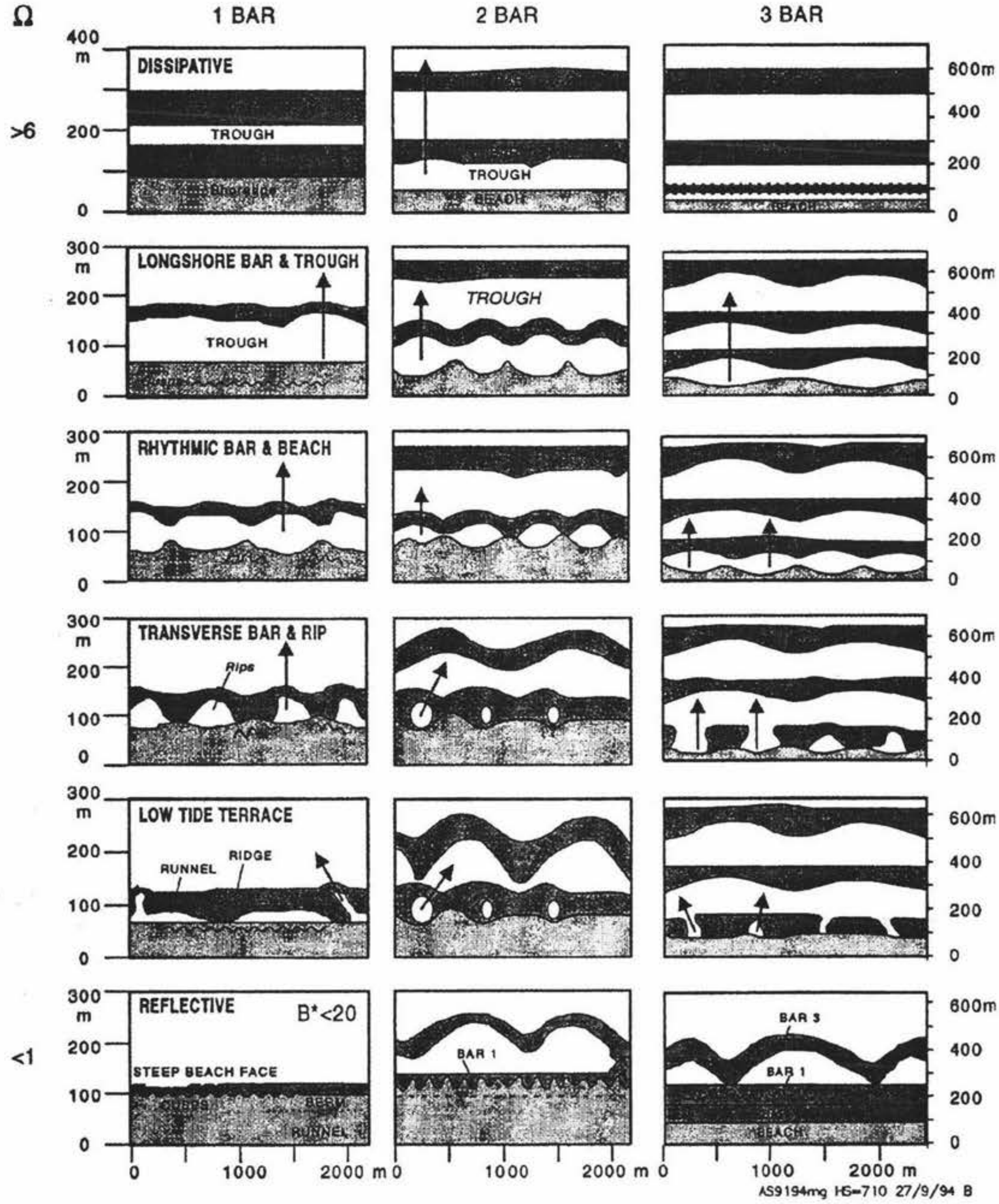


Figure 2.7 Short and Aagaard's (1993) generalised model of one, two and three bar beach systems.

Masselink and Short (1993) extended the micro-tidal beach model of Wright and Short (1984) to include all wave-dominated beaches in all tidal ranges in a conceptual beach model (Figure 2.8). Natural beaches may be grouped into several beach types on the basis of breaker height ($H_b$), wave period (T), high tide sediment fall velocity ($w_s$), and tide range *(TR)*. Two dimensionless parameters quantify these four parameters: the dimensionless fall velocity ($\Omega$) and the relative tide range (RTR = $TR/H_b$). Mean spring tide range is used to calculate the relative tide range. The dimensionless fall velocity value indicates whether reflective, intermediate or dissipative surf zone conditions will prevail, while the relative tide range indicates the relative importance of swash, surf zone and shoaling processes.

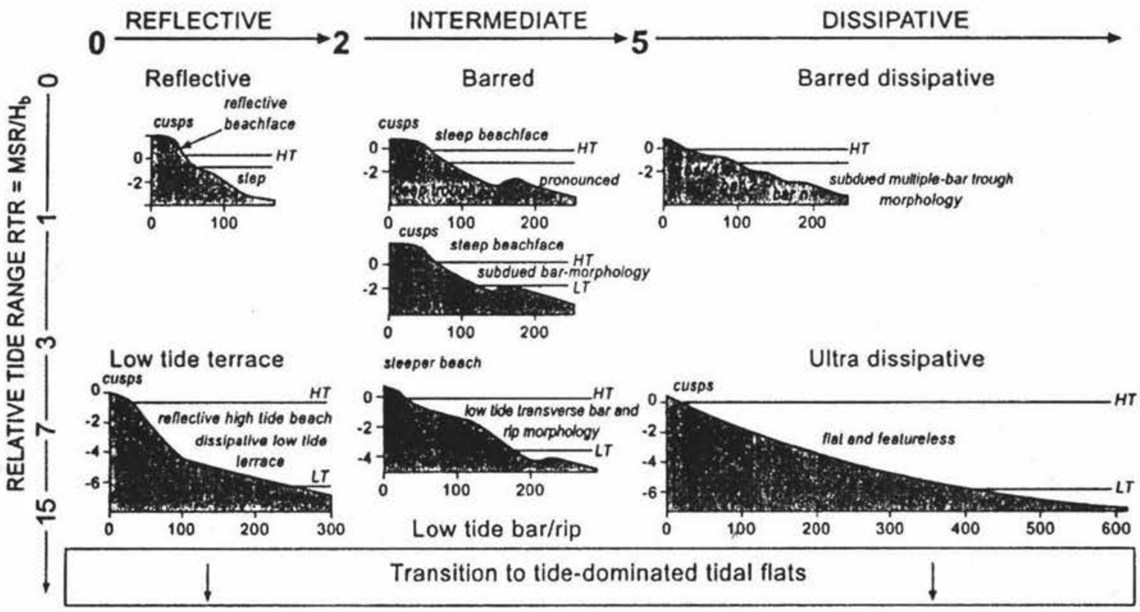


Figure 2.8 Masselink and Short's (1993) classification of beaches on the basis of the modal breaking wave height $H_b$ and period $T$, the high tide sediment fall velocity $w_s$ and the mean spring tide range MSR.

### 2.3.2 Rip Current Evolution Model

Brander (1999b) produced a morphodynamic model, which looked specifically at rip current evolution in a low-energy intermediate system (Figure 2.9). Under decreasing energy conditions, the rip system evolution is characterised by a narrowing and deepening of the rip channel, an increase in the morphologic relief area of the rip channel and a gradual constriction in the area available for rip flow. Therefore, an overall increase in rip channel flow velocity and rip flow occurs as channel cross-sectional area decreases, until the rip channel eventually infills.

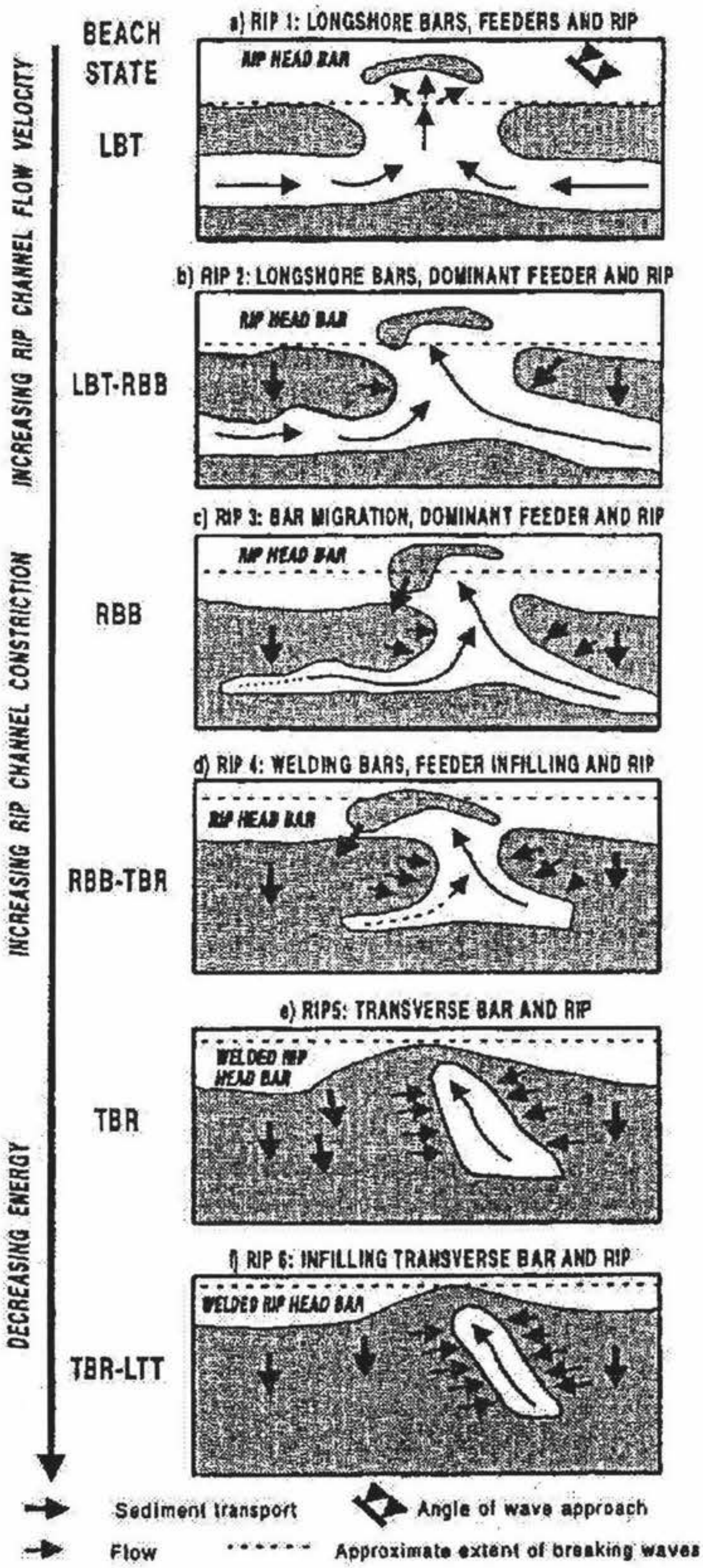


Figure 2.9 Brander's (1999b) rip current evolution model.

## 2.4 RIP TYPOLOGIES

Rip currents have been treated as a component of either erosional or accretionary sequences of morphodynamic beach states (Short, 1979; Wright *et al.*, 1979, 1982, 1985; Short and Hesp, 1982; Wright and Short, 1983, 1984; Gruszczynski *et al.*, 1993). Short (1985) suggested two basic types of rips that occur on beaches: 'erosion rips' that accompany rising seas and general beach erosion when waves are rising, and 'accretion rips' that accompany falling seas and beach accretion where waves are falling (Short, 1979, 1985). In the case of erosional sequences, dissipative beach conditions are highly favourable for the formation of 'megarips' (i.e. large-scale, strong, pulsating, topographically controlled 'erosional' rips; Short, 1985). They persist when wave steepness is increasing, which can be expressed as $\Omega$.

Erosion rips occurred when $\Omega > 2.5$ and waves are rising. As $\Omega$ increases, the rips increase in size and spacing, thereby decreasing in number, until one or two 'mega rips' drain the entire surf zone. Erosion rips are highly variable both spatially and temporally. The rip will rework the morphology to suit the rip spacing, the spacing itself being apparently related to infragravity and/or high edge-wave modes (Bowen and Inman, 1969; Wright, 1982) and the rip circulation controlled by high-energy infragravity pulsing (Shepard and Inman, 1950; Sasaki *et al.*, 1981).

Erosion rips produce morphological changes by removing sand from the beach and inner surf zone and depositing it seaward of the breakers, and are controlled by the surf zone hydrodynamics rather than the antecedent morphology (Short, 1984). Erosion rips are the major mechanism for sediment exchange between intermediate beaches and surf zones and the nearshore and perhaps inner shelf, as suggested by Swift (1975). While erosion rips do not usually possess well-developed channel morphology, if they and/or mega rips, do persist in location, an 'ebb tide' like delta structure can develop seaward of the normal breaker line with flows extending over a kilometre seaward of the surf zone (Shepard and Inman, 1950; Sasaki, 1977; Short, 1979; Wright *et al.*, 1980), even at depth (Reimintz *et al.*, 1976).

A mega-rip is an erosion rip that persists when $\Omega > 6$ due to the influence of nearshore and/or adjacent embayment topography that prevents the development of the fully dissipative state by inducing wave refraction and persistent longshore gradients in surf-zone dynamics (Short, 1985). During extreme wave events when $H_b > 3m$ and $\Omega > 6$, most sandy beaches eventually become fully dissipative (Short and Wright, 1984). Infragravity standing waves and their vertically segregated flow oscillations (Wright *et al.*, 1982a,b) replace the horizontally segregated rip circulation of erosional longshore bar and trough and erosional dissipative beach states.

Accretion rips occur when $\Omega < 2.5$ and waves are constant or falling, usually following the formation of antecedent erosion rips and associated erosion beach states (Short, 1979). Once rip spacing is set, the rips are increasingly held or topographically arrested in locations by the surf-zone morphology. Once the rhythmic bar and beach state is reached, they tend to remain arrested so long as wave height and direction remain constant or fall slowly. During transition to the low tide terrace state the rips infill and disappear (Short, 1985; Brander, 1999b).

The regular spacing of accretion rips is probably initially controlled by the generation of edge waves at infragravity periodicities during the transition from rising to stable wave conditions (Bowen and Inman, 1969; Wright, 1982; Wright and Short, 1984). In the latter stages of longshore bar and trough and particularly in the rhythmic bar and beach and transverse bar and rip state, rips are morphologically very prominent with well-developed rip feeder and rip channels draining the prominent crescentic and transverse bars and megacusp horns and embayments. As the rips become increasingly topographically arrested and the flow confined to smaller, narrower channels, rip velocities may increase between the longshore bar and trough and rhythmic bar and beach states (Wright and Short, 1984). For this reason swift, pulsating rip currents in the order of $1.0ms^{-1}$ can persist on transverse bar and rip beaches when waves are reasonably low (<1m). While accretion rips can move water and sediment seaward of the surf zone, they occur during general beach accretion and the export of sediment from the rips is exceeded by the import from the bars which may eventually infill the rip, resulting in the welded bar of the low tide terrace state (Short, 1985).

### 2.4.1 Embayed beaches

Beach and surf zone morphodynamics can be influenced or controlled by the effect of headlands, rocks, reefs and structures on wave refraction and attenuation, and through the limiting of longshore currents, rips and rip feeder currents (Short and Masselink, 1999). In order to examine such influences, Martens *et al.* (in press; cited in Short, 1999) defined a non-dimensional embayment scaling parameter δ' where:

$$\delta' = S_l^2/100C_lH_b$$

where $S_l$ is the shoreline length, $C_l$ is the embayment width, and $H_b$ is the wave height. The degree of headland impact can be predicted using the non-dimensional embayment scaling predictor δ':

| | |
|---|---|
| $\delta' > 19$ | normal beach circulation |
| $\delta' = 8$-$19$ | transitional circulation |
| $\delta' < 8$ | cellular beach circulation. |

Normal beach circulation consists of the micro and macro tidal models previously described in Section 2.3. Transitional circulation occurs when the shape and size of the embayment begins to influence the surf zone circulation. This is initially characterised by longshore currents flowing seaward against each headland, while some normal beach circulation occurs away from the headlands.

Cellular circulation occurs when the topography dominates the circulation of the entire embayment. This results in the domination of longshore flow within the embayment, and strong, seaward flowing mega-rips (Short, 1985) occurring at one or both ends of the embayment, and in the case of longer embayments also away from the headlands (Short and Masselink, 1999).

## 2.5 RIP SPACING

The regular spacing of rips along shore is a commonly observed feature of rip currents, with this phenomenon noted in many of the early scientific discussions on rip currents (Shepard *et al.*, 1941; Inman and Quinn, 1952; Shepard and Inman, 1951; McKenzie, 1958). Rip spacings have been observed to have wavelengths ranging from 100 to 1000 metres or more (e.g. Komar, 1983; Huntley and Short, 1992).

Surf-zone width has been suggested as one variable that controls rip spacing (Bowen and Inman, 1969; Hino, 1974; Sasaki and Horikawa, 1975; Short, 1985; Huntley and Short, 1992). Hino (1974) suggested a peak in rip spacing ($Y_r$) equal to four times the surf-zone width ($X_s$). However, Bowen and Inman (1969) found this value ranged from 1.5 to 8, which was further confirmed by Sasaki and Horikawa (1975) and Short (1985).

Short (1985) and Huntley and Short (1992) propose the dimensionless fall velocity parameter $\Omega$ as a control on rip spacing, where:

$$\Omega = H_b/Tw_s$$

with $H_b$ the breaker height, T the incident wave period and $w_s$ the sediment fall velocity (Dean, 1973).

Observations by Short (1985) of 3513 rip currents over a 19 month period at Narrabeen Beach, Australia, established a linear relationship between $Y_r$ and $\Omega$ in the form of:

$$Y_r = 81\Omega + 69 \qquad (R^2 = 0.85)$$

$$Y_r = 124\Omega - 53 \qquad (R^2 = 0.95)$$

with the two equations corresponding to different degrees of smoothing of the data into beach state classes (Wright and Short, 1983; Wright *et al.*, 1985).

Huntley and Short (1992) re-examined Short's (1985) extensive data set on rip currents and wave parameters for Narrabeen Beach, Australia, to determine how rip current spacing is related to incident wave conditions. They determined that rip current spacing depends primarily upon breaker height and sediment fall velocity alone, being linear in a dimensionless combination involving $H_b^{3/2}/w_s^2$. The only evidence for any dependence on incident wave period was a trend towards increasing spacing with increasing wave period, but this relationship only had a regression coefficient of 0.1.

Secondly, it was found that simulated surf-zone width (Dean, 1977; Bowen, 1980) provided a better predictor for rip spacing than observed surf-zone width. However, there remained a considerable range in this ratio and regressions with other dimensionless and dimensional variables gave low regression coefficients. It was suggested that edge wave mode number might provide another control variable.

Brander *et al.* (1999) included field measurements of rip spacing along Muriwai Beach, New Zealand. It was found that 'typical' longshore troughs characteristic of dissipative beaches also act as extensive rip channels during oblique wave conditions. The information gained on large-scale rip current systems, was used in further work by Short and Brander (1999), which provided a preliminary description of the scaling relationships of rip spacing found under a range of regional wave environments from a range of different locations. A new dimensionless variable termed 'rip density' (RD) was used where:

$$RD = L_b / Y_r$$

where $L_b$ is beach length and $Y_r$ is rip spacing.

A strong relationship was identified between rip density and levels of wave energy based on the coastal morphogenic approach described by Davies (1964, 1980). A total of five distinct global wave climates were identified, with west coast swell (WCS) beaches recording the lowest rip density of 2 rips/km while fetch-limited bays (SWB) and moderate wind environments (MWS) recorded the highest rip densities of 11-13 rips/km.

A distinct scaling relationship based on rip density was identified. The rip density of SWB and MWS beaches was approximately five times greater than WCS beaches and is twice as great than on east coast swell beaches (ECS). ECS beaches also had 2.5 times the number of rips as WCS beaches, a phenomenon that was confirmed by Brander (1999).

Observation and quantification of rip channels and bar dynamics was carried out at Tairua Beach, New Zealand, using deployment of a computer-controlled video camera by Bogle *et al.* (in press). Rip characteristics were observed for twelve storm events over an eleven month period. Rip spacings varied from approximately 130m to 205m, with rip spacing increasing between the intermediate beach states of transverse bar and rip, and longshore bar and trough (Wright and Short, 1984). Utilising Short and Brander's (1999) rip density parameter, RD, Tairua Beach has a RD value that ranges between 7.69 and 4.88.

## 2.6 RIP VELOCITY

Rip current velocity is difficult to measure, especially in storm wave conditions (Gruszczynski *et al.*, 1993). General velocities range between 0.35 and 1.5 $ms^{-1}$ (Shepard *et al.*, 1941; Ingle, 1966; Cook, 1970; Reimintz, 1971; Wright and Short, 1984; Brander, 1999a), although the velocity of rip currents may approach $2ms^{-1}$ (Sonu, 1972; Brander *et al.*, 1999), or even $3ms^{-1}$ in the case of 'megarips' (Short, 1985).

Brander (1999a) suggests three important factors related to the morphodynamic relationships operating within rip systems: (a) Rip current velocities have a distinct tidal modulation, with maximum flows occurring at low tide and minimum flows at high tide (Masselink and Short, 1993, Aagaard *et al.*, 1997; Brander, 1997; Michel and Howa, 1999; Brander, 1999a,b; Brander *et al.*, 1999); (b) Sediment transport increases with increasing mean rip velocity (Brander, 1999a); and (c) Low energy intermediate beach state evolution, from a longshore bar-trough and rip state through to a transverse bar and rip state, is characterised by an overall increase in rip velocity (Wright and Short, 1984; Brander, 1997; Brander, 1999a,b).

Rip current velocity is highly variable (Huntley *et al.*, 1988). Rip current strength varies on many time scales, and ranges from strong, persistent rip currents, to sporadic, variable rips which fluctuate from weak to strong and back to weak again over a period of a few minutes (Huntley *et al.*, 1988). Smith and Largier (1995) observed unsteady, episodic rip currents that reoccurred periodically but often. The unsteady nature of the rip currents suggests that the offshore 'burst' depletes the nearshore energy reservoir, which in this case is stored up in the longshore flow, and the system is reset.

In field measurements of the large-scale rip current system at Muriwai Beach, Brander *et al.* (1999) found that the maximum lagrangian velocity occurs at the feeder/rip-neck transition where the channel is deepest and the flow turns offshore. Flow velocities in the main body of the feeder channel ranged from 0.4-0.7$ms^{-1}$. Flow maximums in the rip neck ranged from approximately 0.8-1.2$ms^{-1}$ before decreasing again to less than 0.8$ms^{-1}$ in the rip-head. Eulerian rip flow measurements are estimated to be in excess of 1.5$ms^{-1}$ at depth in the rip-neck. A scaling relationship of 2.5 based on mean flow velocity was established between similar beaches with differing energy regimes.

In further work by Brander (1999b) at Palm Beach, Australia, quantitative analysis of a low-energy rip system found that rip velocity increased with decreasing energy conditions (see Section 2.3.2), through morphologic and kinematic adjustments to the rip system, in relation to Wright and Short's (1984) beach state model. Rip flow was maximised when the morphological expression of the rip channel is amplified, as it was during periods of transverse bar-rip morphology, and during low tide at any evolutionary stage.

Huntley *et al.* (1988) used lagrangian techniques to determine rip current strengths on a Caribbean Pocket Beach. Results from the study demonstrated a strong relationship between strong rip currents and higher waves and waves of longer period. These findings are consistent with that of McKenzie (1958), whose observations were made in relatively enclosed bays. This is in direct contrast to Shepard and Inman (1950) who observed large-scale rip currents on an open coast and found that minimum velocities were associated with high waves.

Masselink and Hegge (1995) established that the effect of wave height and angle of approach on rip circulation velocity is dependant upon the orientation of the bar/rip morphology. If the angle of wave approach is in accordance with the bar/rip orientation, an increase in wave height will induce more intense wave breaking and may result in stronger nearshore circulations as observed by Sonu (1972). However, if the orientation of the morphology mismatches the wave angle, an increase in wave height and breaking intensity will tend to decrease or even reverse the current circulation.

## 2.7 SEDIMENT TRANSPORT

Greenwood and Davidson-Arnott (1979) first suggested that large offshore-directed bedforms (megaripples) were due to rip current activity. They concluded that rip currents are important to the transport and circulation of sediment within the surf zone and to the stability of nearshore bars. Rip currents are also the main factor responsible for the transport of coarse sediments from the littoral zone to greater depths (Al-Ghadban, 1990; Gruszczynski *et al.*, 1993).

Tidal modulation of sediment transport and hydrodynamics in a rip channel have been recognised as an important feature (Aagaard *et al.*, 1997). Strong offshore sediment transport was associated with mean flow at low tide. Conversely, weak onshore directed mean flows and/or oscillatory incident waves directing small amounts of sediment onshore, occurred during high tide, when rip channels were relatively inactive.

Studies of the sediment dynamics of a ridge and runnel system have been undertaken by Michel and Howa (1999). Sediment transport was directed onshore onto the ridge, although the ridge was not observed to either grow or migrate during the observation period (Figure 2.10). Offshore transport occurred in the rip channels, with cell circulation enhancement during the rising tide. The longshore transport appeared to be controlled by the strong rip currents concentrated within the runnel during the falling tide.

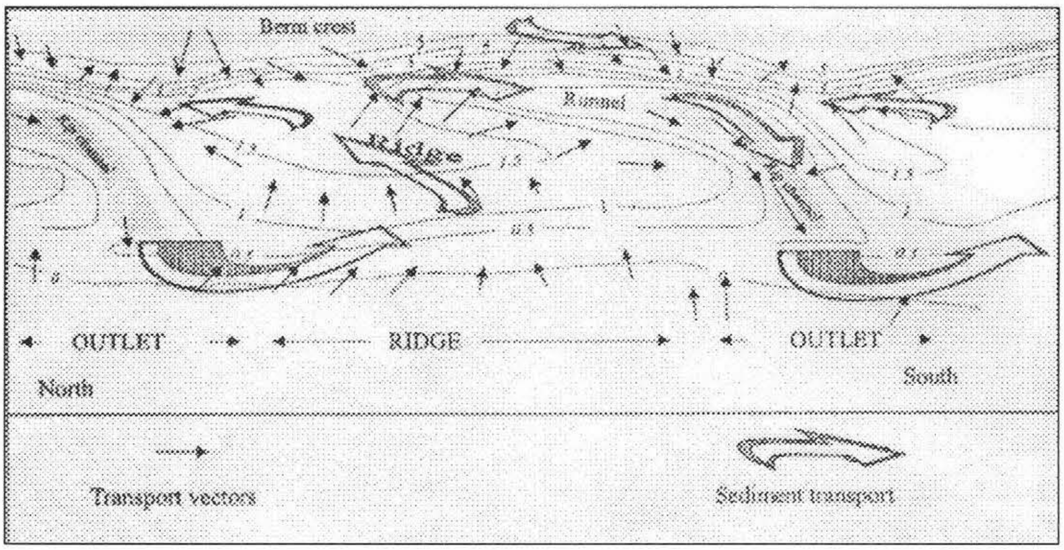


Figure 2.10 Michel and Howa's (1999) conceptual model showing the morphodynamic response of a ridge and runnel system under fair weather conditions.

Quantitative observation of low energy rip currents conducted at Palm Beach, Australia, suggest that the rip-head bar is integral to patterns of sediment transport that produce morphological change (Brander, 1999b). Sediments transported out of the surf zone by the rip current are deposited into a rip-head bar, which, in the presence of a skewed rip channel, eventually becomes attached to the seaward slope of the opposite bar. These sediments are then transported offshore and contribute to the constriction of the rip channel flow and lead to an increase in flow velocity. Thus, greater amounts of sediment are transported by the rip and deposited in the rip-head bar, and the process becomes accelerated. Sediment reintroduced into the surf zone will eventually begin to infill the rip channel, reducing flow and increasing the instability of the system. Therefore, elements of morphodynamic feedback (Cowell and Thom, 1994) are critical to low-energy rip current evolution (Brander, 1999b).

## 2.8 Impact Of Sea Breeze

Pattiaratchi *et al.* (1997) have shown that the sea breeze plays a significant role in driving coastal processes. Results showed that the sea-breeze system changes nearshore and foreshore coastal processes from a swell dominated system to a wind-wave dominated system, with associated changes in wave climate with sea breeze onset. Nearshore currents were modified from a circulatory system with strong oscillatory currents and rips, to a strong longshore unidirectional system with mean speeds up to $1.0ms^{-1}$. This study demonstrated that beach systems with strong sea breezes present, are in a constant state of adjustment to the incident wave energy through the diurnal sea-breeze cycle, and subsequently the beach is not allowed to reach equilibrium conditions.

## 2.9 Video Imaging

The use of automated video imaging is a new technique used for data acquisition that is both simple and cost effective. Measurements over a relatively wide range of spatial scales and time scales can be gained (Holman and Lippmann, 1987; Lippmann and Holman, 1990; Ranasinghe, *et al.*, 1999a,b). Video imaging is particularly advantageous in the documentation of coastal processes as the sub-aerial location of the instrument circumnavigates a number of problems associated with *in-situ* measurements, including bio-fouling, difficulties with turbulent flow conditions, and sensor deterioration under adverse wave conditions (Holland *et al.*, 1997).

Rip currents are visible in time exposure images as low pixel intensity (dark) regions extending seaward, bounded by high pixel intensity (bright) regions on both longshore boundaries of the current (Ranasinghe *et al.*, 1999b). Two years of daily time exposure images of incident waves were collected by Lippmann and Holman (1990) to develop their eight state sand bar morphology model. The use of high quality, continuous, long-term data through video imaging allowed Ranasinghe *et al.* (1999a) to test the various rip generation models suggested in the literature. In New Zealand, work has focussed on the embayed beach of Tairua, where recent investigations have included rip characteristics, evolution and formation (Bogle *et al.*, in press), and the observation of rips and bar type sequences during storm conditions (Bogle *et al.*, 1999).

## 2.10 NEW ZEALAND

Work on rip currents in New Zealand is in its infancy (i.e. Brander *et al.*, 1999; Stephens *et al.*, 1999; Bogle *et al.*, 1999; Bogle *et al.*, in press).

Stephens *et al.* (1999) examined the causative processes in the establishment of arcuate dune embayments at Waihi Beach, New Zealand. Observations of rip currents during the study period were made, and while rip currents eroded small sections of the beach during storm events, a number of rip current systems would fit into a single arcuate dune embayment, suggesting that rip currents were not the primary mode of formation. Stephens *et al.* (1999) suggest wave refraction and focusing over offshore ridges as the most feasible explanation for arcuate dune embayment formation. It is also suggested that this mechanism of embayment erosion could be applied to so called 'rip current embayments' (Komar, 1971, 1983a,b; Komar and Holman, 1986) which have been identified in other coastlines globally.

Muriwai Beach was the site for the examination of rip spacing, flow dynamics, and nearshore morphology within a large-scale, high energy rip system (Brander *et al.*, 1999). 'Typical' dissipative-type longshore troughs were shown to act as extensive rip channels during oblique wave conditions. Rip flows were maximum at low tide, with rip velocities exceeding $2ms^{-1}$ at times.

Work by Bogle *et al.* (1999, in press) has involved the utilisation of video imaging techniques at Tairua, situated on the Coromandel Peninsula. Observations include bar type sequences, with subsequent rip morphodynamics (Bogle *et al.*, 1999) and observations of rip current formation, migration and evolution (Bogle *et al.*, in press) including a pattern termed 'rip extension', where a new rip forms at the far end of an alongshore extension of a pre-existing rip current.

## 2.11 GAPS IN THE LITERATURE

Although there have been numerous qualitative investigations of rip current systems, quantitative field measurements are scarce (Aagaard and Masselink, 1999; Komar, 1998; Huntley *et al.*, 1988). Logistical problems hamper the monitoring of rip current systems, especially as rips are generally highly irregular both in strength and precise location (Huntley *et al.*, 1988).

There is a lack of rigorous verification in the field of both rip current generation mechanisms (Aagaard and Masselink, 1999; Komar, 1998; Trenhaile, 1997), and the subsequent mechanisms that drive rip current spacing (Short and Brander, 1999). The hypothesis proposed by Short and Brander (1999), that there are regional variations in rip spacing (rip density), requires further analysis; firstly because it is a preliminary description, and therefore a potentially rather simplistic model, and secondly because of the relatively small data set on which the assumptions are based.

Few quantitative measurements have been made of sediment transport in rip channels (Aagaard *et al.*, 1997; Brander, 1999b; Michel and Howa, 1999) and the investigations are restricted to low energy rip systems. A small number of quantitative investigations into rip velocities have also been carried out (i.e. Wright and Short, 1983; Huntley *et al.*, 1988; Aagaard *et al.*, 1997; Brander, 1999a) with only one published investigation into rip velocities in a high energy rip system (Brander *et al.*, 1999).

Recent advances have been made, particularly with the use of the video imaging technique, which can provide high quality, long-term field data. This has resulted in the ability to observe rip formation and evolution sequences (Bogle *et al.*, in press) and the capability to test the validity of theoretical rip current generation mechanisms (Ranasinghe *et al.*, 1999). At present the number of beaches that are investigated in this capacity are restricted, limiting the applicability of findings to other types of beaches.

# CHAPTER THREE: METHODOLOGY

## 3.1 INTRODUCTION

The data used in this study is based primarily on an analysis of rip spacing and other surf-zone parameters on intermediate and dissipative beach types. The data has been obtained from aerial photographs taken of the entire New Zealand coastline, with supplementary information used for beach sediments and wave climate. Field investigations were also carried out at Castlepoint, Fitzroy, Oakura and Tairua beaches to further explore rip current dynamics, particularly rip velocity characteristics in relation to rip spacings and surf zone morphology.

## 3.2 AERIAL PHOTOGRAPHS

Two sets of aerial photographs were used. Mosaic aerial photographs held by the Massey University Geography Programme, and individual aerial photographs from the collection at Land Information in Wellington were analysed. The mosaic aerial photographs used from the Massey University collection were at a scale of 1:15,840, with an estimated error range of +/- 15.84m. The aerial photographs used from the Land Information collection were at a scale of 1:25,000, with an estimated error range of +/- 25m. All beaches that displayed rip currents were analysed, although data used was restricted to the inner bar of multiple bar beaches.

The primary beach and morphometric parameters assessed from the photographs consist of rip spacing ($Y_r$), rip density (RD) surf-zone width ($X_s$), rip neck width ($W_r$), rip length ($L_r$) (refer to Figure 3.1), length of beach sampled ($L_b$), total beach length ($L_{bt}$) following Short and Brander (1999) and beach type following Wright and Short (1984) and Short and Aagaard (1993). Rip spacing was measured from the landward edge of the rip neck on the left-hand side, to the corresponding location on the next rip channel. Surf-zone width was measured seaward from the visible high tide mark to the outermost breaking wave. Rip neck width was measured at the narrowest part of the rip current neck. Rip length was measured from the base of the rip current, at the confluence of the feeder channels, to the end of the rip head.

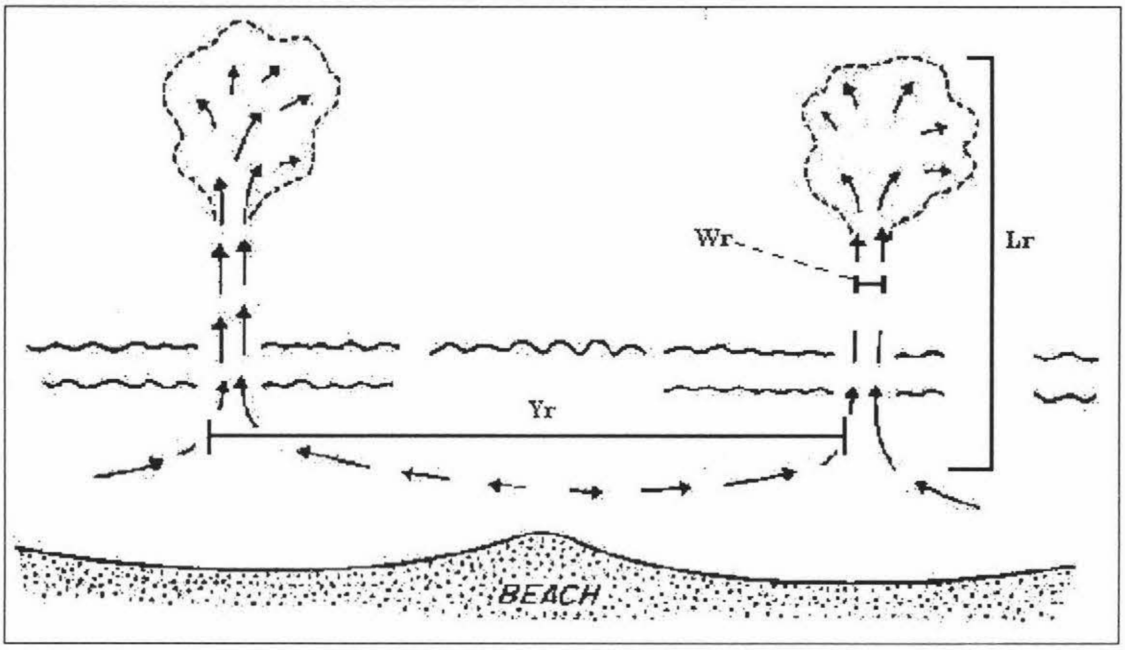


Figure 3.1 Schematic diagram of rip morphometric parameters measured in this study, showing rip spacing ($Y_r$), rip width ($W_r$) and rip length ($L_r$).

Mean values for each beach were obtained for rip spacing, rip neck width and rip length, although in many cases rip spacing, associated rip parameters, and beach type vary along individual beaches. A particularly interesting phenomenon was the occurrence of 'rip clusters' where a group of rip currents of varying sizes would be grouped together in a way that varied from the general rip spacing for the remainder of the beach. These have been identified by Bogle *et al.* (in press), and appeared to be the result of rip formation where a rip-cusp bar splits an existing rip from the shoreward side (Figure 3.2), or a transverse bar splits an existing rip current from either the shoreward or seaward side (Figure 3.3).

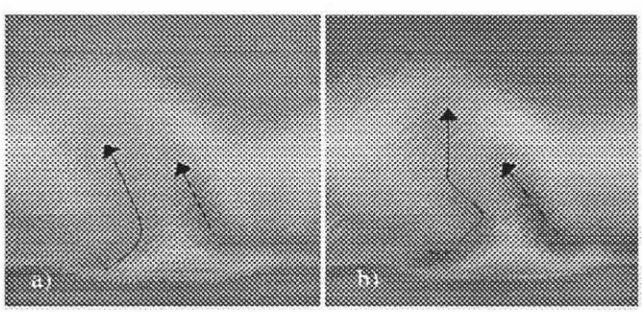


Figure 3.2 Averaged images from the centre of Tairua beach. Solid lines represents to the rip currents. Figure (a) shows the rip-cusp extending outward into the existing rip current. Figure (b) shows the two feeder currents moving apart so that the main rip current is split into two separate rip currents (Bogle *et al.*, in press).

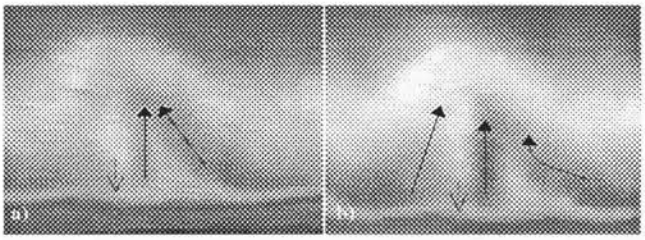

Figure 3.3 Averaged images for the centre of Tairua beach. Solid lines represent the rip currents. Figure (a) shows the first stage in which a transverse bar formed on the northern side of the rip. Figure (b) shows this transverse bar extending shoreward to cut off the feeder channel that is supplying water to the main rip. This water then exited on the northern side of the new transverse bar to form a new rip (Bogle *et al.*, in press).

The sampling techniques used were largely predetermined by the nature of the original data. In the majority of cases, aerial photographs did not reveal rips as they were either not present due to a reflective beach state, or surf zones were in a dissipative beach state. In particular, while the aerial photographs held in the Land Information collection have several photo runs, in most cases only one run displayed rip currents.

A second problem occurred with the mosaic aerial photographs, which are a collection of photographs taken on various days put together to provide coverage of a larger area in a single photograph. In a number of cases, sections of photographs displaying rip currents were adjacent to photographs displaying a very different surf zone morphology, with no rip currents present. This variation caused difficulties, particularly when the area of the photograph displaying rip currents was small, or there was a high degree of variation along the stretch of coastline being analysed. An example of this is shown in Figure 3.4.

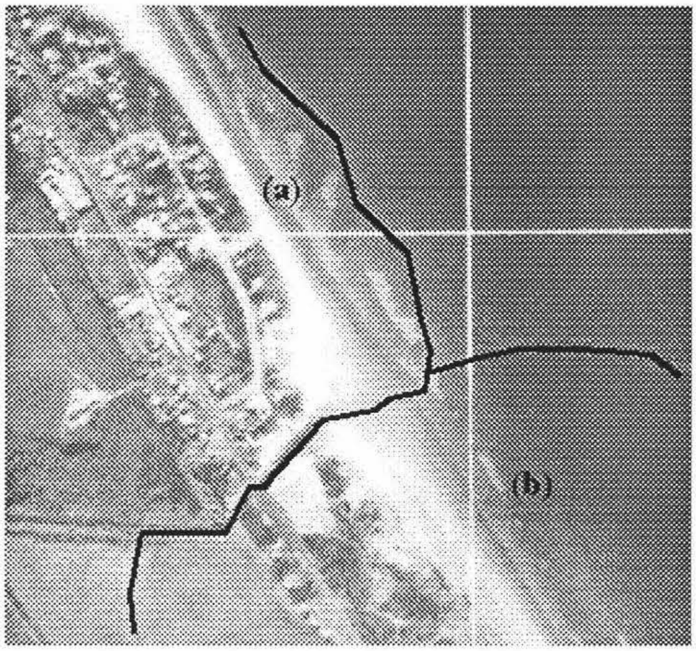


Figure 3.4 An aerial photograph mosaic showing the discrepancies within the photographs with regard to the surf zone conditions. The black lines indicate joins between the photographs in the mosaic. Rip currents are found at (a.) but are not evident in the lower portion of the aerial photograph (b).

### 3.3 WAVE CLIMATE AND SEDIMENT SIZE ASSESSMENT

Data on wave climate, sediment size and sediment fall velocity were used to assess the role that these factors play in controlling rip spacing. Information on wave climate came from two sources. The first source, from O'Dea and Hesp (2000), is a report that attempted to collate wave height, significant wave height and wave period data from a variety of sources around New Zealand. The data is highly variable, with a wide range of time periods over which observations were made, and a broad array of data collection methodologies, from instruments to wave rider buoys and personal observation.

The second source of wave height data is taken from a summary of weather and surf conditions from Surf Life Saving Club beaches around New Zealand over the 1997-1998 summer period (Hesp & O'Dea, 1999a). This wave height data may not provide the best indication of significant wave heights, due to possible observational errors, the way in which data was collected under wave height groups rather than actual values of wave height, and the fact that observations are confined to the summer period.

Sediment data were obtained from Hesp and O'Dea (1999b). Grain size, expressed in the phi (∅) size scale, was utilised for each corresponding beach, with both the graphic mean and moment mean employed. The relationship between grain size and rip spacing was explored since previous work by Sunamura (1988) used the mean grain diameter in millimetres (D) in the dimensionless parameter K*, as a model to assess beach type.

Rip spacings were also compared with sediment fall velocity, which was again acquired from Hesp and O'Dea (1999b). This variable is applied in defining the dimensionless fall velocity, $\Omega$ (Gourley, 1968) and is used to define the beach-surf zone state as proposed by Wright and Short (1984), Short and Aagaard (1993) and Short and Masselink (1993). Sediment fall velocity was also used in an equation proposed by Huntley and Short (1992) as a predictor for rip spacing.

### 3.4 Rip Spacing Measurement in the field

The spacing between rips was measured at Fitzroy and Oakura by pacing out the distance between each rip along the beach. Objects of known length were paced out at the same time (i.e. the distance between two bridges or surf clubs) and these measurements were compared to actual distances as given by relevant topographical maps. Therefore, a relatively accurate measurement of rip spacings could be acquired.

### 3.5 Lagrangian Rip Velocity Measurement Techniques

Rip float experiments were conducted at Castlepoint, Fitzroy, Oakura and Tairua beaches to determine lagrangian rip velocity flows, using the method of Short and Hogan (1994). Rip currents were measured by two methods: the first by using oranges as a rip float at Castlepoint. This method was pioneered by Professor Peter Nielsen of the Department of Civil Engineering at Queensland University. The second method utilised human floaters (Brander *et al.*, 1999) at the other sites, who floated freely in the rip current. Their trajectories were tracked using two compasses at a known distance apart, with recording of positions every 15 seconds. In the case of human floats, measurements were taken from the float's head.

Oranges were used when breaking waves did not limit visibility. They were also particularly useful in situations where the use of human rip floats would have been dangerous. When the impact of breaking waves was too great, human rip floats were used.

## 3.6 RIP DYE TECHNIQUE

Flows through the rip currents were identified by the use of dye within the rip current (Huntley *et. al.,* 1988; Brander, 1999b). Approximately 250 grams of potassium permanganate crystals were dissolved in a bucket of water and dispersed into the rip feeder current. This technique was used at both Castlepoint and Tairua beaches.

## 3.7 LASER LEVEL SURVEY AND DIGITAL ELEVATION MODELLING (D.E.M.)

The surf zone and beach were surveyed to gain an accurate representation of the rip and bar morphology of each study site. The Topcon GTS-701 Total Station laser level was used to survey each site. This automated instrument emits a direct laser beam, which reflects off a prism that is attached to a staff of known height. A precise measurement of the topography can be gained when the instrument is correctly assembled and the staff is held vertically. Data is logged directly into the laser level memory in a three dimensional form (i.e. x, y, and z coordinates).

The laser level was placed on the foredune at each selected beach, which provided an excellent elevated site. Measurements were taken of topographical changes along the rip channel and across the bars on either side of the rip channel. Further measurements were made where applicable, particularly where the rip was in an oblique state.

Once the data points were downloaded, analysis was carried out using SURFER software. Three-dimensional contour maps, (Digital Elevation Models or D.E.M's), of the nearshore topography were produced using the software.

## 3.8 SEDIMENT ANALYSIS

Analysis was undertaken of the sediment size and fall velocity of sediment taken from the mid tide swash region of Oakura Beach. Sample weights were approximately 400 grams with sample depths to a maximum of five centimetres. Samples were first rinsed with fresh water to remove salt and then oven dried.

### 3.8.1 Sediment size analysis

Sub-samples of 100 grams were obtained using a sample divider to reduce bias to the results. The sub-samples were then mechanically sieved at half phi intervals for 20 minutes. Calculations of sediment size parameters were carried out using the PC-GRAN computer software package. The Folk-Ward (Folk, 1974) sediment size parameters used in this study are (1) moment mean size; (2) graphic mean size (3) deviation (sorting); (4) skewness; and (4) kurtosis.

### 3.8.2 Sediment Fall Velocity

For each sediment sample at least 50 randomly selected individual grains of sand were timed as they dropped through a 400-millimetre column of water. The following formula:

$$v = d / t$$

where v velocity ($ms^{-1}$), d is distance in metres, and t is time in seconds was then utilised. The average of the samples then gives a value for the sediment fall velocity ($w_s$).

# CHAPTER FOUR: BEACH TYPES, SEDIMENT CHARACTERISTICS, WAVE CLIMATE, RIP DENSITY AND MORPHOMETRY

## 4.1 INTRODUCTION

A total of 71 beaches from around New Zealand were used in the following investigation. The total data set is listed in Appendix I. The primary objective of this chapter is to test the hypothesis suggested by Short and Brander (1999) that the spacings between rips (and therefore rip density), and other rip morphometric parameters, can be classified into distinct groups based on their regional wave climate, as originally suggested by Davies (1980).

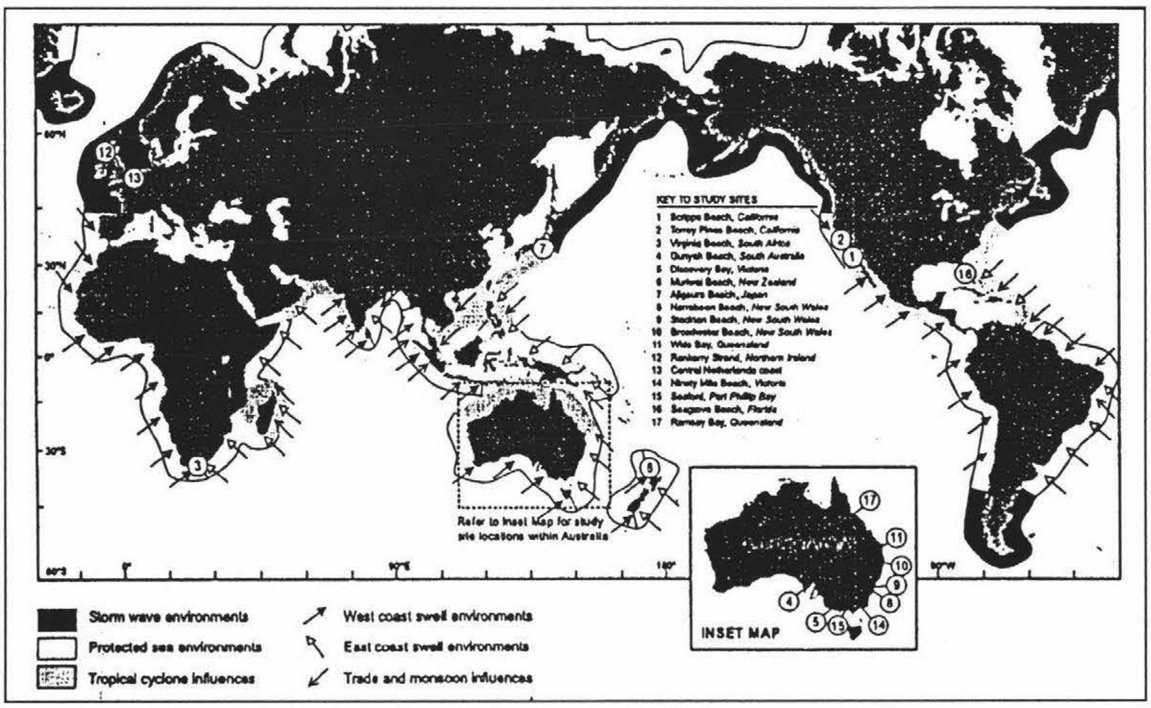


Figure 4.1 Davies (1980) original regional wave climate classification as modified by Short and Brander (1999).

As revealed in Figure 4.1, the New Zealand coastline can be placed into two of the five regional wave classifications; West Coast Swell (WCS) dominated coasts, and East Coast Swell (ECS) dominated coasts. It has been suggested that a scaling factor of 2.5 exists between WCS and ECS systems, with ECS beaches typically having 2.5 times as many rips as WCS beaches (Short and Brander, 1999). This is further illustrated in Figure 4.2. In Short and Brander's investigation, the majority of examples used were taken from the Australian coastline, complemented by published research of rip spacing measurements. Twenty-one beaches were employed, with 15 examples from six beaches for the WCS regional wave climate and 35 examples from 10 locations for the ECS regional wave climate. Only one New Zealand case was used, Muriwai beach, as an example of a 'typical' WCS beach system. This chapter will also assess the extent to which Muriwai beach, in a similar state as utilised by Short and Brander, represents an example of a typical New Zealand WCS beach.

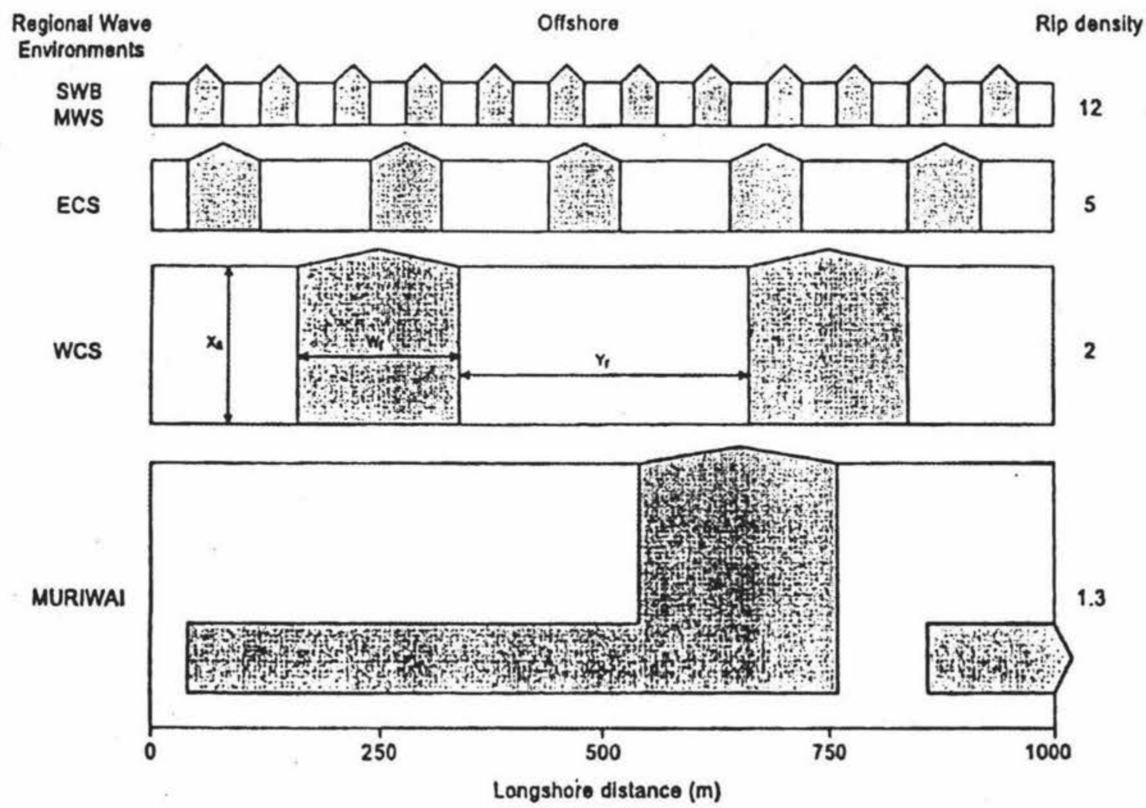


Figure 4.2 Variations in rip spacing, length and width between regional wave climates, as proposed by Short and Brander (1999).

Rips most commonly occur on beaches in an intermediate surf zone state, particularly that of transverse bar and rip (TBR) and rhythmic bar and beach (RBB) types (Wright and Short, 1984). Surf zone state has been found to influence the spacings between rips, with larger spacings found with RBB beaches as compared with beaches in a TBR state (Short, 1985; Huntley and Short, 1992; Bogle *et al.*, 1999). Other rip morphometric parameters have been found to be influenced by surf zone types, with narrower rip widths and smaller rip lengths found for TBR rip channels, as compared with RBB states (Brander, 1999b). The effects of beach state on rip morphology and velocity are summarised in Figure 4.3. Therefore, analysis will include the classification of the data into their respective beach states, to assess whether this classification can improve predictions for rip spacings and other rip morphometric parameters.

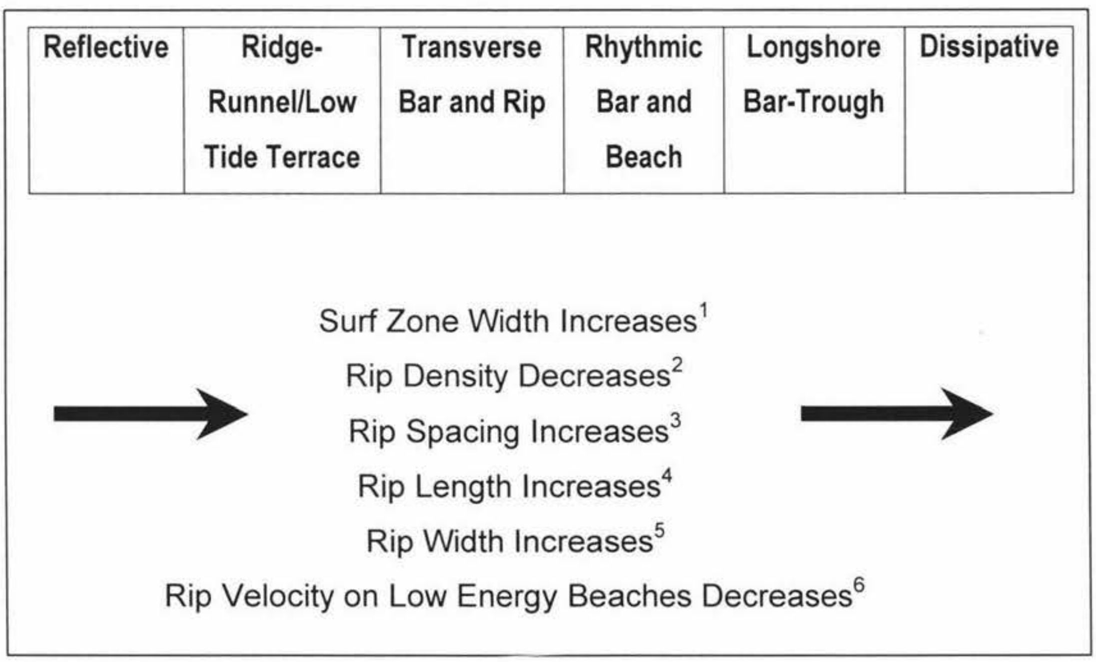


Figure 4.3 Changes to surf zone and rip morphology and rip velocity as beaches go through the six state Wright and Short (1984) morphodynamic beach state model.

[1] Wright and Short (1984); Short and Aagaard (1993)
[2] Short and Brander (1999)
[3] Short (1985); Huntley and Short (1992); Bogle *et al.* (1999)
[4] Brander (1999b)
[5] Brander (1999b)
[6] Brander (1997); Wright and Short (1984); Brander (1999a,b)

## 4.2 RIP SPACING AND SURF ZONE WIDTH

The relationship between rip spacing ($Y_r$) and surf zone width ($X_s$) is shown in Figure 4.4. The mean ratio of rip spacing to surf-zone width was 1.82,[7] with ratio values ranging from 0.43 to 4.55. In comparison, Sasaki and Horikawa (1975), Short (1985) and Huntley and Short (1992) found a scatter in this ratio between 1.5 and 8.

The overall low $R^2$ value of 0.37 (p-value <0.01) for the relationship between rip spacing and surf zone width provides a better predictor than the value of 0.20 found by Short (1985), which was based on observed surf zone width. However, the $R^2$ value of 0.49 found by Huntley and Short (1992) using simulated surf zone width indicates a slightly better fit for their data.

A comparison of rip spacing to surf zone width based on the two regional wave climates produced weaker relationships (Figure 4.5), with $R^2$ values of 0.33 and 0.35 for ECS and WCS beaches respectively. These relationships are statistically significant, with p-values of <0.01 for ECS and 0.003 for WCS. Overall, WCS beaches produced slightly larger rip spacings than ECS beaches for the same surf zone width, however the 2.5 scaling factor suggested by Short and Brander (1999) was not evident.

Comparisons between beach types (Wright and Short, 1984) produced greater $R^2$ values (Figure 4.6), particularly RBB with an $R^2$ value of 0.58, and TBR with an $R^2$ value of 0.40. P-values for both beach types are <0.01. These relationships also confirm aspects of Wright and Short's (1984) beach type model, demonstrating that beach type and surf zone width are related to some extent. There is an overall trend for larger surf zone widths associated with beaches in a RBB state, as compared with TBR beaches.

[7] Rip spacing length is 1.82 times the surf-zone width

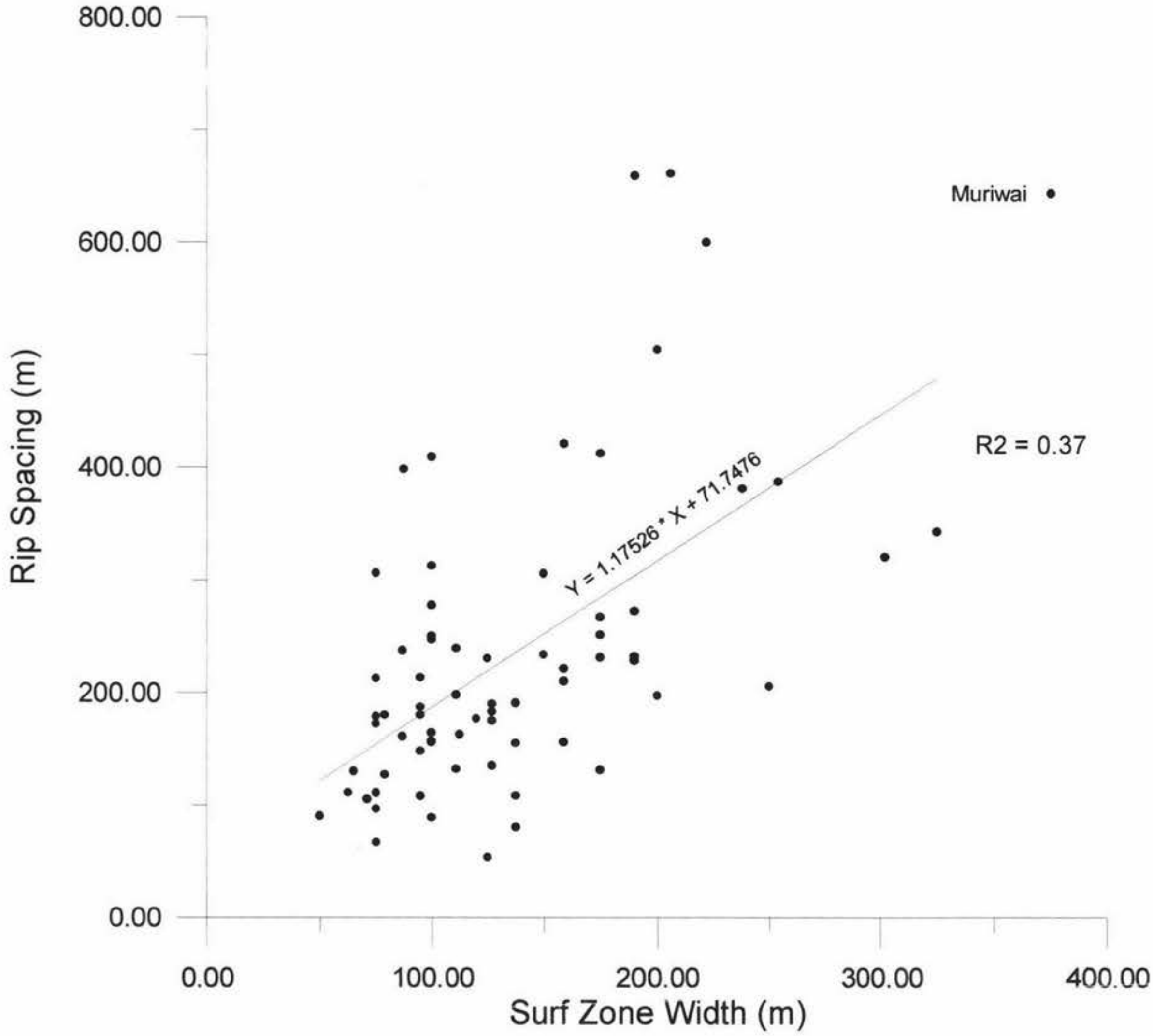


Figure 4.4 Rip spacing verses surf zone width.

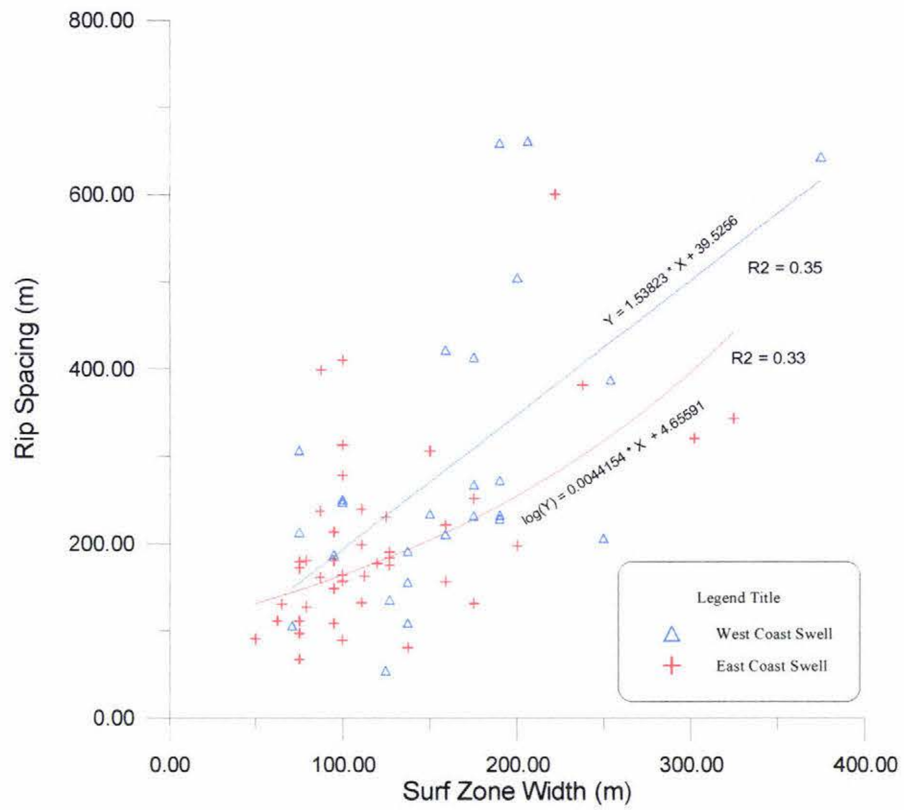


Figure 4.5 A comparison between rip spacing and surf zone width based on regional wave climate.

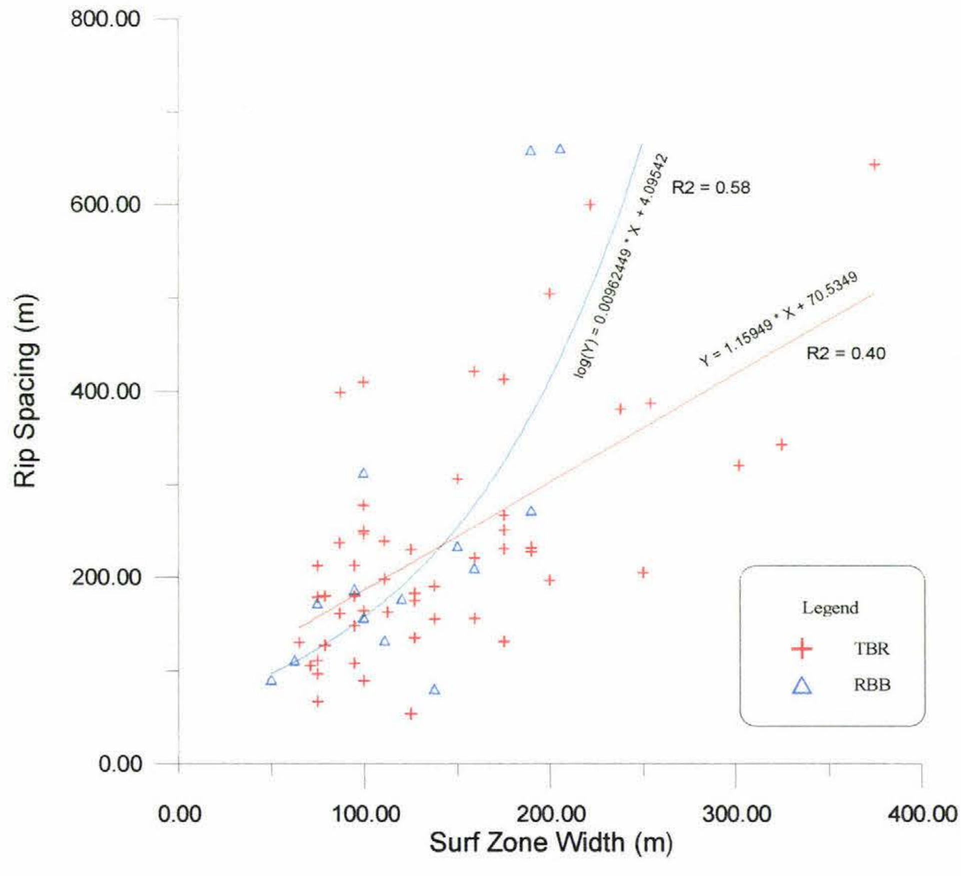


Figure 4.6 Comparison of rip spacing with surf zone width based on beach type.

## 4.2 RIP SPACING AND RIP NECK WIDTH

Figure 4.7 plots rip spacing against rip neck width ($W_r$) and shows that the $R^2$ value is surprisingly low, at 0.35, although it is still statistically significant, with a p-value of <0.01. Figure 4.8 shows a slight relationship based on wave climate, with greater overall rip spacings with comparable rip neck widths for WCS beaches. However, the difference between WCS and ECS examples does not exhibit the proposed scaling relationship by Short and Brander (1999) of 2.5. Correlations within regional wave climates were low, with $R^2$ values of 0.34 and 0.21 for WCS and ECS respectively.

The comparison between beach types (Wright and Short, 1984) produced outcomes that are of particular interest, and are shown in Figure 4.9. A stronger $R^2$ value of 0.77 was found for RBB states, although it is noted that only 15 values were used for this beach type. The $R^2$ value for TBR beach states was considerably weaker, at 0.28. This may be a reflection of the greater number of values in the data set as compared with RBB. No particular scaling relationship was present in this comparison. However, it was assumed that a scaling relationship would occur between TBR and RBB beach types, since RBB states are characterised by wider rip spacings (Short, 1985; Huntley and Short, 1992; Bogle *et al.*, 1999) and wider rip channels (Brander, 1999b) in comparison to the TBR beach state.

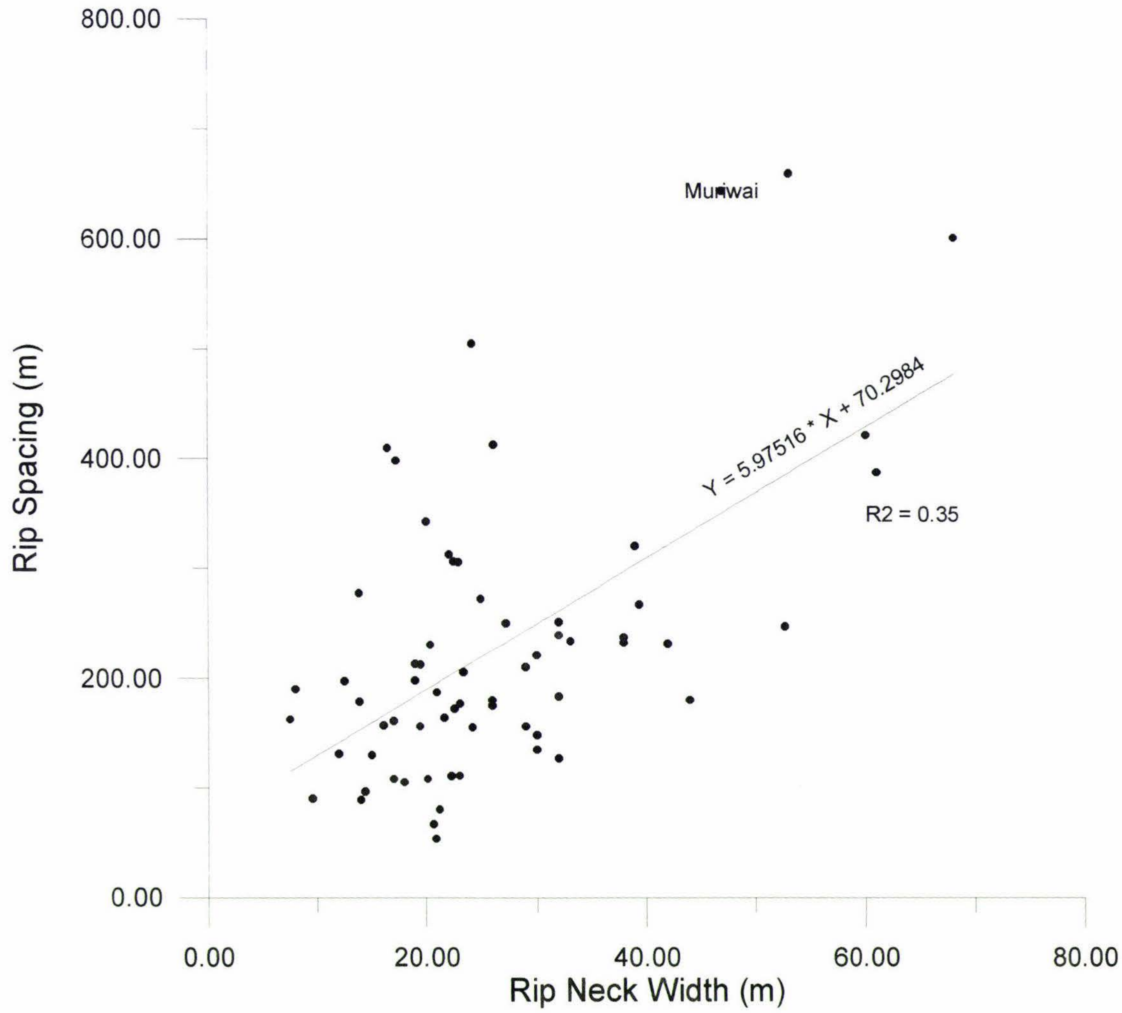


Figure 4.7 Rip spacing verses rip neck width.

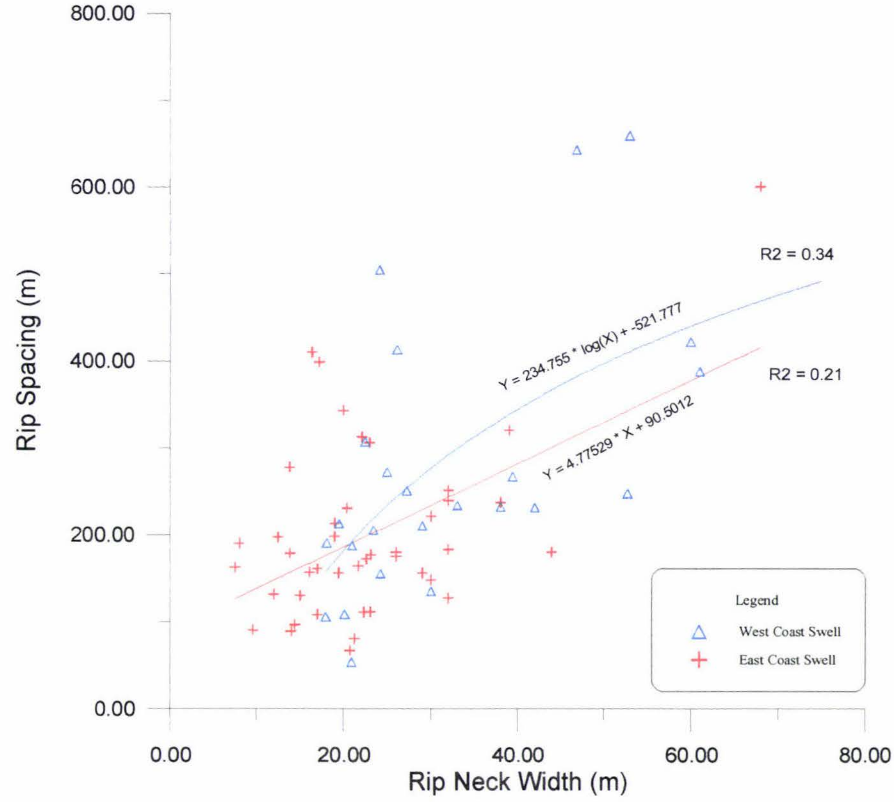


Figure 4.8 Comparison of rip spacing with rip neck width based on regional wave climate.

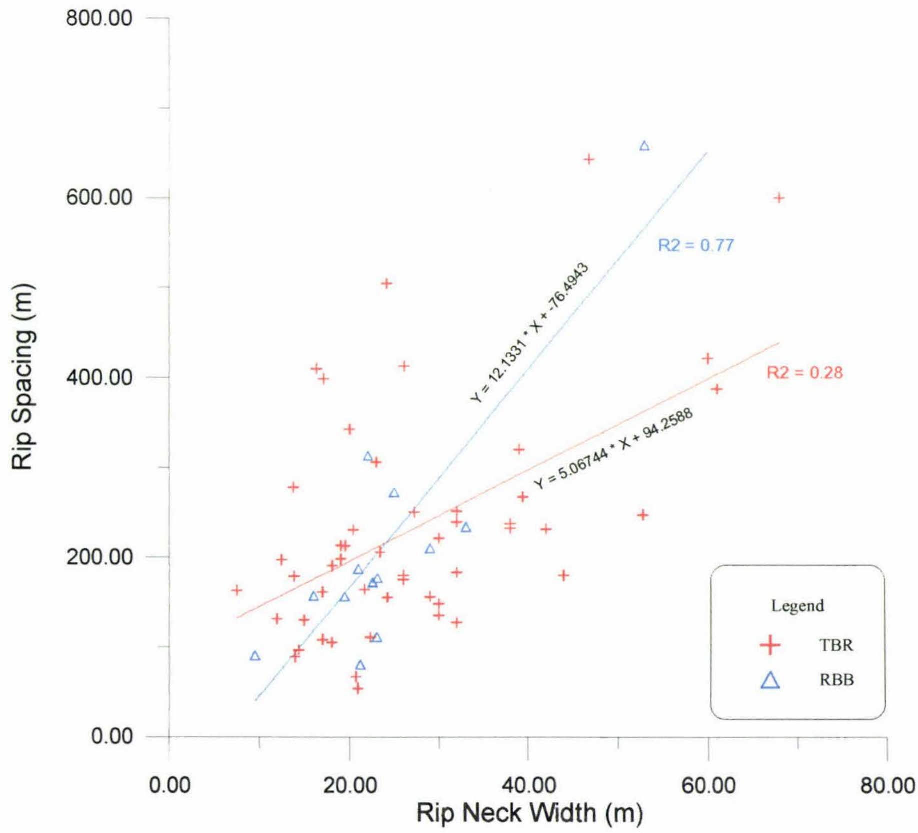


Figure 4.9 Comparison of rip spacing with rip neck width based on beach type, after removal of significant outliers.

## 4.4 RIP SPACING AND RIP LENGTH

Figure 4.10 shows the relationship between rip spacing verses rip length ($L_r$). A moderate correlation was found with an $R^2$ value of 0.43 and a p-value of <0.01. The three outliers labelled in Figure 4.10 are particularly interesting, although their removal does not improve the $R^2$ value (Figure 4.11). Haldane Bay is a classic example of a 'mega-rip' (Short, 1985) and is pictured in Figure 4.12. Muriwai represents an example of a longshore bar and trough beach state (Figure 4.13), while Ruatoria is an example of a transverse bar and rip state in oblique wave conditions. In all three cases the rips displayed elongated morphology resulting from either topographic control (Haldane Bay), or oblique wave conditions (Ruatoria and Muriwai Beach). This is of considerable interest in regard to Short and Brander's (1999) use of Muriwai as an example of a WCS beach, since this data is in a similar beach state to that used by Short and Brander (1999), as a representative WCS beach. In contrast to both the total data set and other WCS beach examples (Figure 4.14), the relationship between rip spacing and rip length for Muriwai beach is atypical.

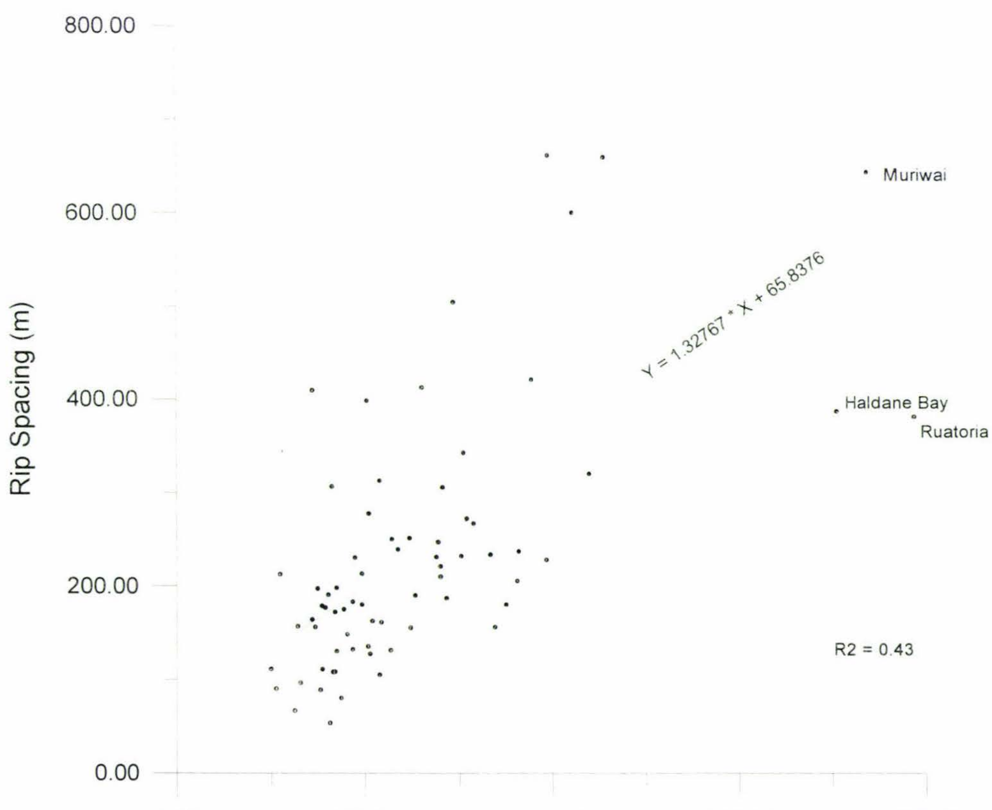


Figure 4.10 The relationship between rip spacing and rip length, displaying the three significant outliers of Muriwai, Ruatoria and Haldane Bay.

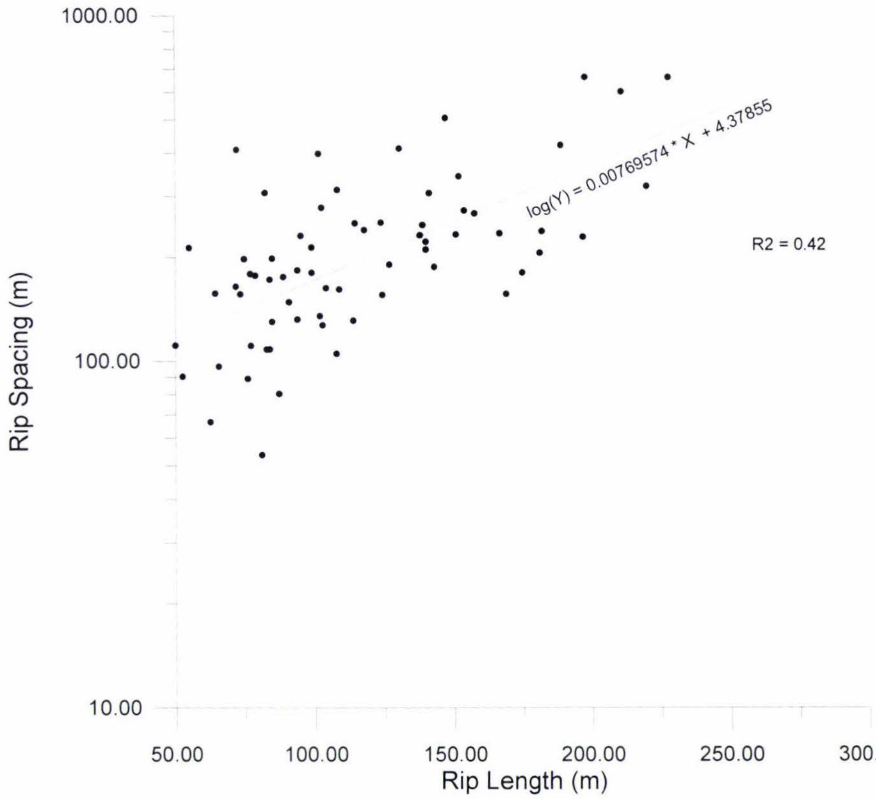


Figure 4.11 The relationship between rip spacing and rip length, after the removal of the three outliers, Ruatoria, Muriwai and Haldane Bay.

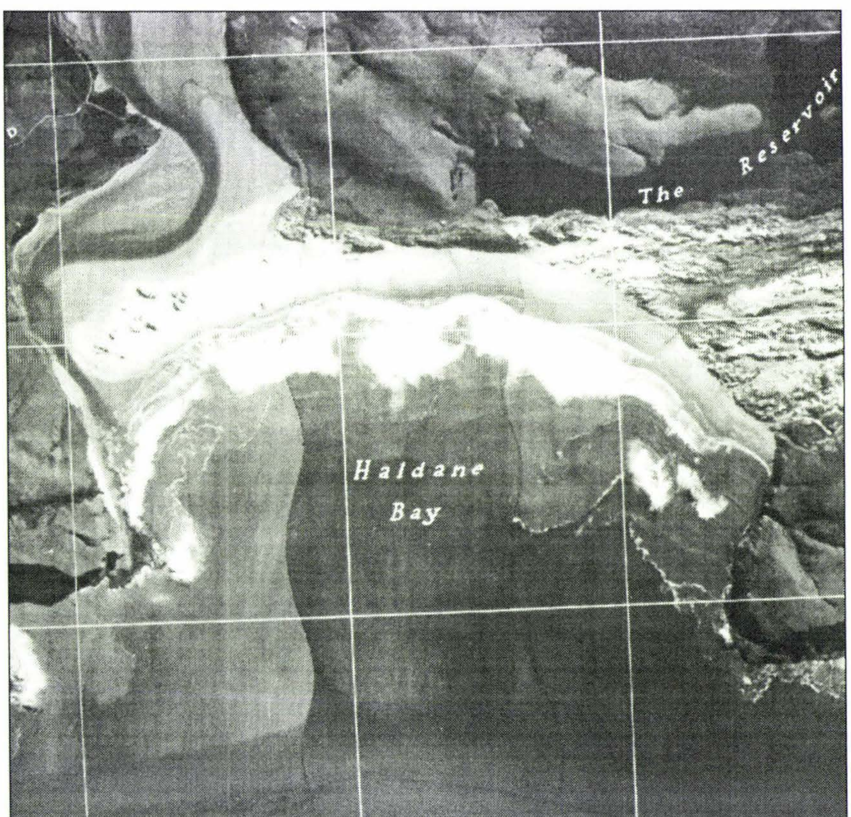


Figure 4.12 Haldane Bay: an example of a structurally controlled surf zone exhibiting mega rip morphology. Distance between gridlines is 900 metres.

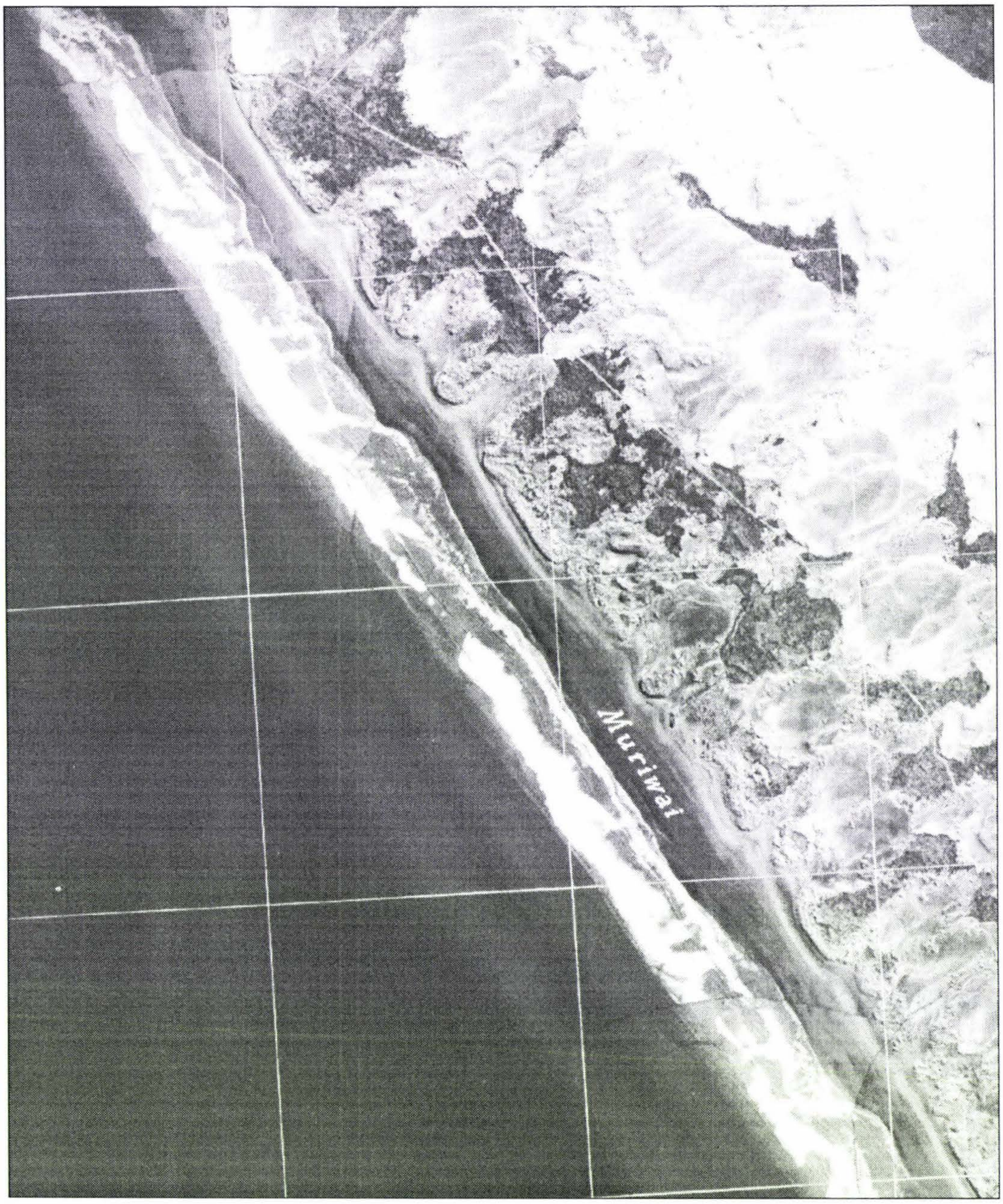


Figure 4.13 Muriwai Beach in a longshore bar and trough state with rip currents occurring within the troughs. The distance between the gridlines is 900 metres.

A weak relationship is present in the comparison between rip spacing and rip length, based on wave climate (Figure 4.14), with WCS beaches experiencing larger rip spacing values than ECS beaches, for similar rip lengths. However this relationship does not exhibit the scaling relationship of 2.5 suggested by Short and Brander (1999). $R^2$ values for both WCS and ECS are slightly lower than the total data set, at 0.42 for both regional wave climates.

There is no obvious scaling factor between rip spacing and rip length based on beach type (Wright and Short, 1984) (Figure 5.15), with $R^2$ values of 0.73 and 0.40 occur for RBB and TBR respectively. Again, RBB may have a greater $R^2$ value in part due to the small data set used.

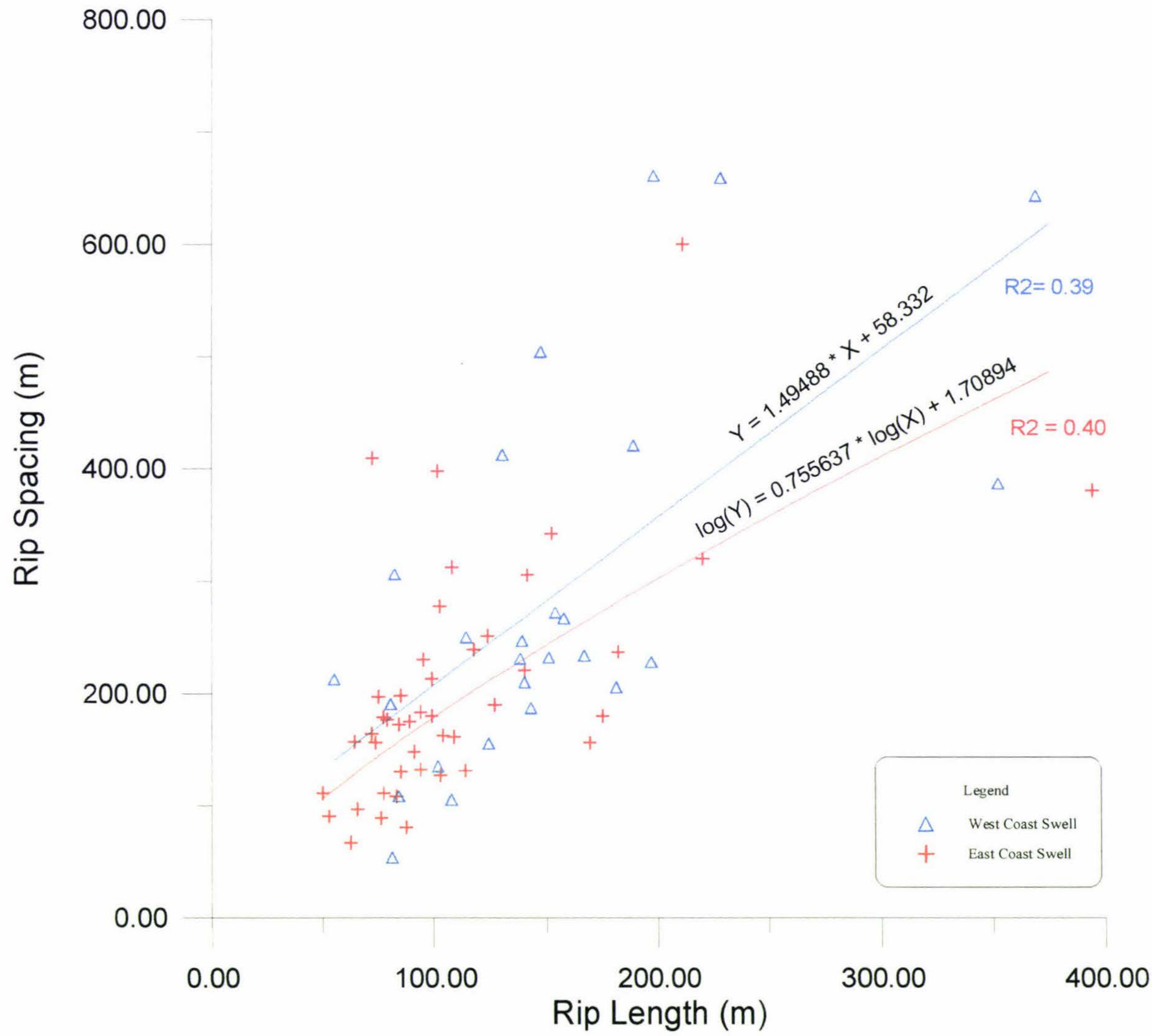


Figure 4.14 The relationship between rip spacing and rip length based on a comparison between regional wave climate.

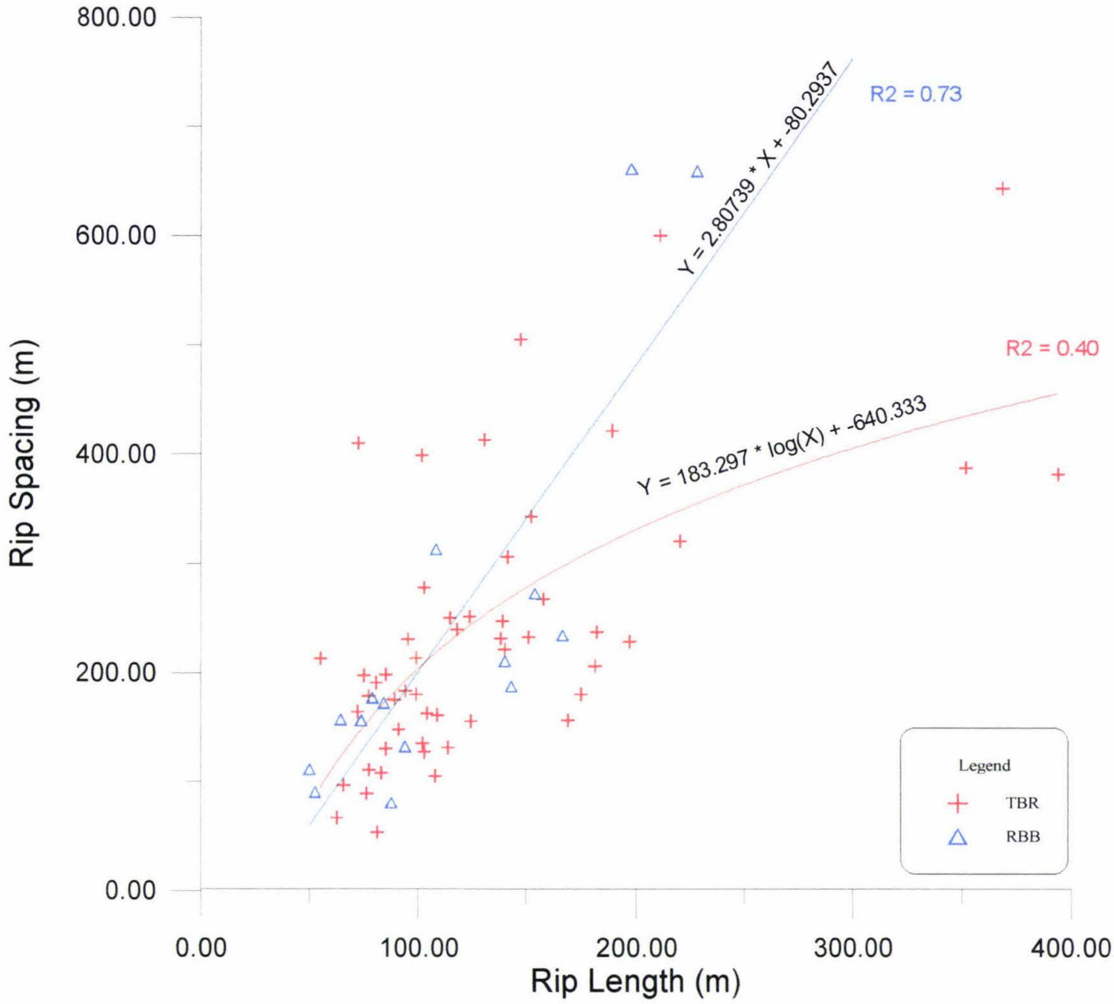


Figure 4.15 The relationship between rip spacing and rip length, based on a comparison between beach types.

## 4.5 RIP NECK WIDTH AND RIP LENGTH

The relationship between rip neck width and rip length is shown in Figure 4.16. The outliers of Ruatoria, Muriwai and Haldane Bay are again significant in their representation of beach states displaying atypical rip morphology, having a considerably longer rip length as compared with the rip width. This is due to topographic control during dissipative beach state conditions in the case of Haldane Bay, and oblique wave conditions for Ruatoria and Muriwai Beach. Muriwai is also distinguished as it is in a longshore bar and trough state. An $R^2$ value of 0.45 is gained for the total data set, with an improved value of 0.51 when the outliers are removed (Figure 4.17). Both relationships have a p-value of $<0.01$. There are no significant scaling relationships obtained based on wave climate (Figure 4.18) with $R^2$ values of

0.41 and 0.53 for ECS and WCS respectively. Scaling relationships between beach types are also minimal (Figure 4.19), with a major deviation between the lines of best fit only occurring with beaches in a TBR state due to the effect of the outliers of Ruatoria and Haldane Bay. $R^2$ values were 0.54 for RBB beaches, and 0.66 for TBR beaches.

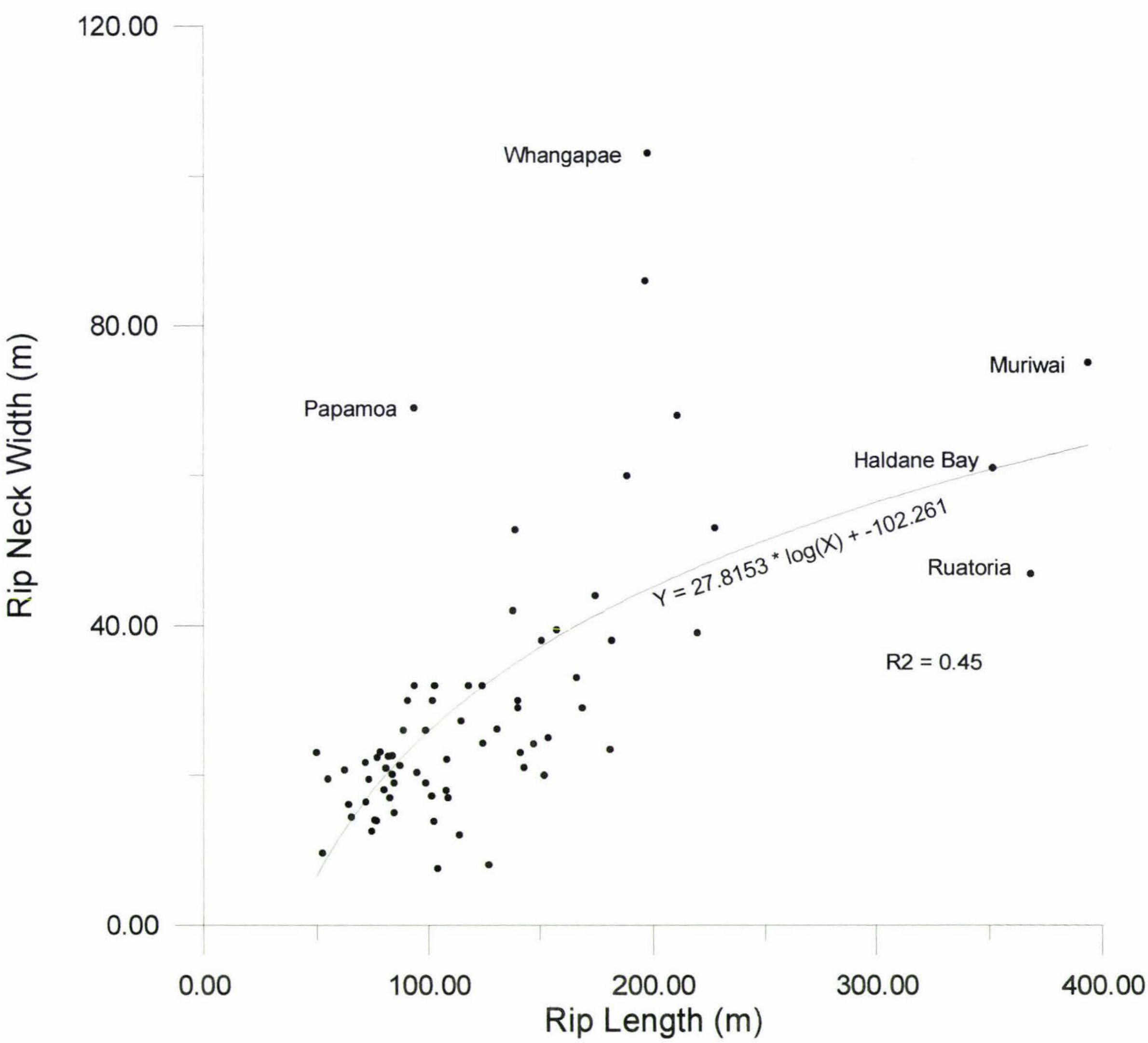


Figure 4.16 The relationship between rip neck width and rip length, showing significant outliers.

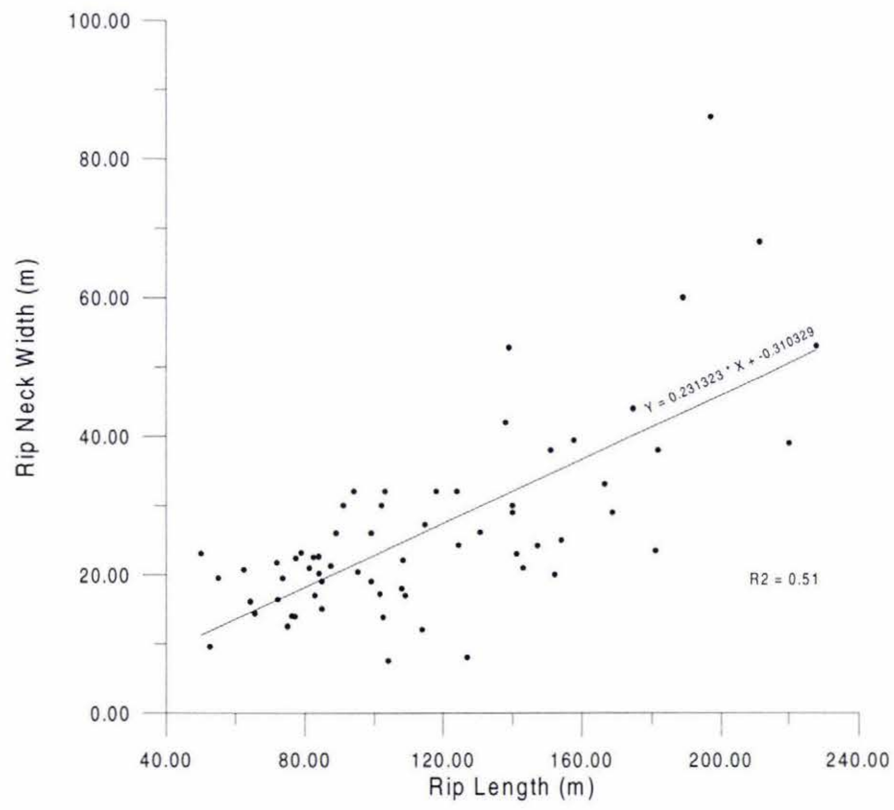


Figure 4.17 The relationship between rip neck width and rip length with removal of significant outliers.

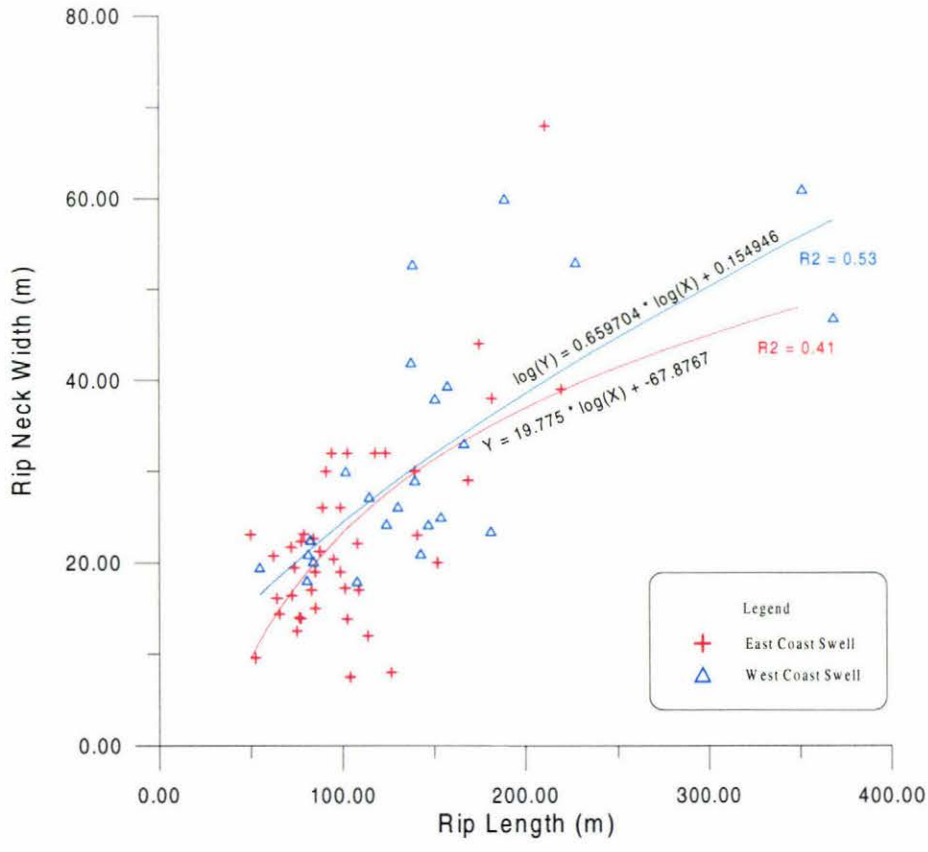


Figure 4.18 The relationship between rip neck width and rip length based on a comparison between regional wave climates.

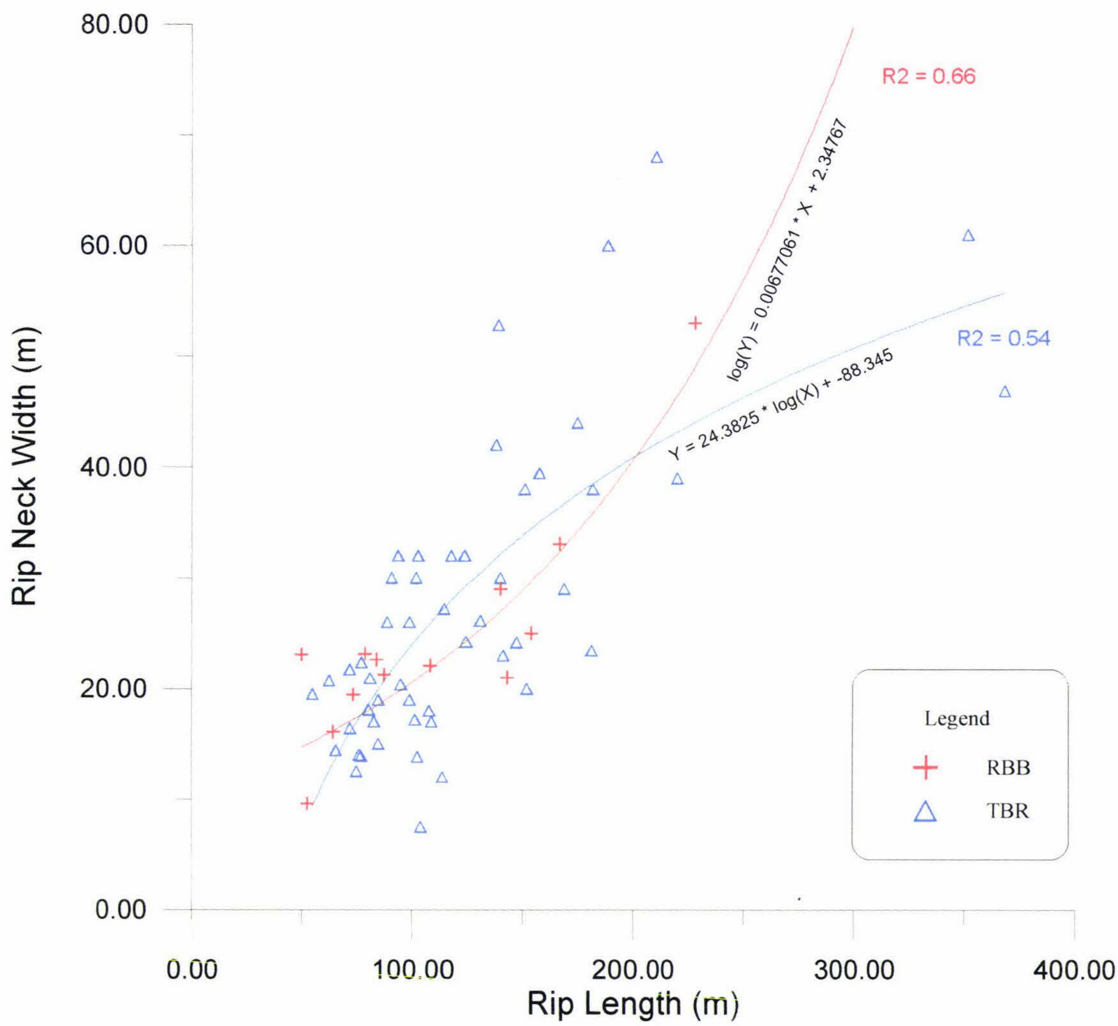


Figure 4.19 The relationship between rip neck width and rip length, based on a comparison between beach types.

## 4.6 SEDIMENT CHARACTERISTICS

In this section, rip spacing is compared with sediment size and sediment fall velocity. Data on sediment size was not available for a large proportion of beaches in this investigation, thus resulting in a data set of only 46 beaches.

### 4.6.1 Rip Spacing and Sediment Size

The initial relationship between rip spacing and sediment size is extremely poor (Figure 4.20), with an $R^2$ value of just 0.07 and a p-value of 0.067. There are seven distinct outliers that are labelled on this graph. Of particular note are the beaches of

Piha, North Piha, Ohope, Waihi Beach and Akaroa, which are characterised by a relatively fine sediment grain size but small rip spacings. It may be that on the particular day of aerial photography, these beaches were affected to varying degrees by the end effects of headlands present. Martens *et al.* (in press, citied in Short, 1999) found that for embayed beaches, as wave height increases and shoreline length decreases, beaches become increasingly modified by end effects. Therefore, topographical controls on rip formation and persistence may provide a possible explanation with regard to the significant outlier status of these particular beaches.

$R^2$ values are improved greatly once the outliers are removed, with values of 0.60 for the graphic mean, and 0.61 for the moment mean (Figure 4.21). Both equations have p-values of $<0.01$, indicating a statistically significant relationship. The relationships are log-linear, with rip spacing increasing exponentially as sediment size decreases. Values for both moment mean and graphic mean are shown, indicating the high similarity between these values. In further analysis moment mean values will be used.

The trend shown in Figure 4.21 indicates that as sediment size decreases rip spacing increases. This phenomenon has been noted throughout the relevant literature (e.g. Wright *et al.*, 1985; Short, 1985). There is a slight relationship evident in Figure 4.22 between wave climates, with slightly larger rip spacings for WCS beaches as compared with ECS beaches with similar sediment sizes. Regression coefficients for WCS and ECS are 0.47 and 0.44 respectively. A similar relationship occurs between TBR and RBB states, with TBR beaches having somewhat larger rip spacings, as shown in Figure 4.23. Regression coefficients based on beach type are somewhat higher than those gained for regional wave climate, with a value of 0.57 for TBR beaches and 0.55 for RBB beaches.

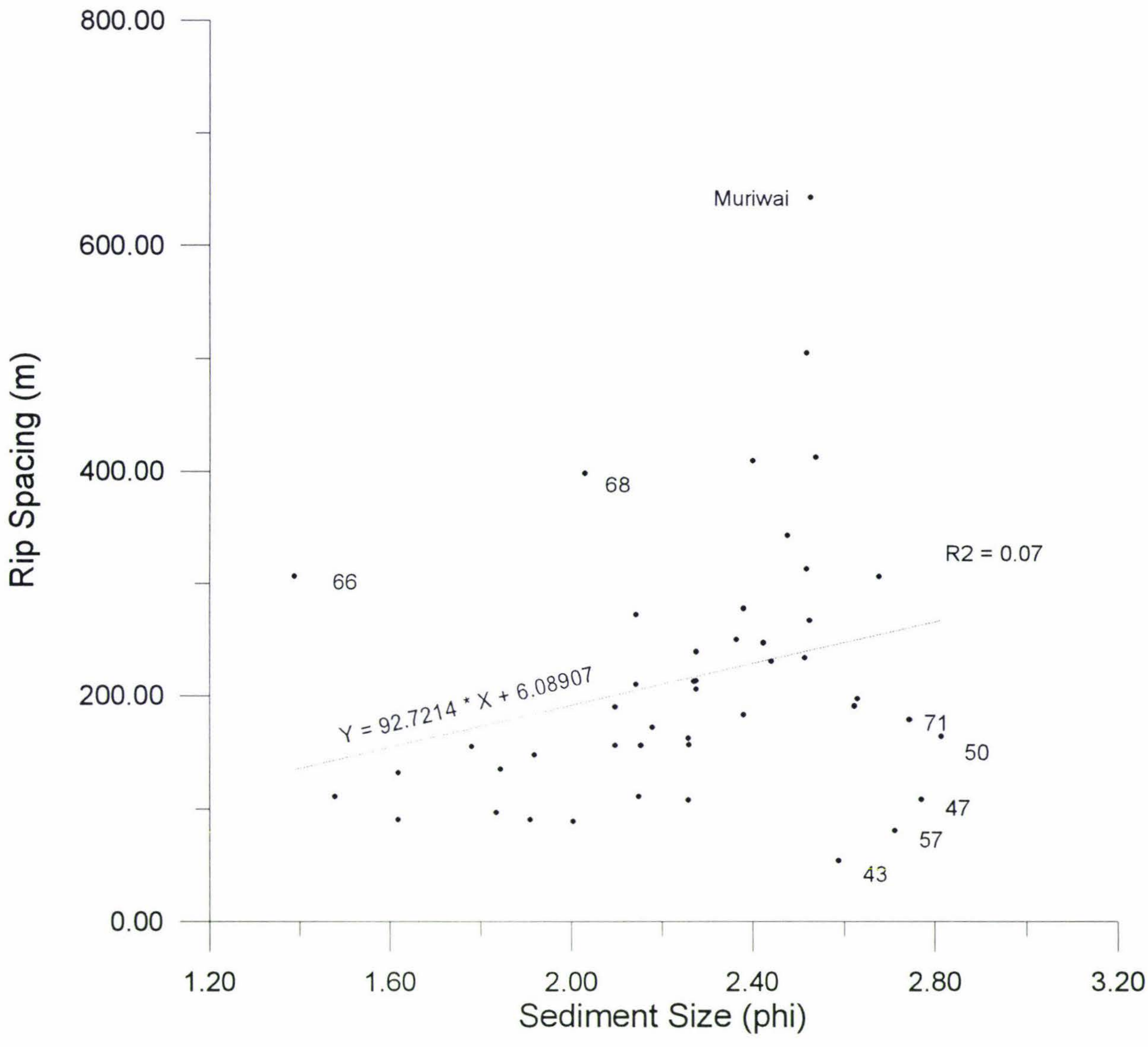


Figure 4.20 The relationship between rip spacing and sediment size, using the graphic mean for each beach. Significant outliers are: (66) Ocean Beach; (68) Mangawhai Heads; (71) Ohope; (50) Waihi Beach; (47) North Piha; (57) Akaroa; (43) Piha.

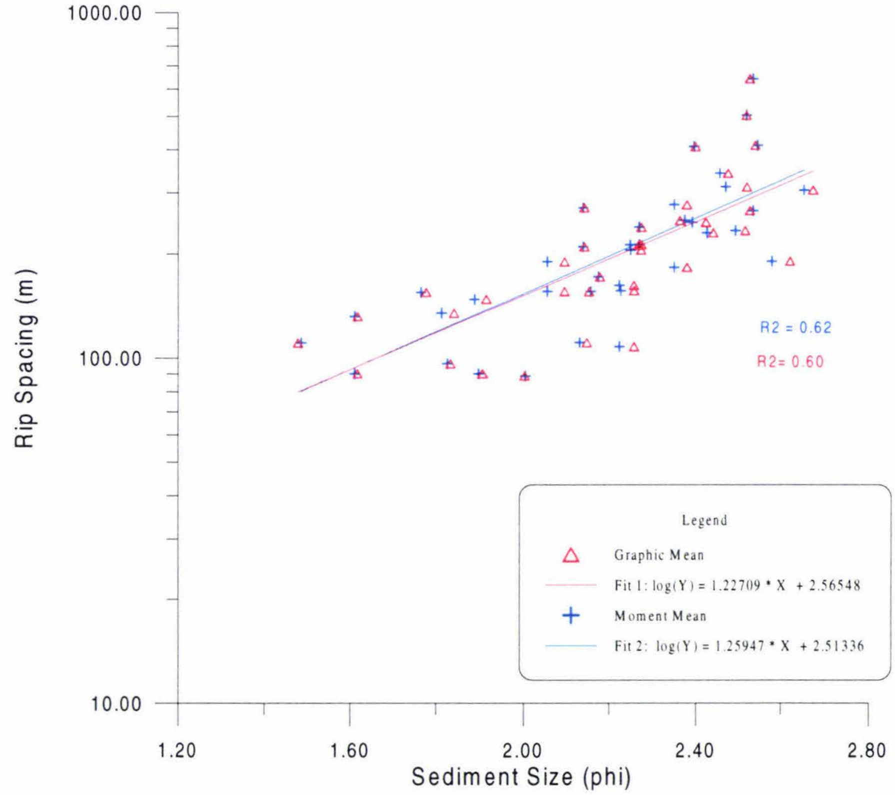


Figure 4.21 The log-linear relationship between rip spacing and sediment size after the removal of significant outliers. Both the graphic mean and moment mean are shown.

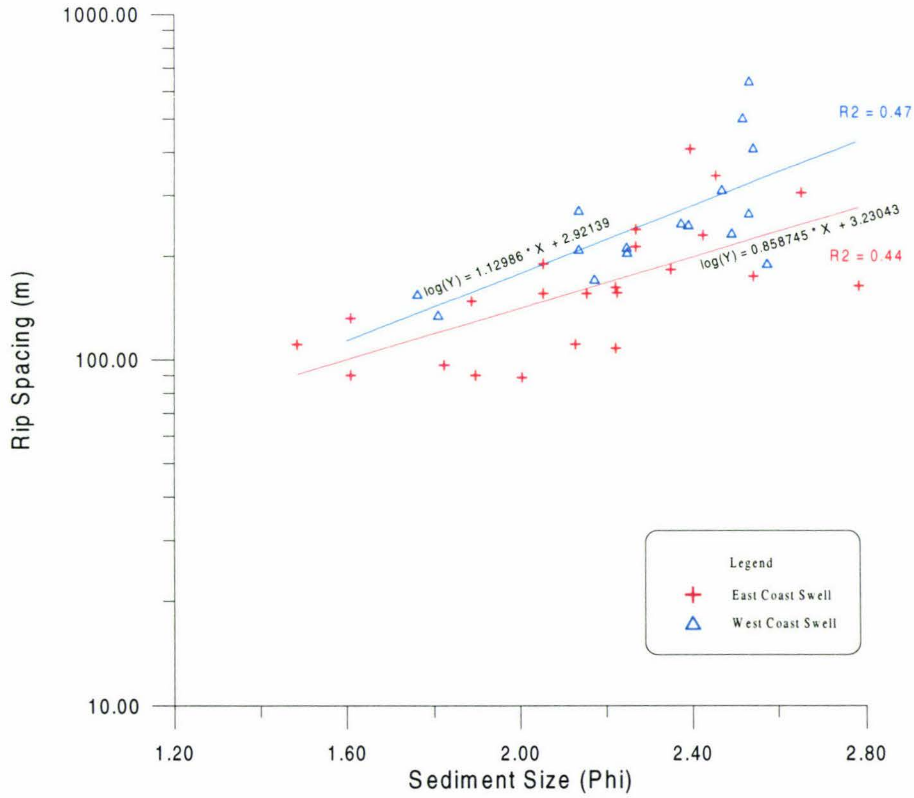


Figure 4.22 The log-linear relationship between rip spacing and sediment size (moment mean), after the removal of significant outliers, based on regional wave climates.

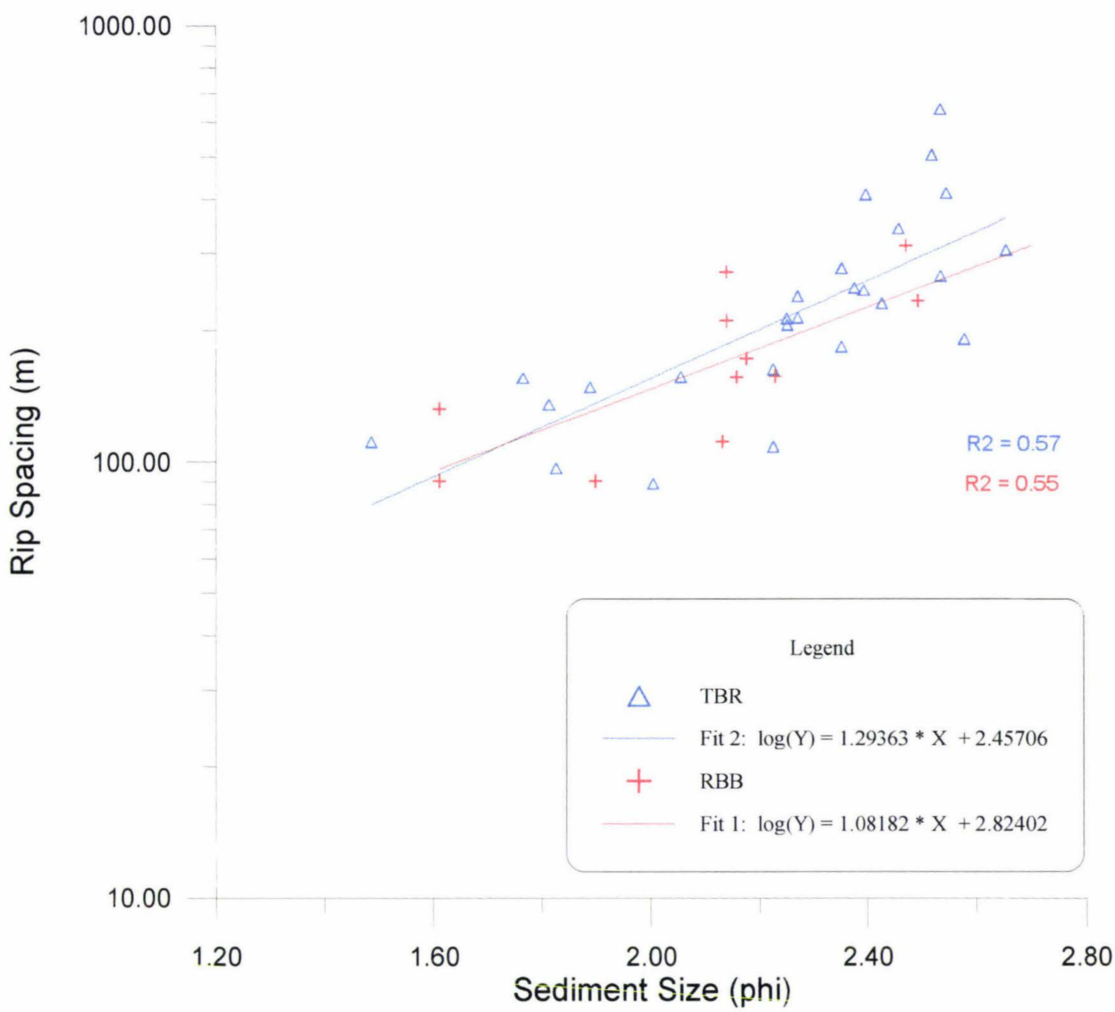


Figure 4.23 The log-linear relationship between rip spacing and sediment size (moment mean), based on a comparison between beach types.

### 4.6.2 Rip spacing and sediment fall velocity

Figure 4.24 shows that there is no statistically significant relationship between rip spacing and sediment fall velocity ($w_s$) as the p-value of 0.296 indicates there is no statistical significance, and the regression coefficient value is 0.04. This is surprising, since Short (1985) found relationships based on this parameter, in the form of the dimensionless fall velocity, Ω (Gourley, 1976) where:

$$\Omega = H_b/Tw_s$$

where $H_b$ is significant wave height, T is significant wave period, and $w_s$ is the sediment fall velocity, while Huntley and Short (1992) suggest a rip spacing predictor based on the equation:

$$Y_r = H_b^{3/2}/w_s^2.$$

There is no trend apparent when sediment fall velocity is compared to wave climate (Figure 4.25) or beach type (Figure 4.26). The later outcome is fairly predictable. The sediment fall velocity parameter is an integral component of the dimensionless fall velocity parameter, which is used to predict beach state (Wright and Short, 1984). However Wright *et al.* (1985) state that although Ω is reasonably good at predicting the extreme states (which do not generally exhibit rip currents) it is a poor predictor for intermediate states that can persist through a relatively wide range of Ω values.

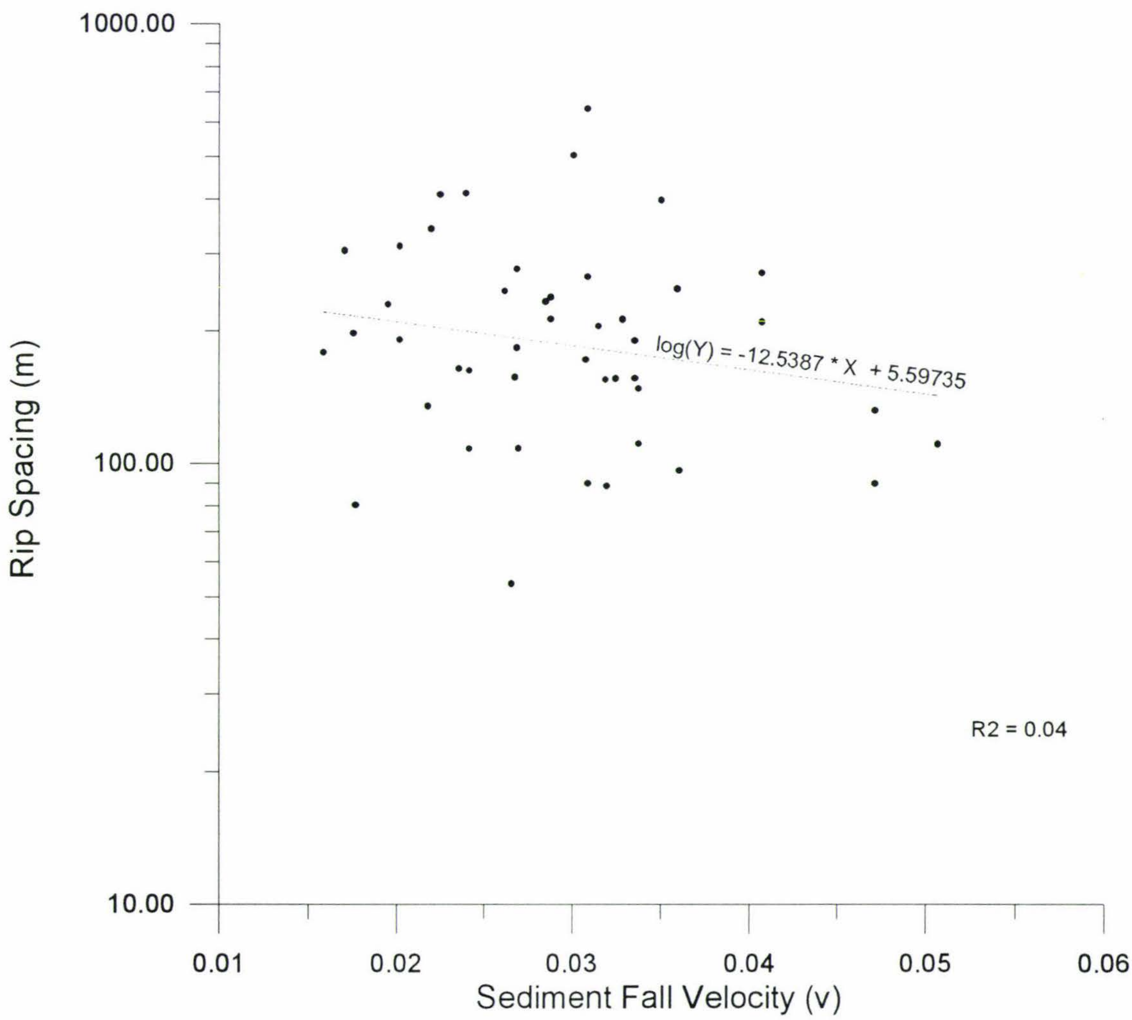


Figure 4.24 The relationship between rip spacing and sediment fall velocity.

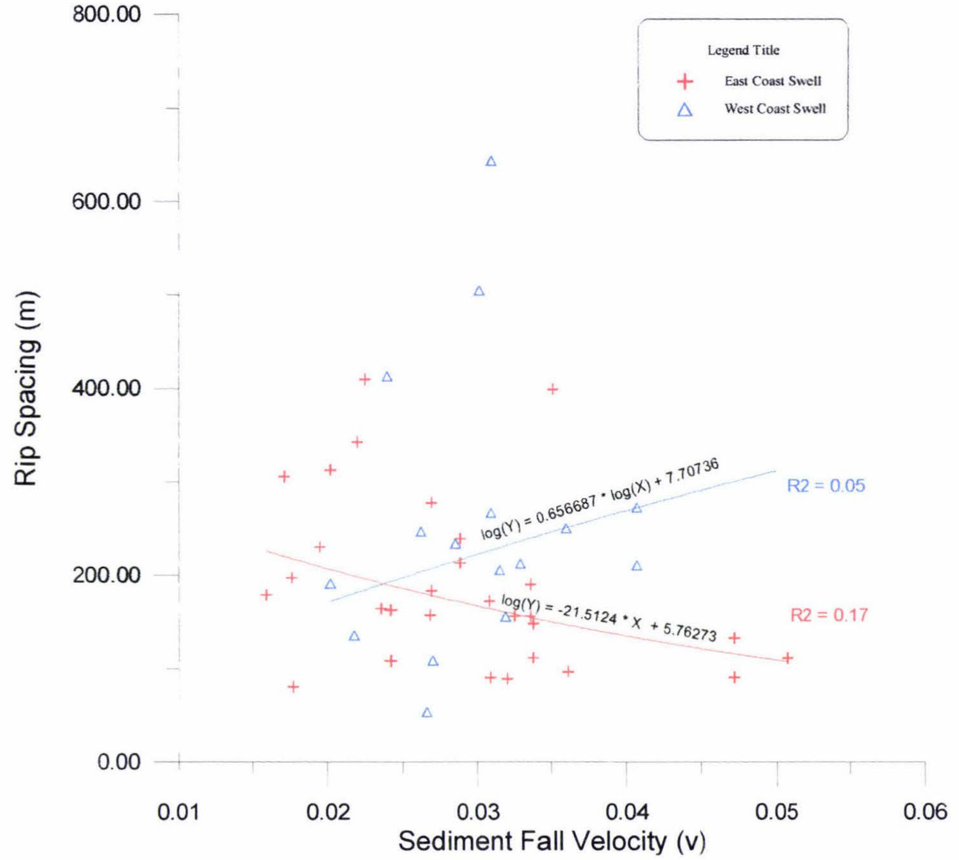


Figure 4.25 The relationship between rip spacing and sediment fall velocity, based on a comparison between regional wave climates.

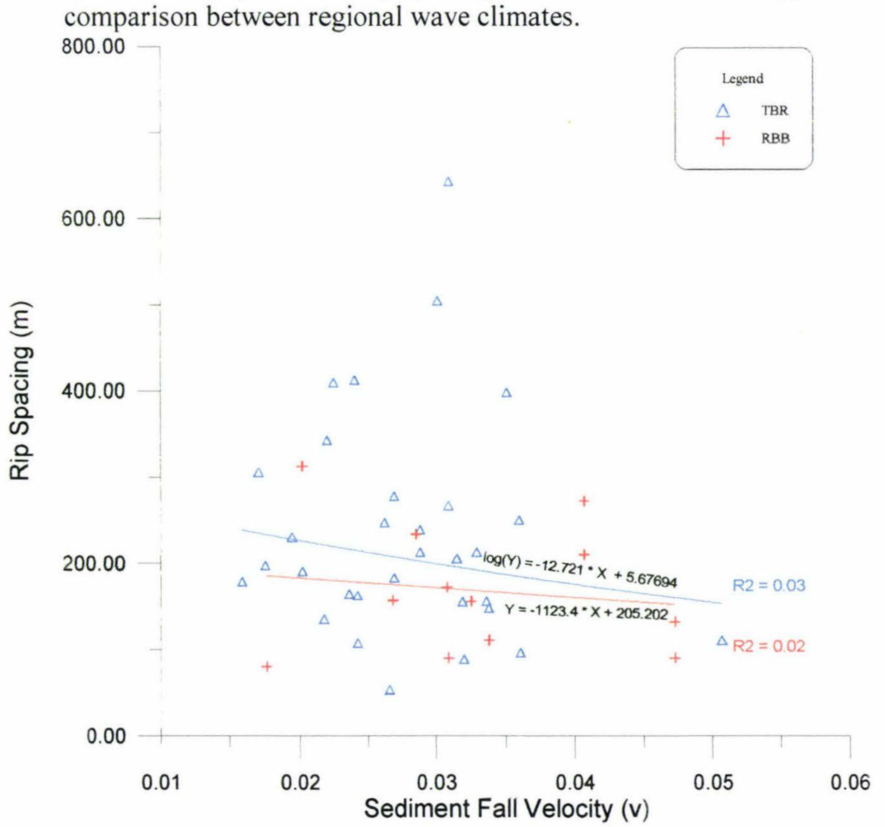


Figure 4.26 The relationship between rip spacing and sediment fall velocity based on a comparison with beach types.

### 4.6.3 Sediment Size and Sediment Fall Velocity

An interesting outcome found in this investigation is the inconsistency between the results for sediment size and sediment fall velocity. Sediment size and sediment fall velocity measurements for each beach were taken from the same sediment sample. However, the outcomes for each parameter are very different, with a reasonable relationship found between rip spacing and sediment size, but no relationship found between rip spacing and sediment fall velocity. Short (1985) and Wright *et al.* (1985) found that both values for grain diameter and sediment fall velocity decrease as beaches go from a reflective to a dissipative state, while rip spacing increases. Therefore, it would be expected that both outcomes would be relatively similar. An investigation into the relationship between the sediment size and sediment fall velocity of beaches in this data set was carried out to establish if the sediment fall velocity measurements were correct.

Figure 4.27 shows the comparison between the sediment size and sediment fall velocity data. The results are particularly interesting, as they indicate a moderate relationship with an $R^2$ value of 0.56 and a p-value of $<0.01$, demonstrating that the sediment fall velocity measurements are likely to be correct.

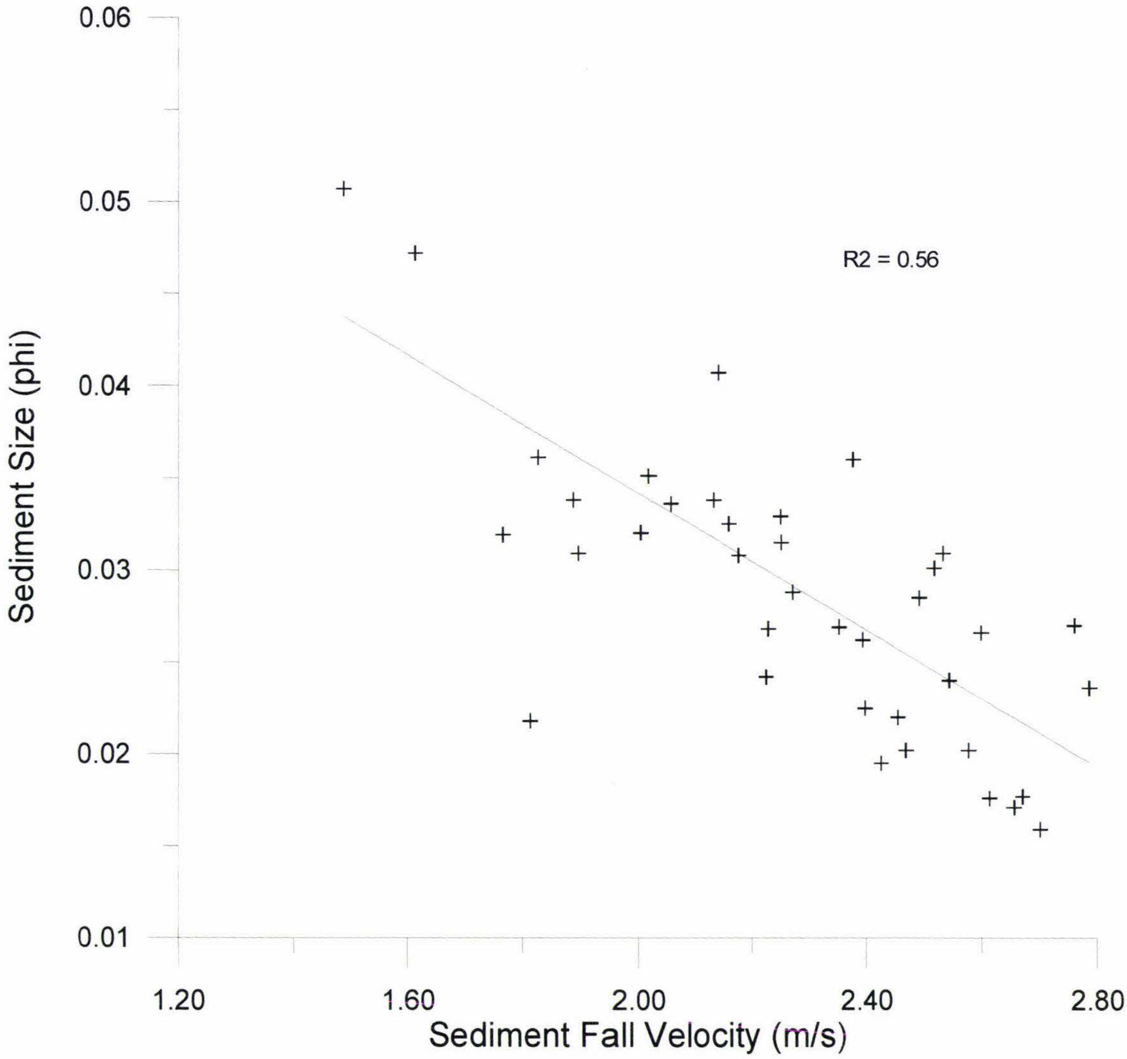


Figure 4.27 The relationship between sediment size and sediment fall velocity.

An important aspect of the New Zealand coastline is the differences between the sediment composition of the east and west coasts. The west coast of the North Island is characterised by titanomagnetite sands, which are denser and generally finer than the quartzo-feldspathic sands that are characteristic of east coast beaches. Therefore, a comparison of the sediment size, sediment fall velocity relationship based on regional wave climate was carried out, with the outcome displayed in Figure 4.28. The results of this particular investigation are especially interesting due to the differences between ECS and WCS relationships. ECS beaches had a strong relationship, with an $R^2$ value of 0.89 and a p-value of <0.01. In contrast, WCS beaches had an extremely weak relationship with an $R^2$ value of just 0.10, and a p-value of 0.24 indicating a relationship that is not statistically significant. However, two noteworthy outliers are present in the WCS data, Punakaiki Beach and Tauranga Bay, the only examples of

WCS beaches from the South Island in this dataset. Their removal greatly improves the $R^2$ value for WCS beaches (Figure 4.29), to 0.66 with a p-value of <0.01, although this is still weaker than the value obtained for ECS beaches.

Although a relatively good relationship between sediment size and sediment fall velocity is apparent, it does not suggest any reasons for the lack of a relationship between sediment fall velocity and rip spacing. It may be that the fine to very fine, iron-dominated sediments of the North Island west coast are exhibiting some control over beach type and therefore rip spacing.

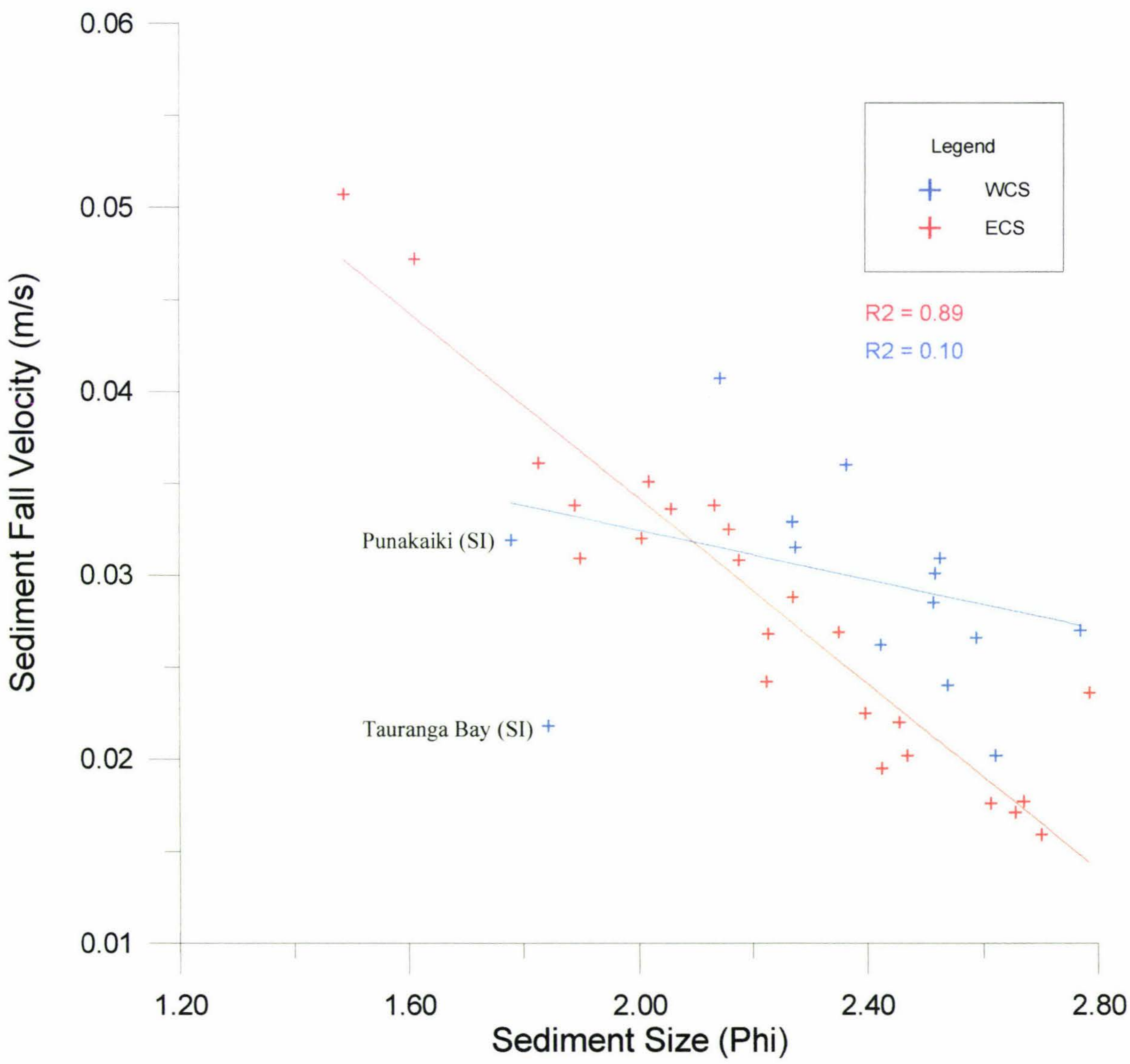


Figure 4.28 The relationship between sediment size and sediment fall velocity based on a comparison between wave climates. Of note are the outliers of Tauranga Bay and Punakaiki.

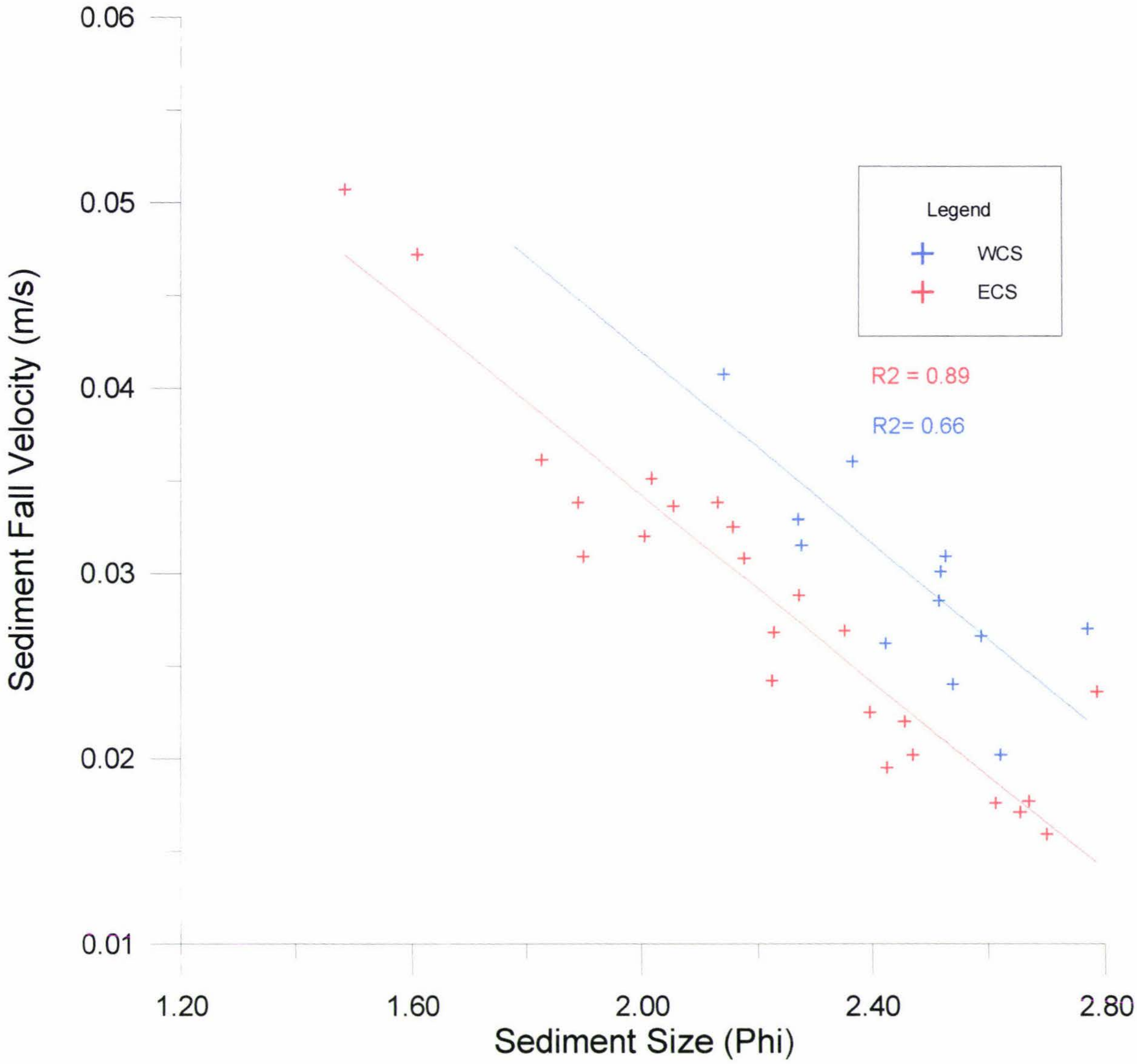


Figure 4.29 The relationship between sediment size and sediment fall velocity based on wave climate, after the removal of the two significant outliers noted in Figure 4.28.

## 4.7 WAVE CLIMATE

In this section rip spacings are compared with the wave climate parameters of significant wave height ($H_b$) and significant wave period (T). A large proportion of beaches did not have any wave climate data available for them. This resulted in a reduction in both data sets, with 44 beaches examined for significant wave height and only 18 beaches examined for significant wave period.

### 4.7.1 Rip Spacing and Significant Wave Height

There is a very poor relationship between rip spacing and significant wave height, as shown in Figure 4.30. The $R^2$ value for the total data set is 0.01, with a p-value of 0.964, indicating that there is no statistically significant relationship. This outcome is vastly different to that suggested by Short (1985), Huntley and Short (1992), and Short and Brander (1999), that rip spacing should increase with increased wave height. Comparisons based on wave climate (Figure 4.31) and beach type (Figure 4.32) yield no further evidence to explain the lack of a relationship.

Noteworthy outliers include both Muriwai Beach and Rimmers Beach. The significant wave height value of 2.5 metres used for these two beaches is taken from Brander *et al.* (1999) and is the same value as used in Short and Brander's (1999) scaling relationship hypothesis. It is again suggested that this value, if correct, is an extreme value and therefore atypical of west coast beaches, as shown in Figure 4.30. Therefore the use of Muriwai Beach as a typical WCS example appears erroneous.

The suggested significant wave height values for Muriwai do not compare well with those of Piha, an adjacent beach, which has had daily wave height data collected for at least ten years and has a significant wave height value of 1.46 (O'Dea and Hesp, 2000). Therefore, this value was inserted for Muriwai and Rimmers Beach, with the results shown in Figure 4.33. However the regression value was not improved, with a value of 0.01.

Although a relationship as poor as the one gained here was not expected, it was intuitive to anticipate a rather weak relationship, due to the temporal and spatial variability of wave heights on coastlines. Significant wave height may not necessarily produce rip currents for all beaches. Without knowing the exact wave conditions at the time of aerial photography, this relationship is difficult to assess properly. Secondly, the antecedent wave conditions are an important consideration that is unknown for the data set. Finally, the quality of the wave height data is extremely variable, and may be another explanation for the extremely poor relationships found here.

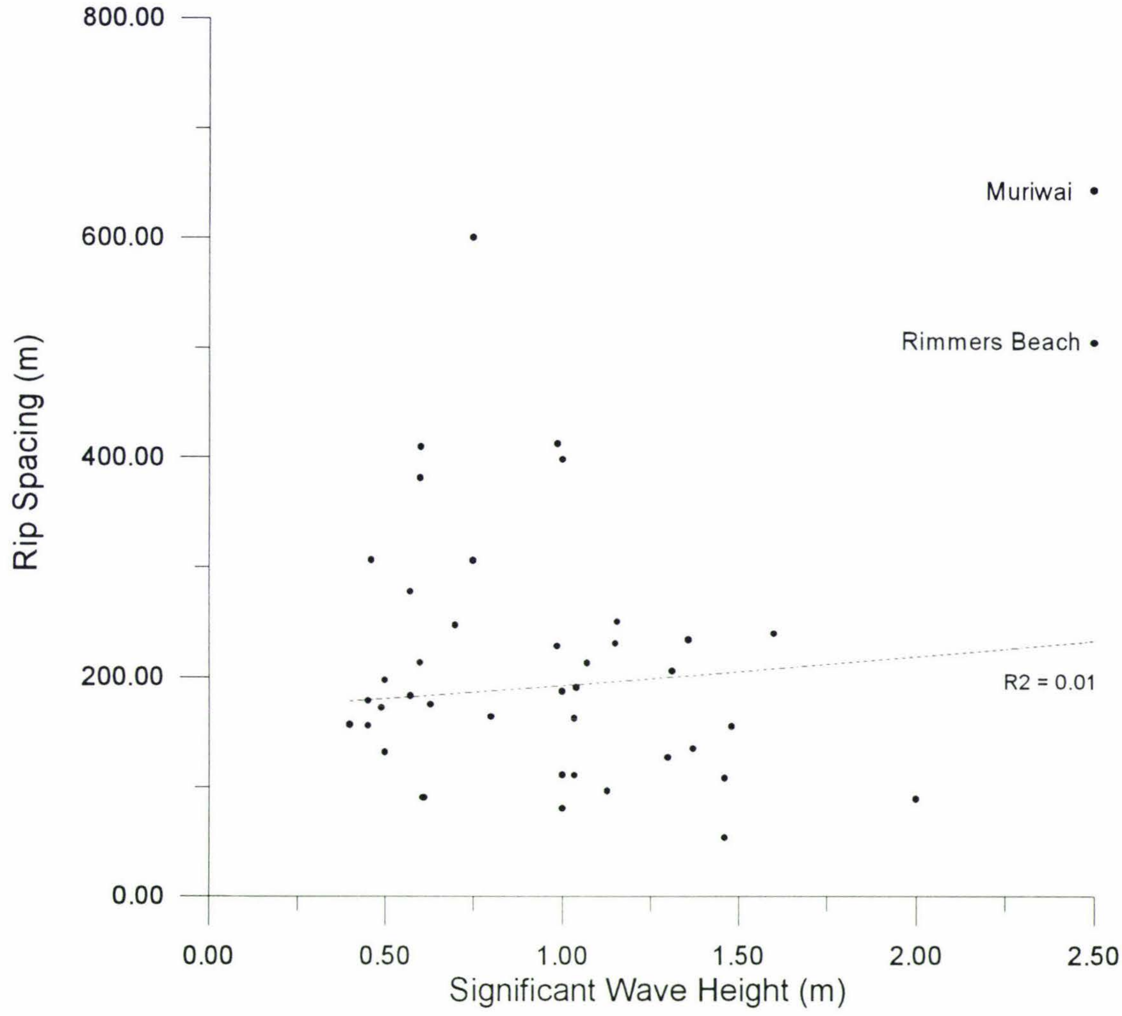


Figure 4.30 The relationship between rip spacing and significant wave height, showing the values used by Short and Brander (1999) for Muriwai and Rimmers Beach.

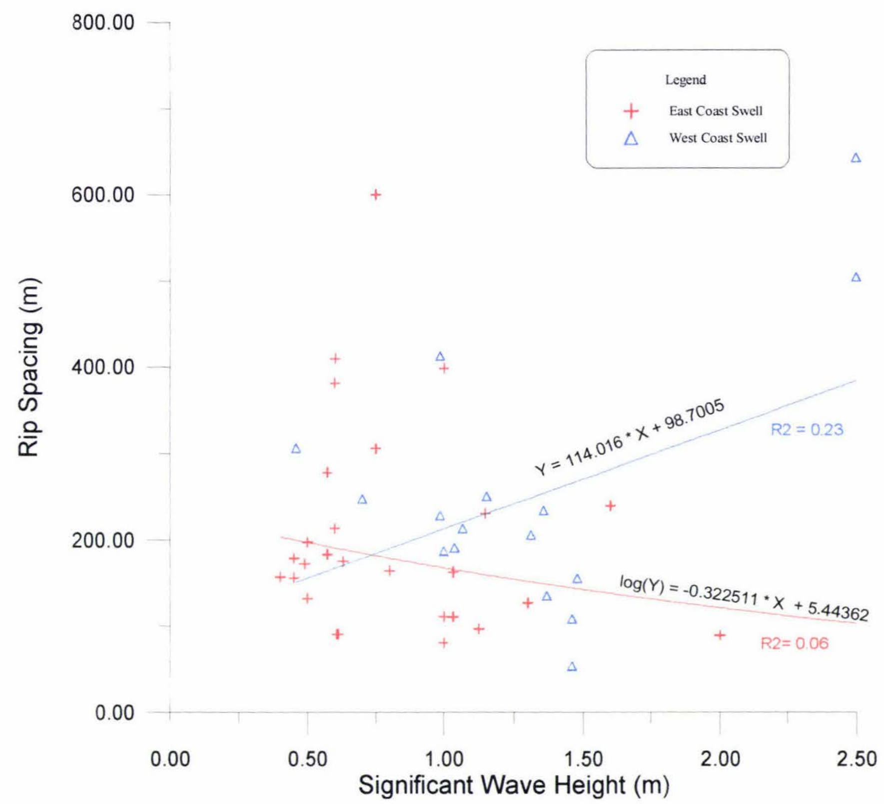


Figure 4.31 The relationship between rip spacing and significant wave height based on comparison with regional wave climates.

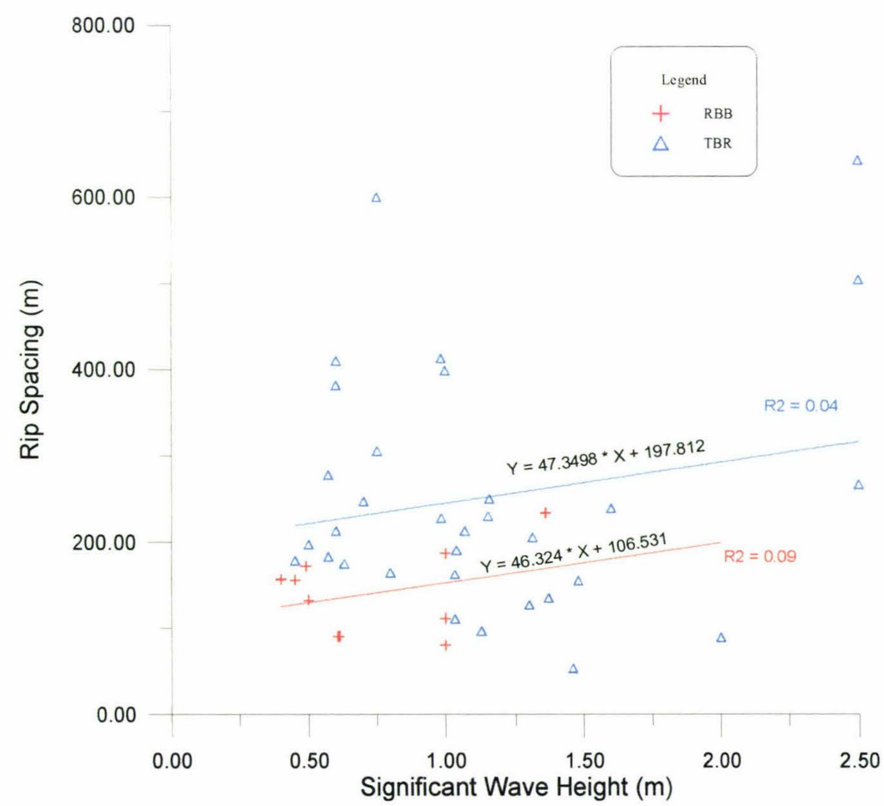


Figure 4.32 The relationship between rip spacing and significant wave height based on a comparison between beach types.

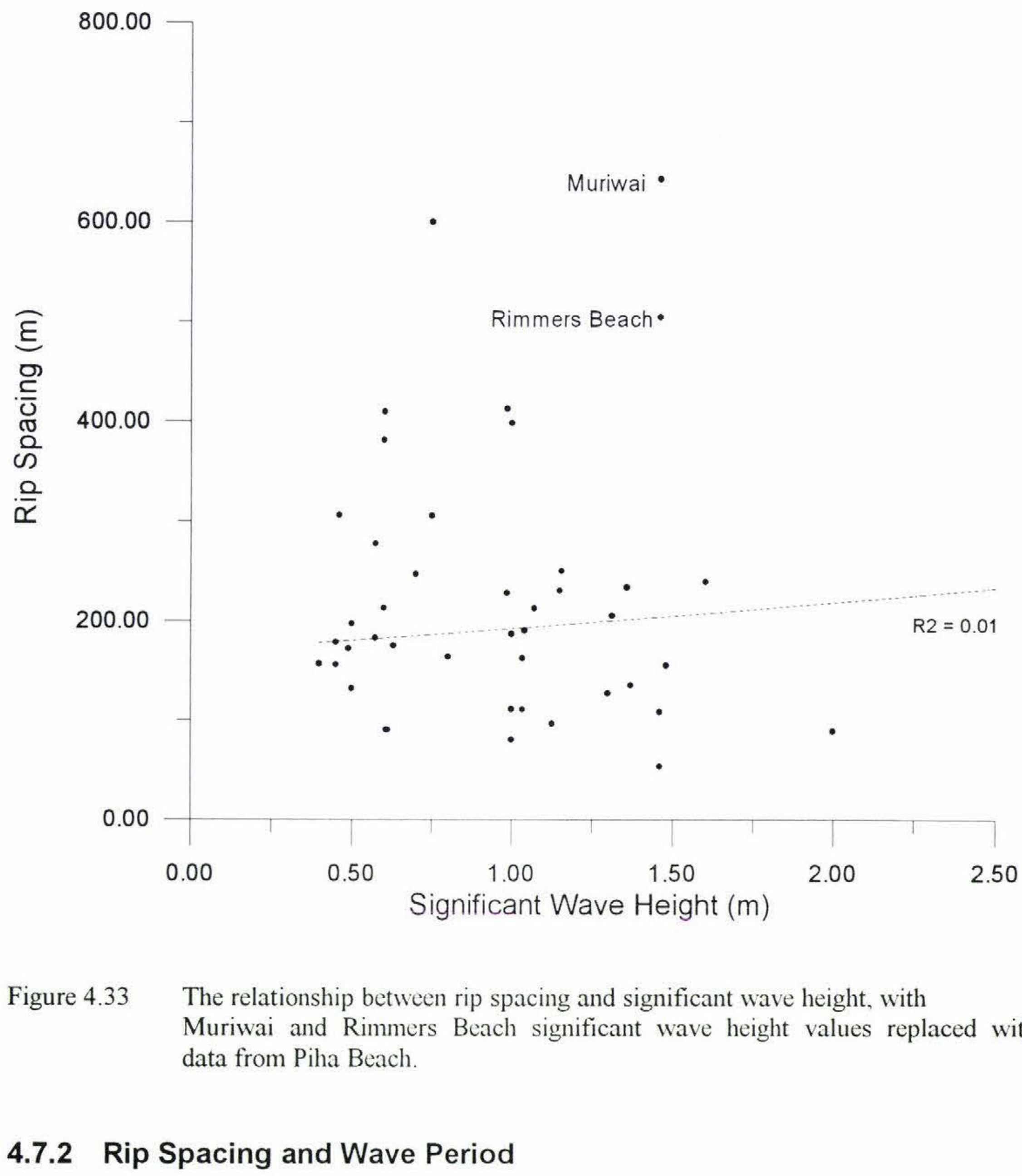


Figure 4.33 The relationship between rip spacing and significant wave height, with Muriwai and Rimmers Beach significant wave height values replaced with data from Piha Beach.

### 4.7.2 Rip Spacing and Wave Period

No relationship was found between rip spacing and wave period, with a correlation coefficient value of 0.06 and a p-value of 0.37, as shown in Figure 4.34. This result is expected because of the negligible relationship found by Huntley and Short (1992) with an $R^2$ value of just 0.1. Secondly, a weak relationship was likely to occur due to the temporal variability of wave periods. The significant wave period value for a particular beach may not be what it is experiencing at the time the aerial photograph was taken. The antecedent wave conditions, which are not present in the data, are also likely to have had an impact. Finally, the quality of the wave period data may be highly variable.

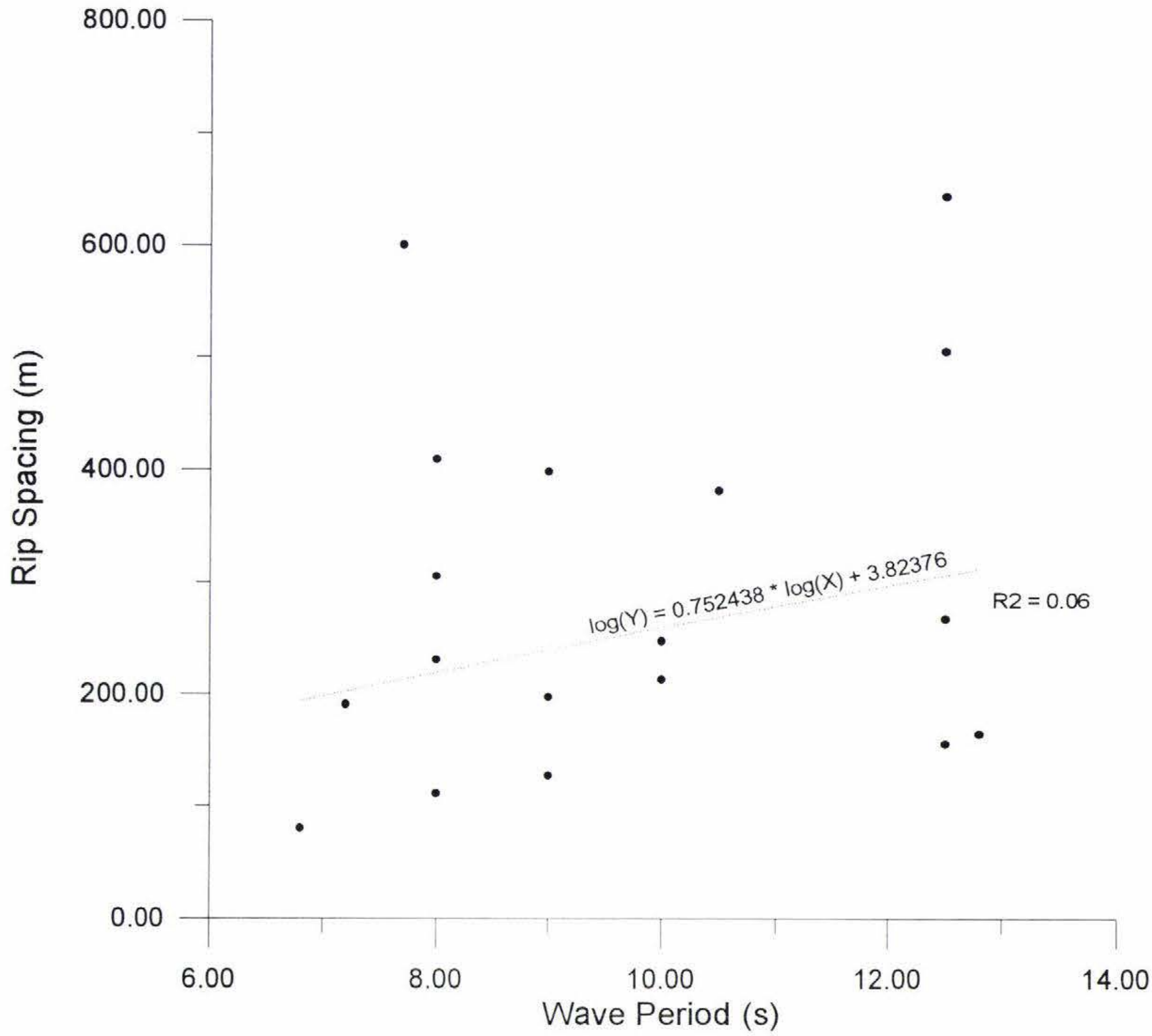


Figure 4.34 The relationship between rip spacing and significant wave period.

## 4.8 RIP SPACING PREDICTOR (HUNTLEY AND SHORT, 1992)

Huntley and Short (1992) proposed a rip spacing ($Y_r$) predictor based on the equation:

$$Y_r = H_b^{3/2}/w_s^2$$

where $H_b$ is significant wave height, and $w_s$ is the sediment fall velocity. To test this theory, significant wave height and sediment fall velocity, in the form of the Huntley and Short (1992) equation, was plotted against the actual rip spacing for each applicable beach. It is notable that neither significant wave height, nor sediment fall velocity produced any significant relationship when compared with rip spacing.

However, it would be assumed that, at least, the significant wave height data could be used to suggest modal rip spacing for particular beaches.

In spite of this, no relationship emerged, as shown in Figure 4.35. The correlation coefficient was 0.035, with a p-value of 0.75, implying that there is no statistically significant relationship. In fact, predicted rip spacing ranged from approximately 200 metres to 3500 metres, while actual rip spacings ranged from just 50 metres to 650 metres.

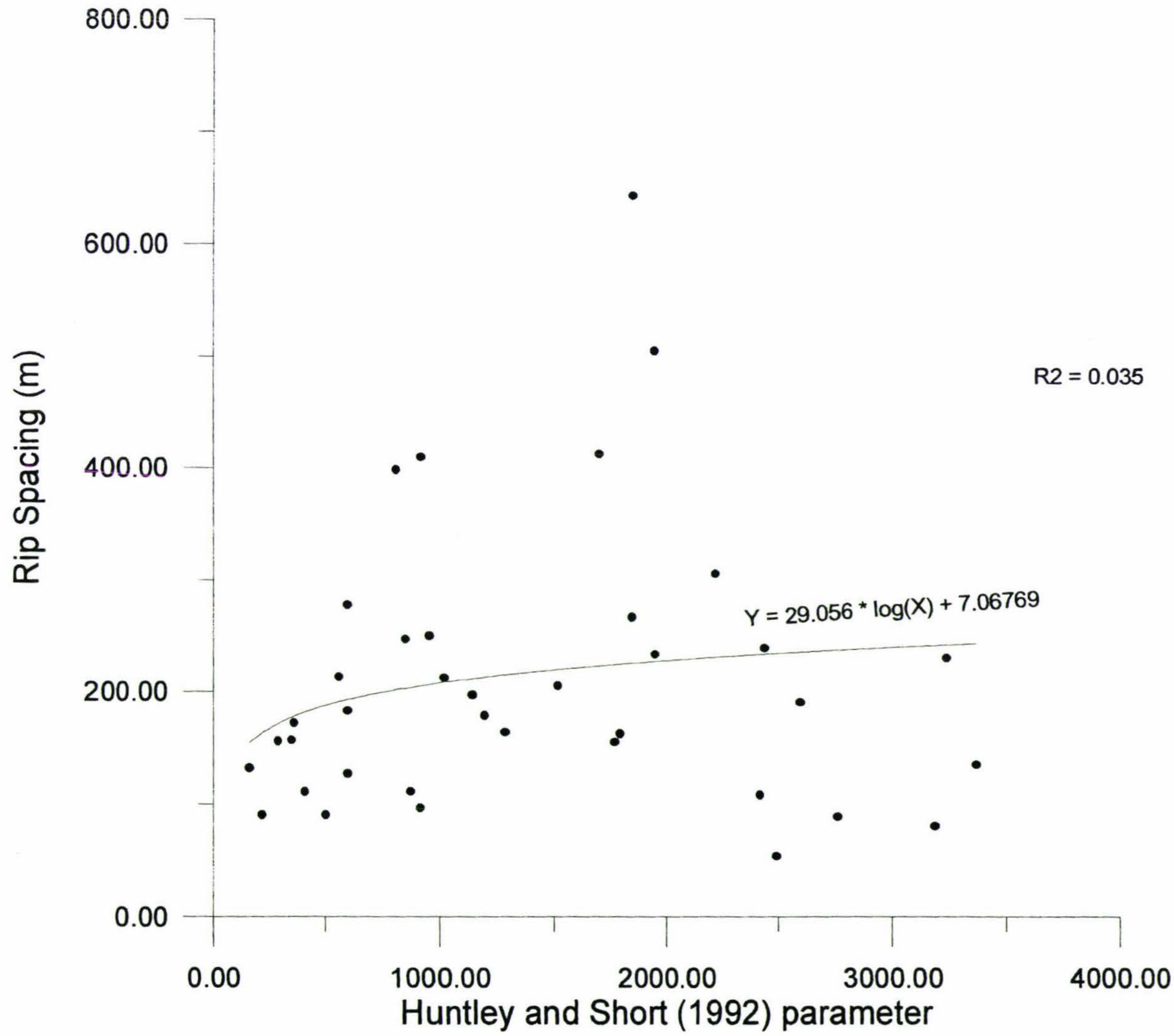


Figure 4.35 The relationship between actual rip spacings and predictions based on Huntley and Short's (1992) parameter that $Y_s = H_b^{3/2}/w_s^2$.

## 4.9 Comparison With The Dimensionless Fall Velocity Parameter

A comparison between rip spacing and the dimensionless fall velocity parameter $\Omega$ where:

$$\Omega = H_b/Tw_s$$

with $H_b$ the breaker height, T the incident wave period and $w_s$ the sediment fall velocity (Dean, 1973) is shown in Figure 4.36. A slight negative relationship is apparent, with an $R^2$ value of 0.23. The p-value is 0.15, suggesting that the relationship is approaching statistical significance. This outcome is somewhat un-anticipated, since Short (1985) and Huntley and Short (1992) demonstrated that the spacing between rips increased from reflective to dissipative state beaches. Furthermore, Short (1985) obtained an $R^2$ value of 0.85, with a regression equation of:

$$y = 81\Omega + 69.$$

This outcome suggests that either there are some problems with the quality of the data used, particularly in respect of the wave climate data, or the results shown are realistic and therefore demonstrate that when one examines a wider range of beaches, the Short (1985) and Short and Huntley (1992) conclusion is suspect.

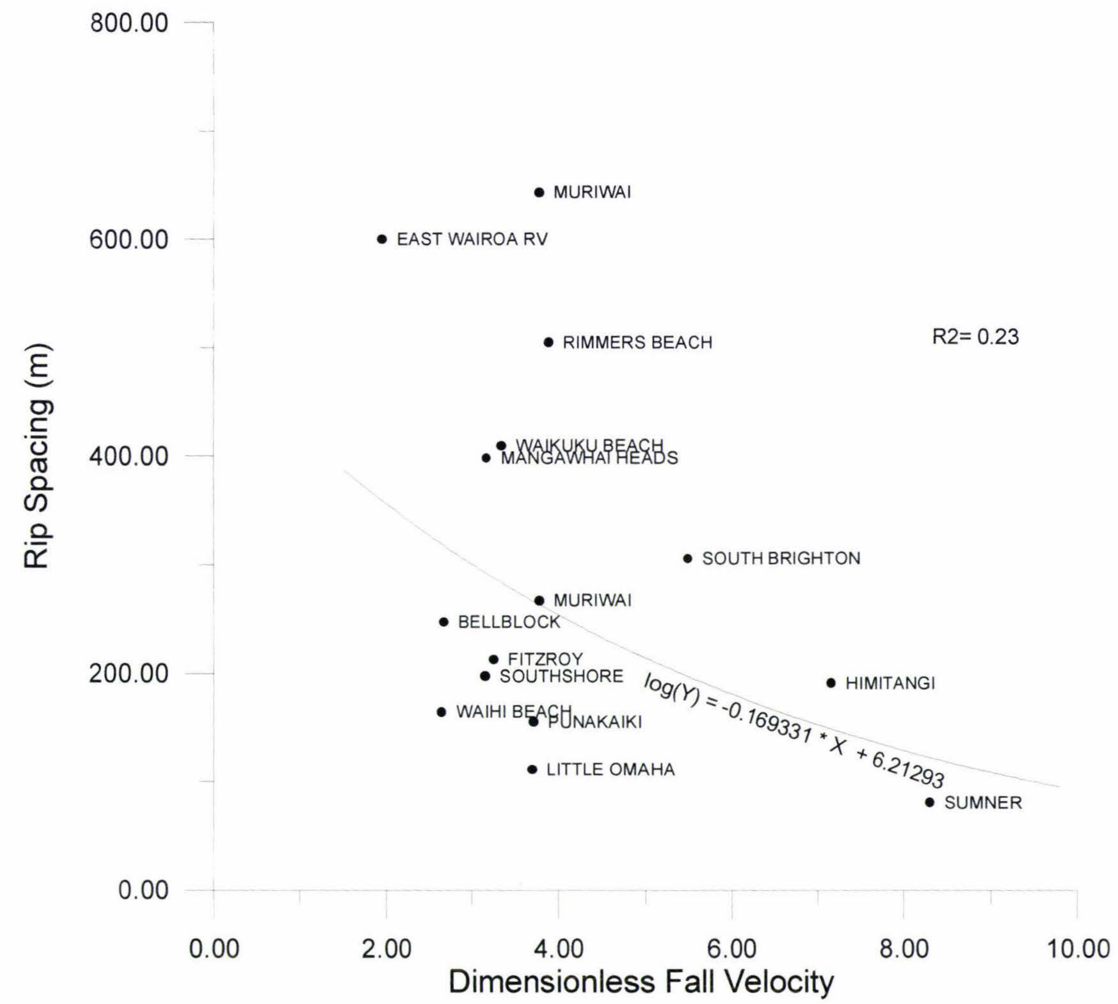


Figure 4.36 The relationship between rip spacing and the dimensionless fall velocity parameter $\Omega$.

## 4.10 RIP SPACING AND COMPARISON WITH SHORT AND BRANDER (1999)

The hypothesis put forward by Short and Brander (1999) suggests that a scaling relationship may be found between rip current spacing and is based on classifying beaches within their respective regional wave climate, as previously proposed by Davies (1980). Under this premise, New Zealand can be divided up into two of the five wave climates: West Coast Swell (WCS) for the western coastline; and East Coast Swell (ECS) for the eastern coastline (see Figure 4.1).

To test this hypothesis, rip spacing and its relationship to a wide range of parameters were evaluated based on their regional wave climate. The results from this research, summarised in Table 4.1 show that in no case is there a scaling factor between WCS and ECS beaches that is comparable to the value of 2.5 suggested by Short and Brander (1999). In fact, the scaling factors for rip spacing and associated morphological parameters between WCS and ECS beaches do not have values greater than 1.44. The mean rip spacing value for New Zealand ECS beaches is similar to Short and Brander's (1999) mean value of 211 metres for this wave climate. However, the WCS mean rip spacing found by Short and Brander (1999) is 545 metres, which is 1.89 times larger than the mean value found for New Zealand's WCS beaches.

| Parameter | NZ WCS mean | Short and Brander's WCS mean | NZ ECS mean | Short and Brander's ECS mean | NZ Scaling relationship | Short and Brander's Scaling Relationship |
|---|---|---|---|---|---|---|
| **Rip Spacing** | 289 | 545 | 200 | 211 | 1.44 | 2.58 |
| **Rip Neck Width** | 30 | | 22 | | 1.38 | |
| **Rip Length** | 154 | | 110 | | 1.41 | |
| **Surf Zone Width** | 162 | 183 | 120 | 81 | 1.35 | 2.26 |

Table 4.1 Comparison between New Zealand and Short and Brander's (1999) mean and scaling relationships for rip spacing and other rip morphometric parameters.

A second factor is the $R^2$ relationships of each wave climate group in relation to the total data set. In no case were regression coefficients significantly improved when beaches were classified into their respective wave climate.

The best illustration of the contrast between the two sets of data is shown in Figure 4.37 where a comparison is made between rip spacing and surf zone width, presenting both the New Zealand data and Short and Brander's (1999) data. The ECS and WCS examples from Short and Brander (1999) produce distinct regional variations. Their WCS beaches are characterised by surf zone widths ranging from approximately 100 to 300 metres, with rip spacings extending from 500 to 590 metres. Short and Brander's ECS beaches have a surf zone width ranging from approximately 65 metres to 90 metres, with the spacing between rips extending from approximately 150 metres to 275 metres. In contrast, the New Zealand data has far greater ranges in both rip spacing and surf zone width for both ECS and WCS.

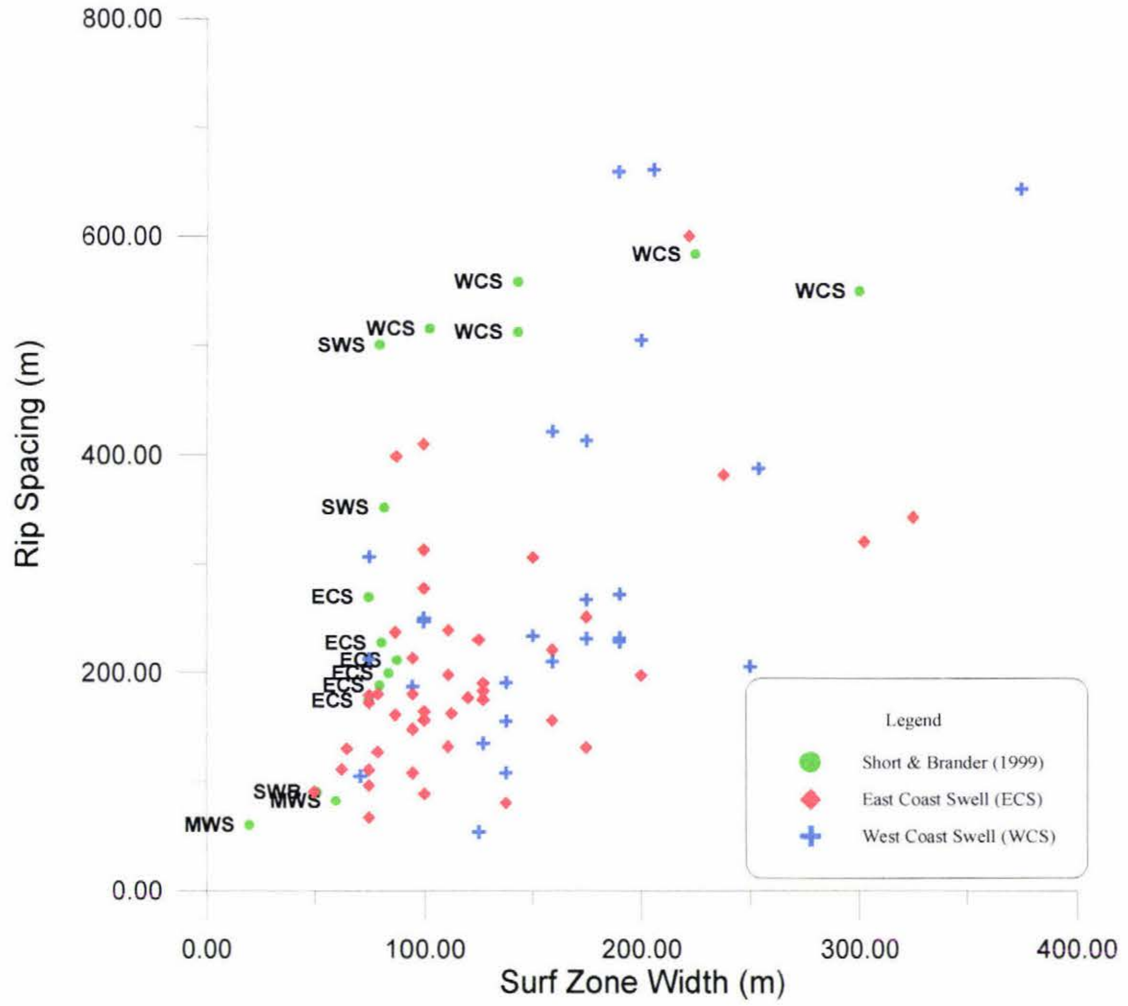


Figure 4.37 Comparison of current data showing the relationship between rip spacing and surf zone width, with that of Short and Brander (1999). All data has been classified into their respective regional wave climates: WCS (west coast swell); ECS (east coast swell); SWB (strong wind bays); SWS (strong wind seas); MWS (moderate wind seas).

### 4.10.1 Muriwai Beach

In the dataset used by Short and Brander (1999), Muriwai Beach was the only site used from New Zealand, as a 'typical' WCS beach. From this current research, it is disputable whether Muriwai is in fact a characteristic WCS beach, especially when it typically experiences strongly oblique wave conditions, producing a longshore bar and trough morphology with troughs acting as rip feeder channels. In particular, Muriwai Beach in an oblique state is considered to be a significant outlier along with Ruatoria, in a similar oblique wave condition, and Haldane Bay, which exhibited the characteristics of a classic 'megarip' (Short, 1985). These outliers are especially apparent in relationships between rip spacing and surf zone width, rip neck width and rip length, and rip spacing and rip length.

Secondly, the significant wave height value used for Muriwai Beach of 2.5 metres (Brander *et al.,* 1999) was considerably higher than any other wave height data obtained, suggesting that it may have been overestimated, and is therefore a poor value to use as the significant wave height. This is further substantiated by the fact that Piha Beach, which has eight years of daily wave height recordings, has a significant wave height of only 1.46 (O'Dea and Hesp, 2000).

These outcomes suggest that the regional swell wave classification for rip spacings proposed by Short and Brander (1999) is not appropriate in the New Zealand context. Both the east coast and west coast of New Zealand have variable wave climate and sediment conditions, which control beach type and ultimately rip spacing and morphology.

### 4.11 Proposed New Zealand Regions For Wave Climate

Following the analysis of rip spacing and its relationship to a wide range of parameters, a tentative attempt was made to identify specific regional variations in wave climate around the New Zealand coastline.

The regions were initially based on four broad regional groupings suggested by Pickrill and Mitchell (1979), which were established from 17 years of wave records from shore-based and deepwater stations around New Zealand. The divisions consist of:

- The exposed, high energy shores of the west coast;
- The exposed, high energy shores of the south coast;
- The low energy lee shore sheltered from the prevailing westerly to south-westerly winds of the east coast;
- The northern coast from North Cape to East Cape, which is characterised by a low energy system, although it can be affected by subtropical disturbances.

Further variations within the regions were established based both on observations of the New Zealand surf (Hesp and O'Dea, 1999; O'Dea and Hesp, 2000) and trends that developed within the data.

Nine regions are proposed (Figure 4.38):

- Region One is from Albatross Point to North Cape;
- Region Two is from North Cape to East Cape;
- Region Three is from East Cape to Cape Palliser;
- Region Four is from Cape Palliser to Owaka;
- Region Five is from Maniaia to Albatross Point;
- Region Six is from Cape Farwell to Puysegur Point;
- Region Seven encompasses the Wanganui, Manawatu and west Wellington coastline;
- Region Eight is from Puysegur Point to South Cape/Whiore;
- Region Nine is from South Cape to Owaka.

Regions Five, Seven, Eight and Nine are only tentatively suggested, due to the limited data obtained for these areas. Correlation coefficient values are only stated for regions with over six values. The limited amount of data severely restricts the ability to satisfactorily assess relationships based on modified regional wave climates. Although these limitations inhibit the validity of the proposed regions, general trends are to some extent evident in the following graphs. Figures 4.39, 4.40, and 4.41 display the relationships between rip spacing and surf zone width, rip length, and sediment size respectively.

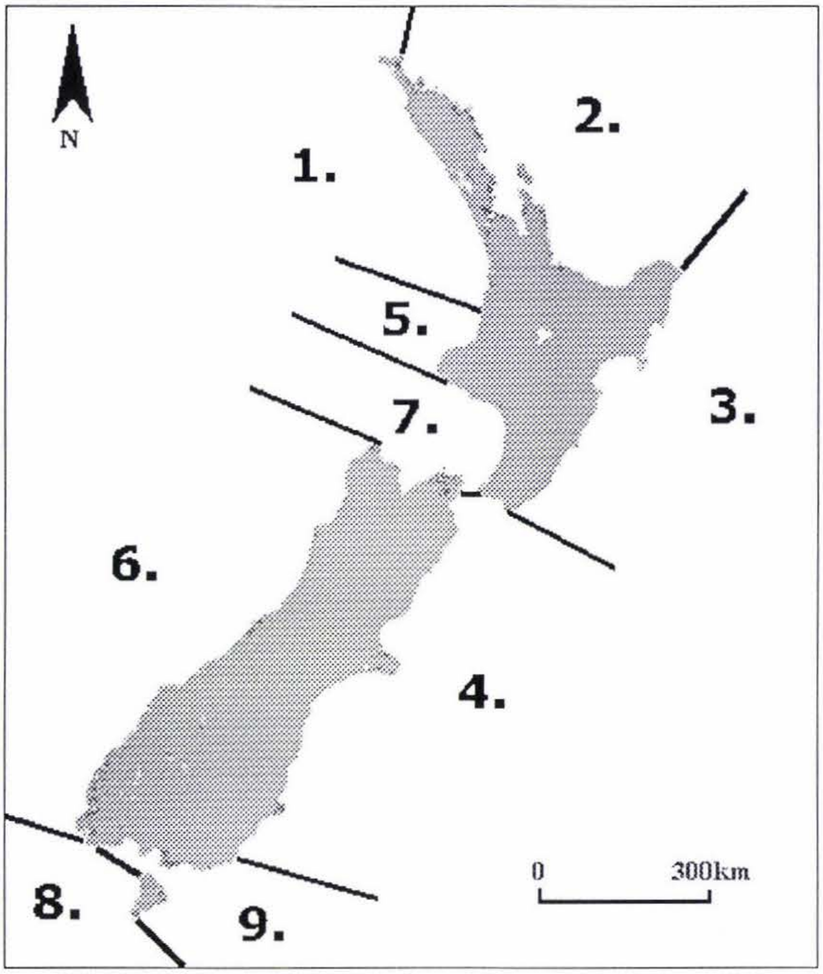


Figure 4.38 Proposed New Zealand regional wave climate classification.

The relationship between rip spacing and surf zone width is improved dramatically from the total $R^2$ value of 0.37, to 0.63 for Region Three. Other regions are not improved, however a small degree of scaling is evident between the regions. The relationships for Region One and Three are greatly improved in the comparison between rip spacing and rip length, with $R^2$ values of 0.57 and 0.60 respectively, as compared with 0.43 for the total data set. Again there is a slight scaling trend evident between regions.

The results from the analysis of the relationship between rip spacing and sediment size are particularly interesting. The data set is more limited in this comparison, however $R^2$ values are all lower than the total value of 0.61. Regions One and Three have an $R^2$ value of 0.56, while Region Two has a $R^2$ value of just 0.25. It is surprising, firstly that Region One does not have a higher correlation due to the relatively consistent sediment size along the west coast. Secondly, Region Three has a similar $R^2$ value, although there is a wide range of sediment types along this coastline. This result further validates the use of sediment size as a general predictor of rip spacing.

The regional classifications presented here are very tentative, and are suggested with caution, due to the relatively small data set used. However the ability to define more localised variations in rip spacing and associated parameters suggests that the use of globally based, regional wave climate regimes, as a foundation for rip spacing classification, is too simplistic for the New Zealand context.

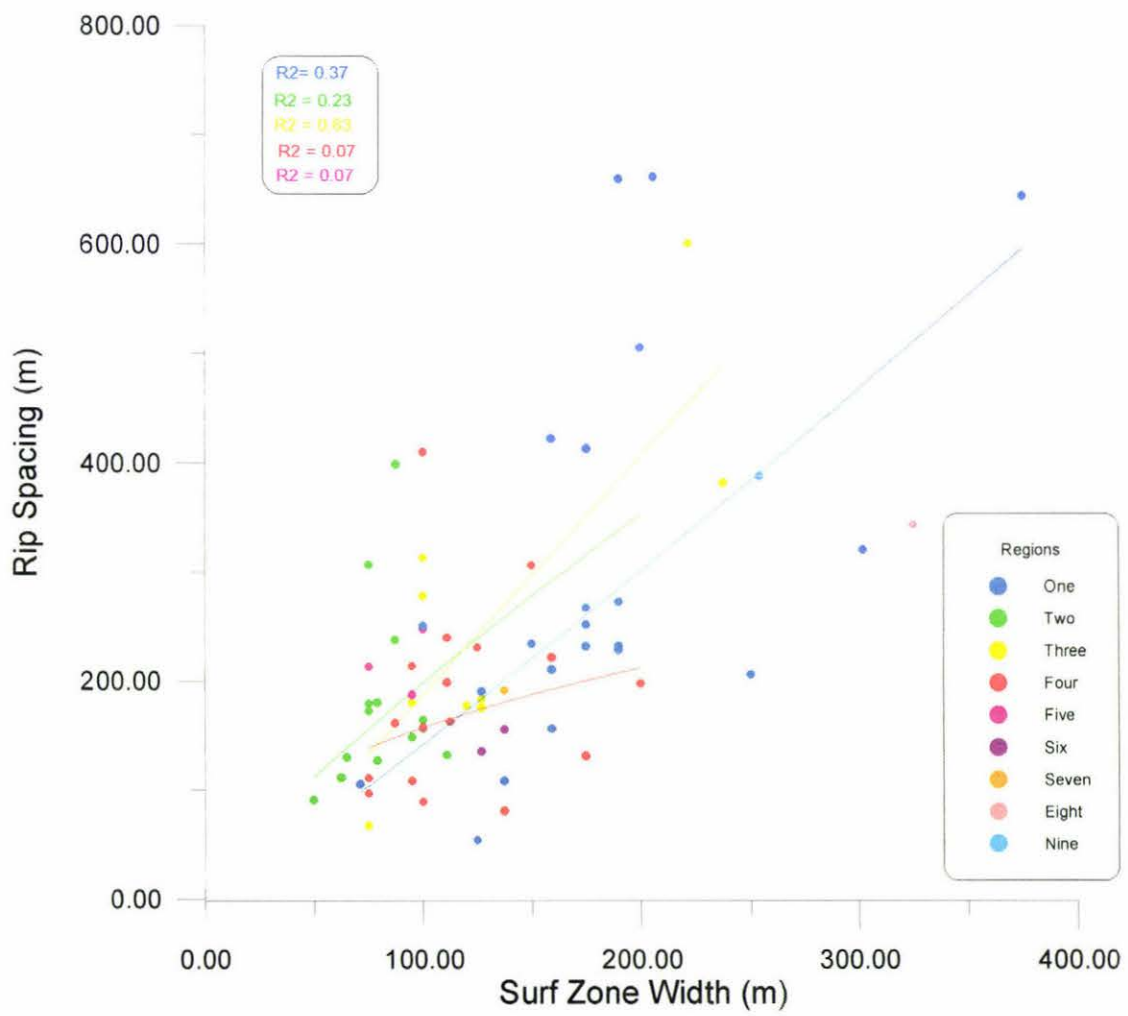


Figure 4.39 The relationship between rip spacing and surf zone width, showing the variations between proposed regions.

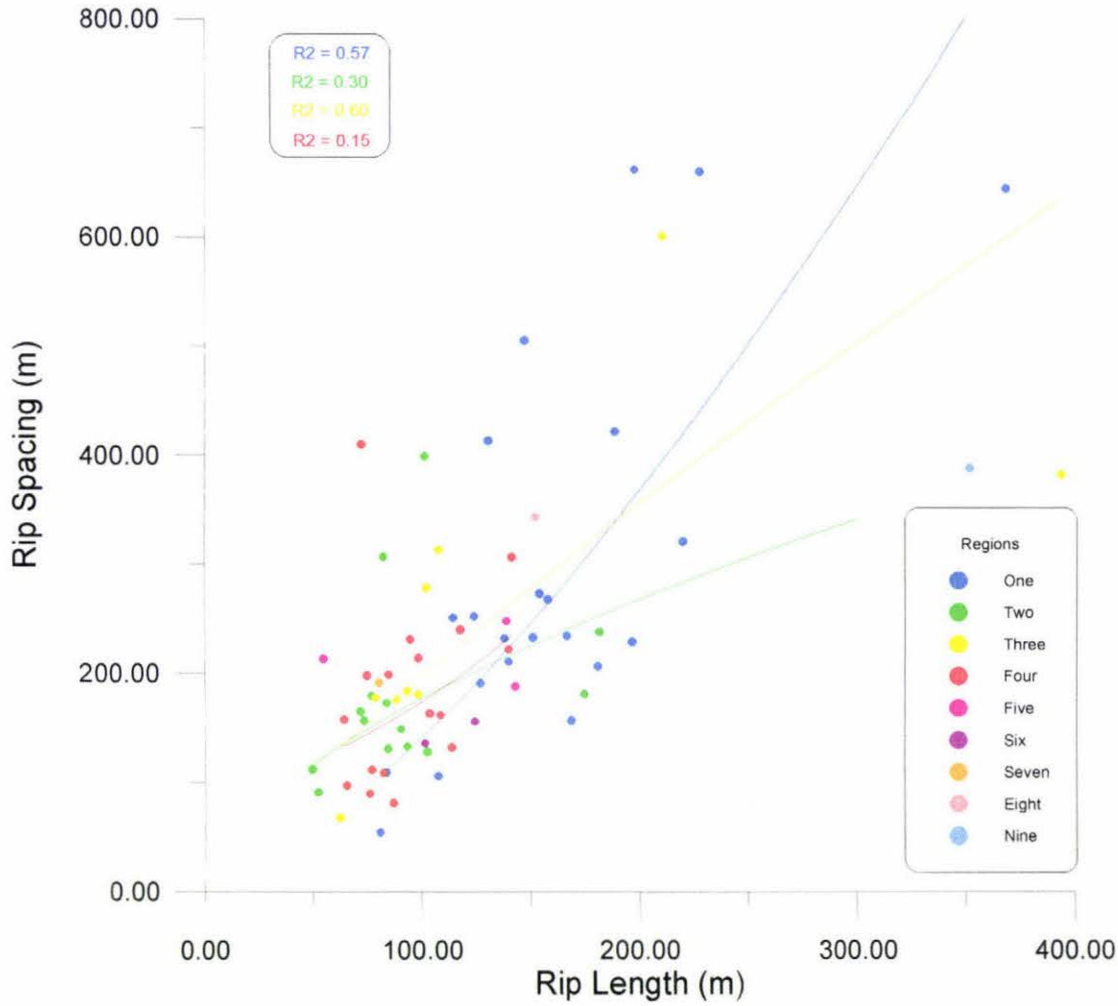


Figure 4.40 The relationship between rip spacing and rip length, showing the variations between proposed regions.

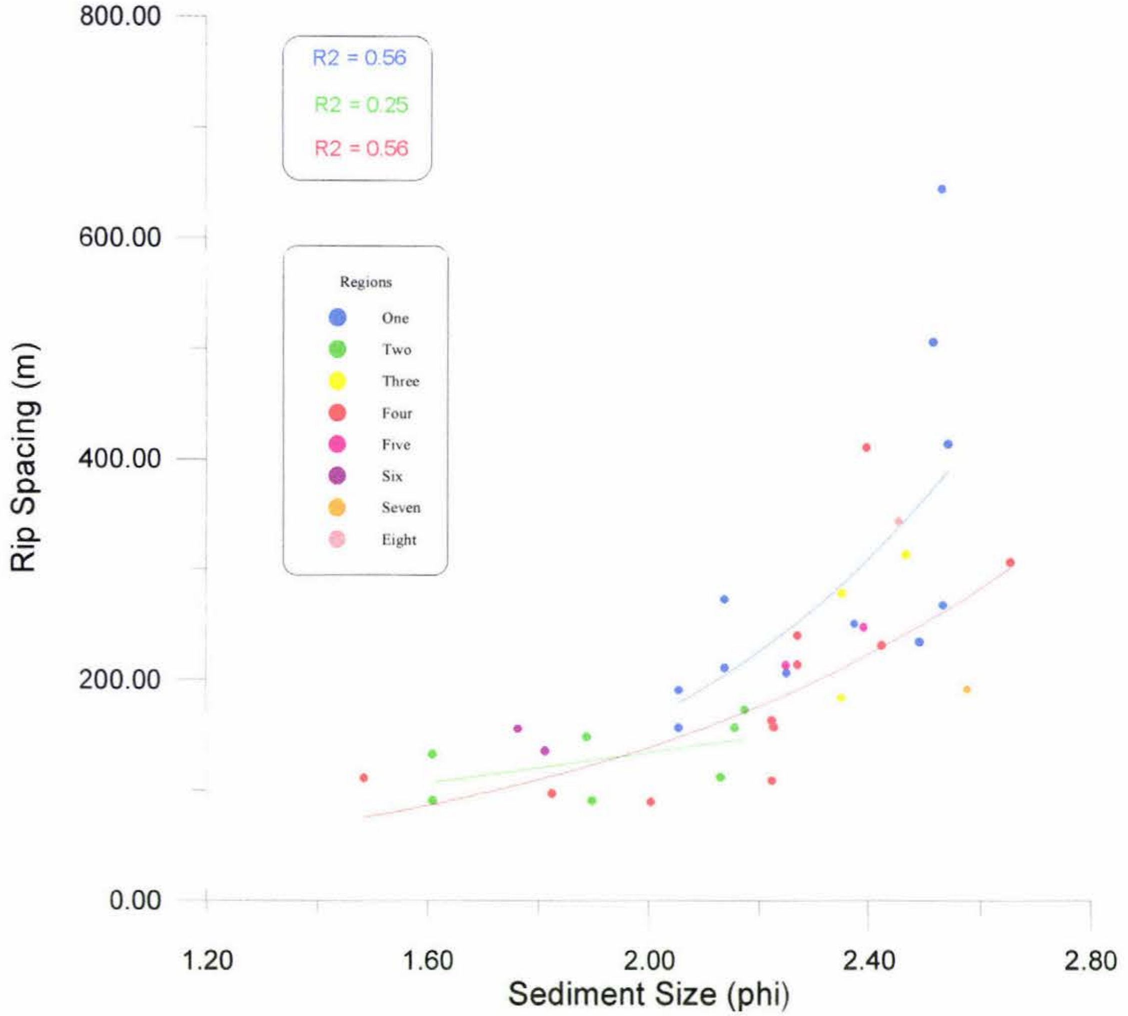


Figure 4.41 The relationship between rip spacing and sediment size, showing the variations between the proposed regions.

# CHAPTER FIVE: THE GAP, CASTLEPOINT: the effect of topographic control on surf zone and rip characteristics.

## 5.1 INTRODUCTION

Figure 5.1 Photograph of the Gap, Castlepoint on the 3-09-2000.

Rip currents occur on a wide range of beaches and are particularly prevalent on beaches exhibiting intermediate type surf zone morphology (Short and Wright, 1984). Rip currents are the most evident component of the nearshore cell circulation (Goldsmith *et al.,* 1992) and although there have been numerous qualitative investigations of rip current systems; quantitative field measurements are scarce (Aagaard and Masselink, 1999; Komar, 1998; Huntley *et al.,* 1988; Wright and Short, 1983). This is primarily due to the many logistical difficulties facing field investigation and has resulted in concentrated efforts on low energy rip current systems (i.e. Huntley *et al.,* 1988; Aagaard *et al.,* 1997; Symonds *et al.,* 1997; Brander, 1999). Field data for rip currents on high-energy beach systems are rare, with one of the few examples provided by Brander *et al.* (1999).

The research presented here is obtained from field work on a longshore bar and trough system with a rip current occupying the trough in the enclosed bay of 'The Gap' at Castlepoint, on the Wairarapa coastline. The aims of this chapter are to investigate rip current velocities and their relationship to morphology, and, to a small degree, the effects of tidal control on rip velocity.

## 5.2 THE SITE

Castlepoint is located on the east coast of the North Island, approximately 27 kilometres by road from Masterton (Figure 5.2). It is comprised of a prominent headland, 'the Castle', and 'the Reef' composed of a sequence of Opoitian and Nukumaruan rocks (Johnston, 1972). The Castle is 162 metres high, with shear sides, while the Reef to the northeast of the Castle, is a low linear feature rising to a height of 50 metres. It is connected to the mainland by a tombolo that is covered at high spring tides, and encloses a small harbour, known as The Gap (Johnston, 1972). A 165 metre gap between the Castle and the Reef provides access to the harbour. Holocene sand deposits overlie older rocks particularly on the hillside west of the Reef after being blown from the beaches surrounding the harbour.

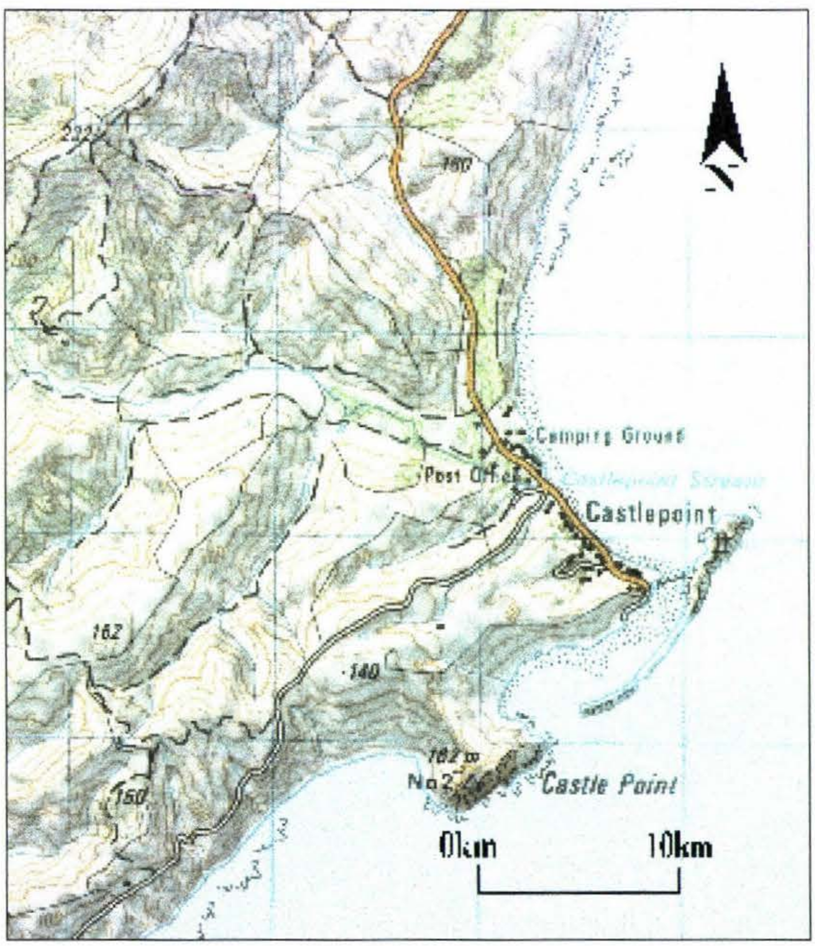


Figure 5.2 Map of Castlepoint, Wairarapa (Source: 260-U26 Castlepoint, Land Information).

A major rip exiting the northeast end of the Gap, as shown in Figure 5.3 is the focus of this investigation. The Gap exhibited quite complex topographic features, related to topographical controls of the headland and the Reef. Figure 5.4 clearly demonstrates the existence of a pronounced trough running along the edge of the beach. This was occupied by a rip current, which ran south to north. An inflow of water from a small embayment located behind the Reef added an additional volume of water to the northern end of the system. The Rip exited through the gap alongside the reef. The nearshore bar was actually attached (or welded) to the southern end of the beach, where it exhibited features also characteristic of a low tide terrace. A second smaller trough may have occurred approximately 160 metres from the shoreline. A small rip current exited the southern end of the bay, around the rocks at the base of the Castle.

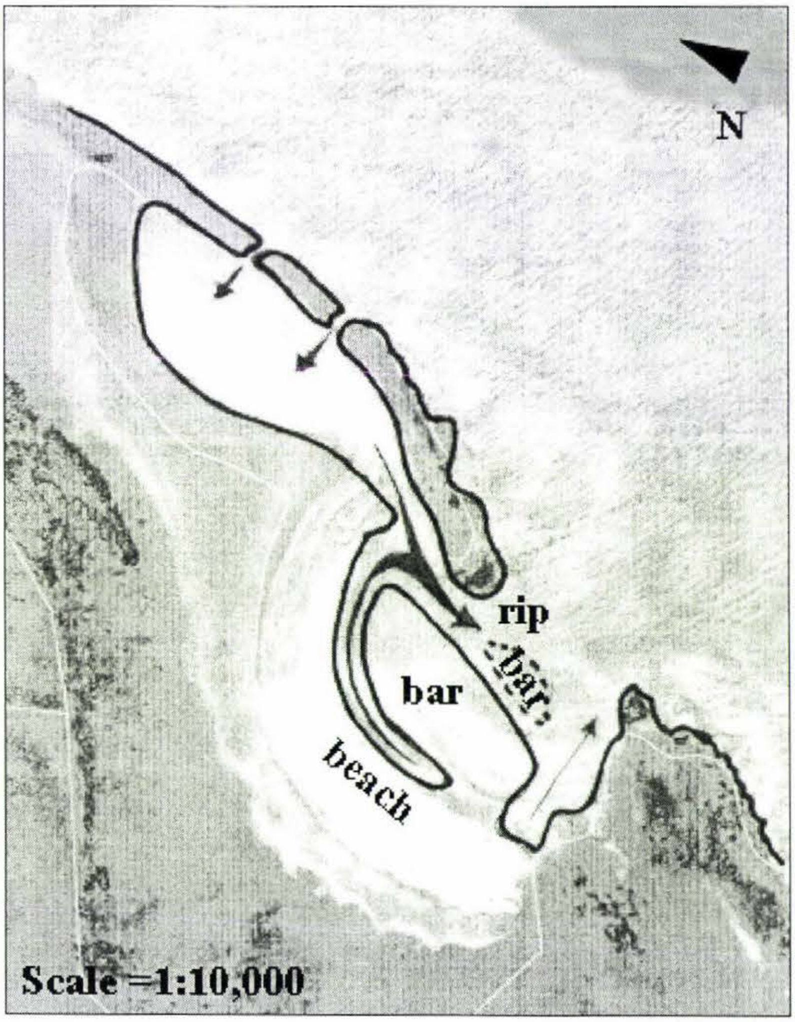


Figure 5.3 Enhanced vertical aerial photograph of the Gap, Castlepoint. Rip currents are depicted with arrows. The rip current exiting at the left-hand side of the Gap is the focus of this investigation.

Figure 5.4 The Gap embayment, Castlepoint. The longshore trough can be seen as the calm stretch of water along the edge of the Gap beach.

The tidal regime for Castlepoint on the fourth of September 2000 is shown in Table 5.1. Wave height at the entrance to the Gap embayment was approximately two metres, with wave heights of approximately 1.5 metres in the embayment itself.

| Time | Height (m) |
|---|---|
| 0345 | 0.5 |
| 0949 | 1.7 |
| 1616 | 0.5 |
| 2216 | 1.7 |

Table 5.1 Tidal regime for Castlepoint, 3-9-2000 (Ministry of Transport, 2000).

## 5.3 TOPOGRAPHY SURVEYS

The morphology of the Gap system and the location of the survey points are shown in Figure 5.5. The topographic survey was carried out through the use of manual dumpy levels for station surveys and the Topcon GTS-701 Total Station laser level for the remaining points.

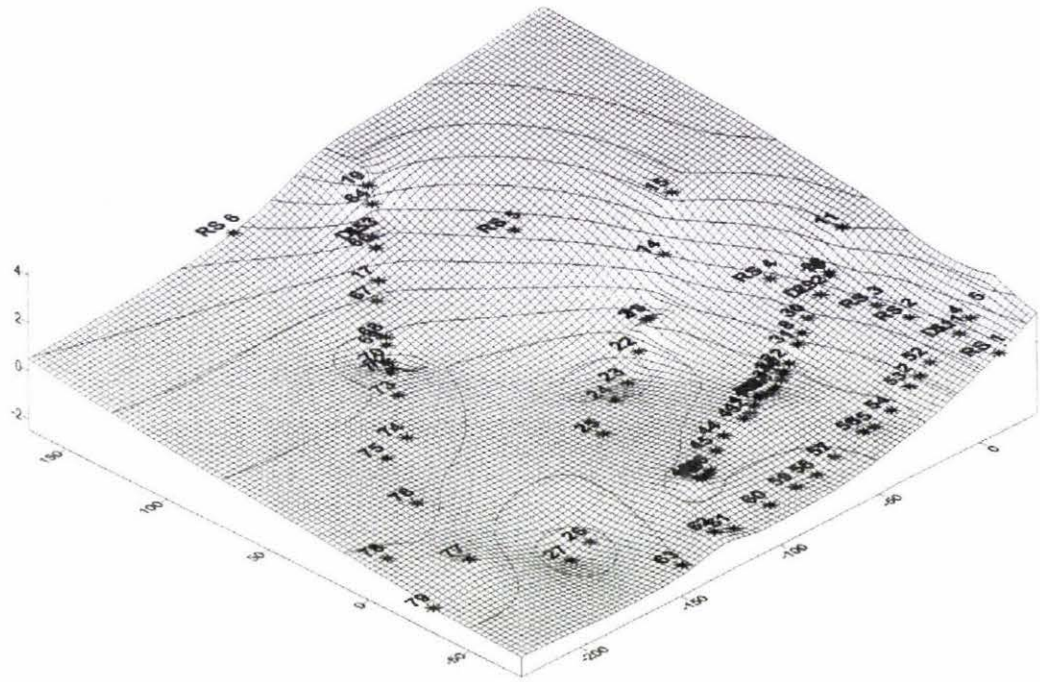

Figure 5.5 Digital Elevation Model of The Gap surf zone morphology.

The rip is difficult to distinguish in the topographical survey. However, Figure 5.4 illustrates the extent of the longshore trough and rip current more clearly. The morphology of the trough and bar system was surveyed at each station site. As depicted in Figure 5.6 the northern survey (station one) exhibited a pronounced longshore trough and bar system. In contrast, although the longshore trough is still evident from the middle (station two, Figure 5.7) and southern (station three, Figure 5.8) surveys, the prominence of the longshore trough decreases in a southerly direction. The topography of the transverse bar is also more undulating, and smaller trough like features are evident.

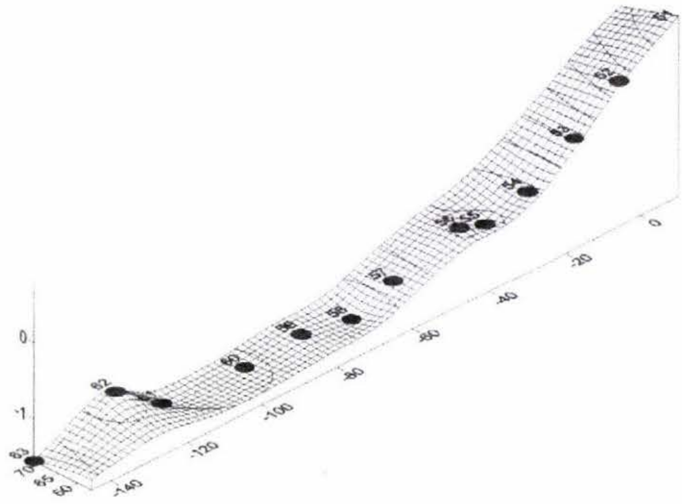

Figure 5.6a Digital Elevation Model for the northern survey (station one).

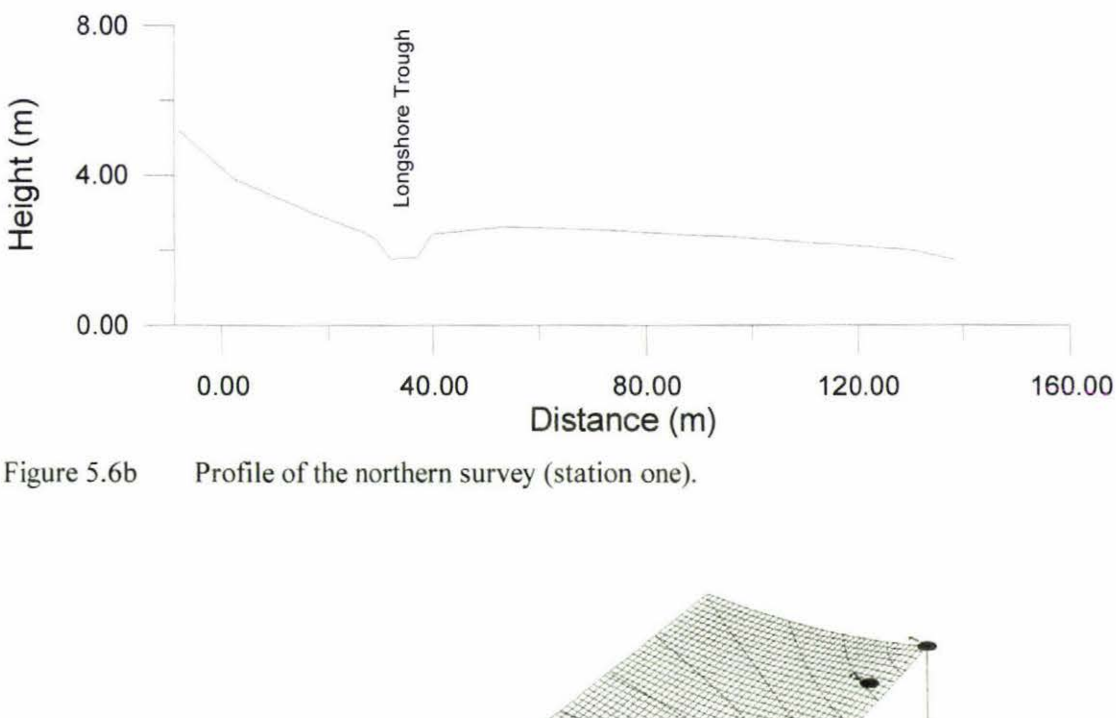


Figure 5.6b Profile of the northern survey (station one).

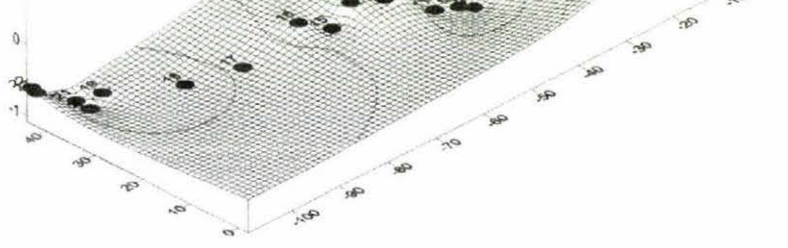

Figure 5.7a Digital Elevation Model of the middle survey (station two).

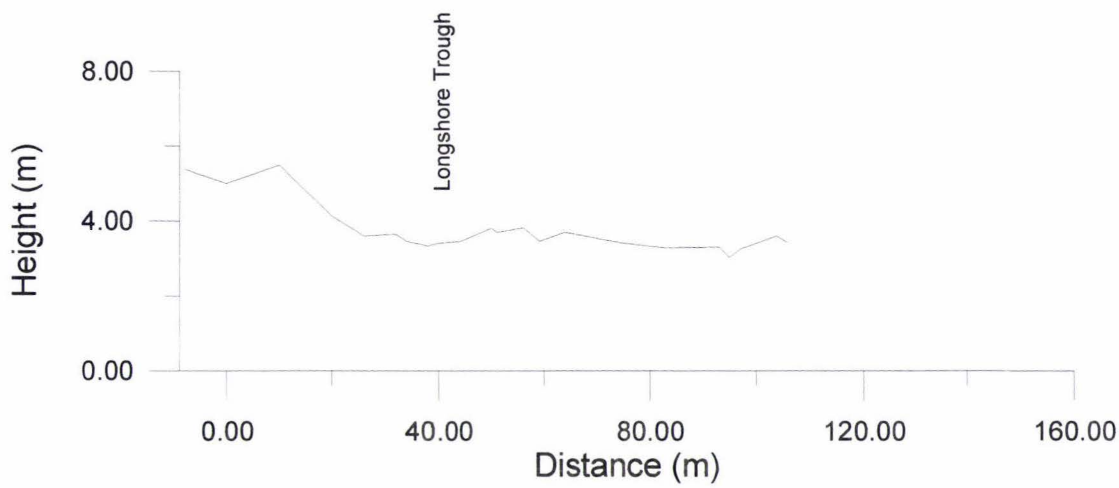


Figure 5.7b Profile of the middle survey (station two).

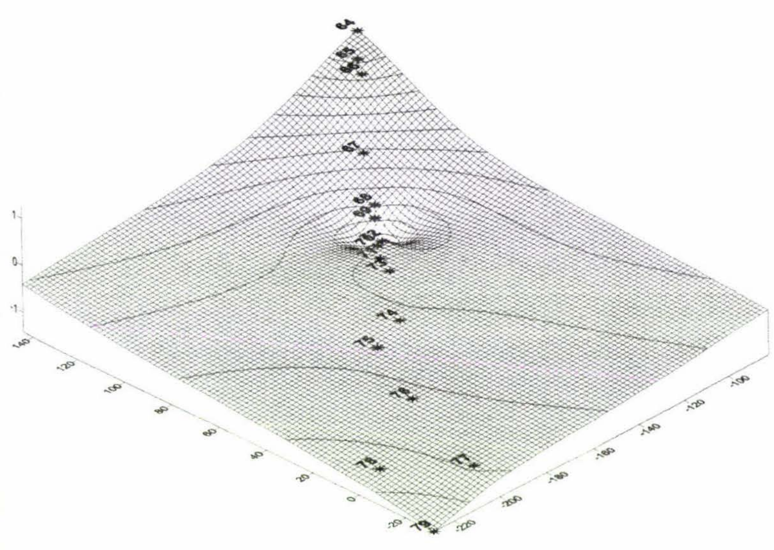

Figure 5.8a Digital Elevation Model of the southern survey (station three).

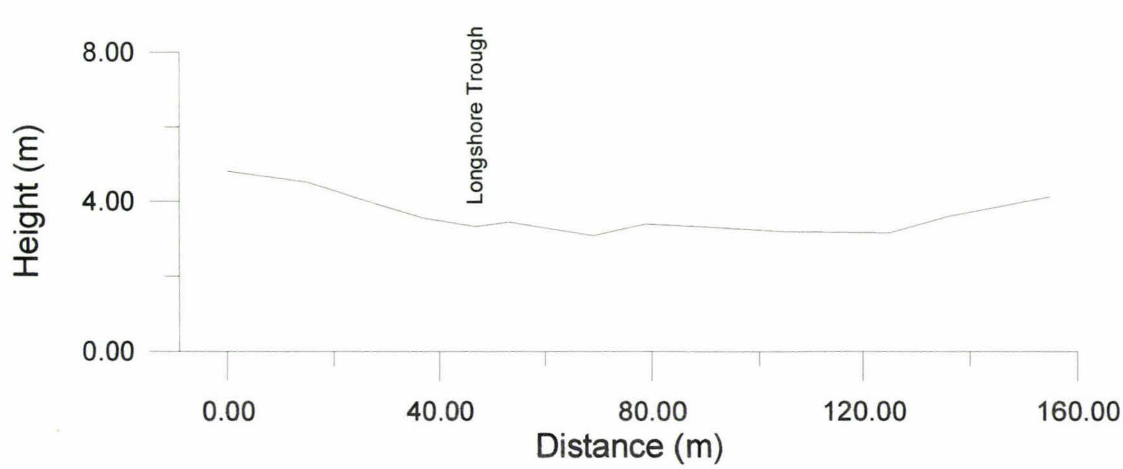


Figure 5.8b Profile of the southern survey (station three).

## 5.4 Rip Dye Technique

The rip current was identified by the use of dye within the rip (Huntley *et al.*, 1988; Brander, 1999b). Approximately 250 grams of potassium permanganate crystals were dissolved in a bucket of water and dispersed into the rip feeder current, between the northern and middle stations. Figure 5.9 show the path of the rip current as it flows north, exiting the Gap along the edge of the Reef.

Figure 5.9a Initial release of dye into the rip current.

Figure 5.9b Dye can be seen in the rip current as it heads towards the Reef.

Figure 5.9c Dye in rip begins to turn out of the Gap.

Figure 5.9d The dye is travelling past the Reef, and can be seen to the left of the black tyres in the centre of the photograph.

## 5.5 RIP FLOAT TRAJECTORIES

Rip float experiments were conducted to determine lagrangian rip velocity flows. This involved the use of the method as described by Short and Hogan (1994). Rip currents were measured through the use of oranges as a rip float, a technique pioneered by Professor Peter Nielsen of the Department of Civil Engineering at Queensland University. The limited impact of breaking waves in the longshore trough allowed for easy observation of the oranges as they travelled in the rip current. They were also particularly useful as the employment of a human rip float would have been extremely dangerous, particularly at the northern end of the Gap.

The trajectories of the oranges were tracked using two compasses at a known distance apart, with recording of positions every 15 seconds. Three stations were set up at each topographic survey site. Each of the eleven runs were carried out simultaneously at all three sites. Gaps in the data are due to lost sightings of oranges early in a run, or beaching of the orange in the initial stages of the run.

The trajectories of all runs undertaken are shown for stations one, two and three in Figures 5.10, 5.11 and 5.12 respectively. The trajectories at station one are of particular note. Only four floats, runs three, six, nine and 11, were measured for a substantial distance into the outer surf zone. These runs were not only distinguished by their spatial nature, but also by the distinct increase in velocity, demonstrated by the large distances between readings.

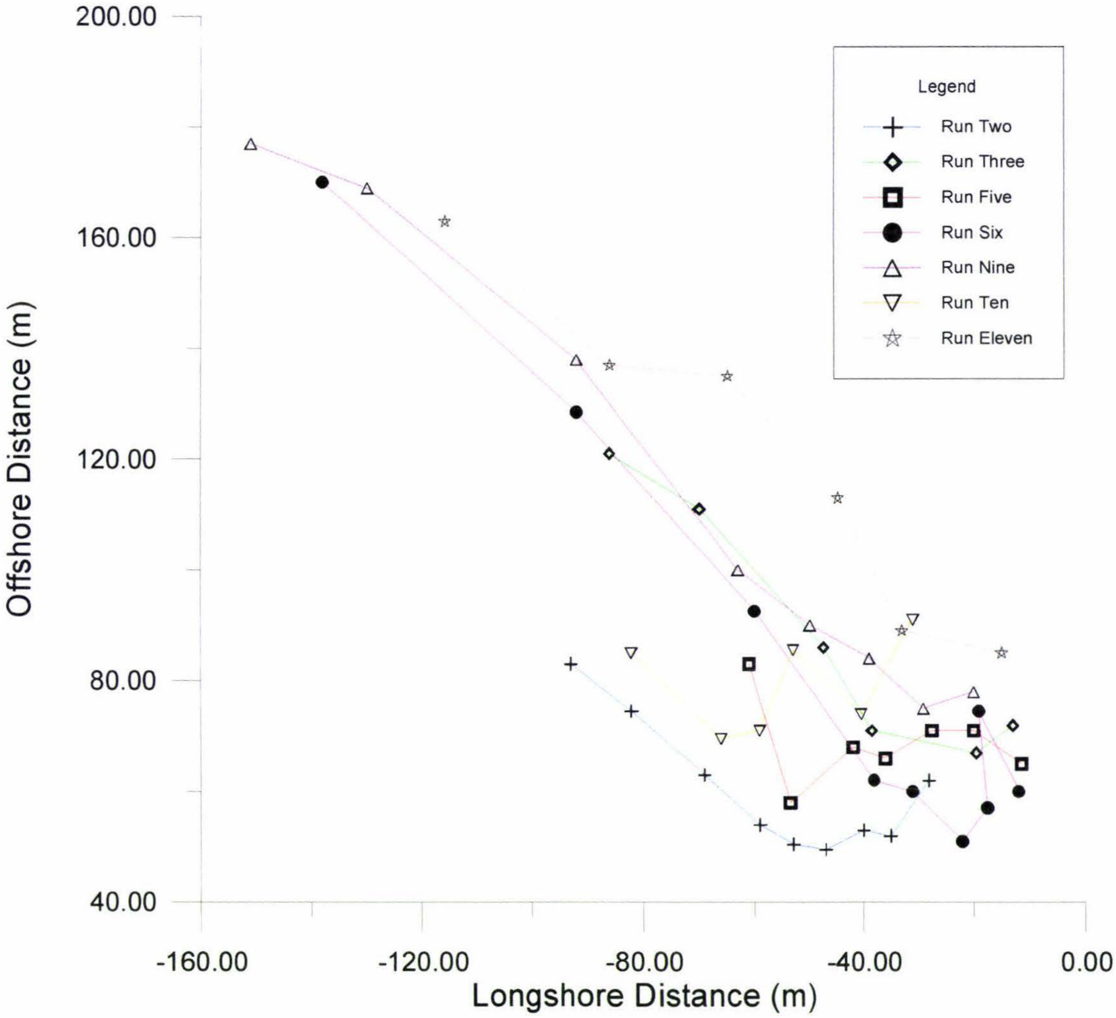


Figure 5.10 Station one (northern): rip float trajectories, relative to the southern measuring point.

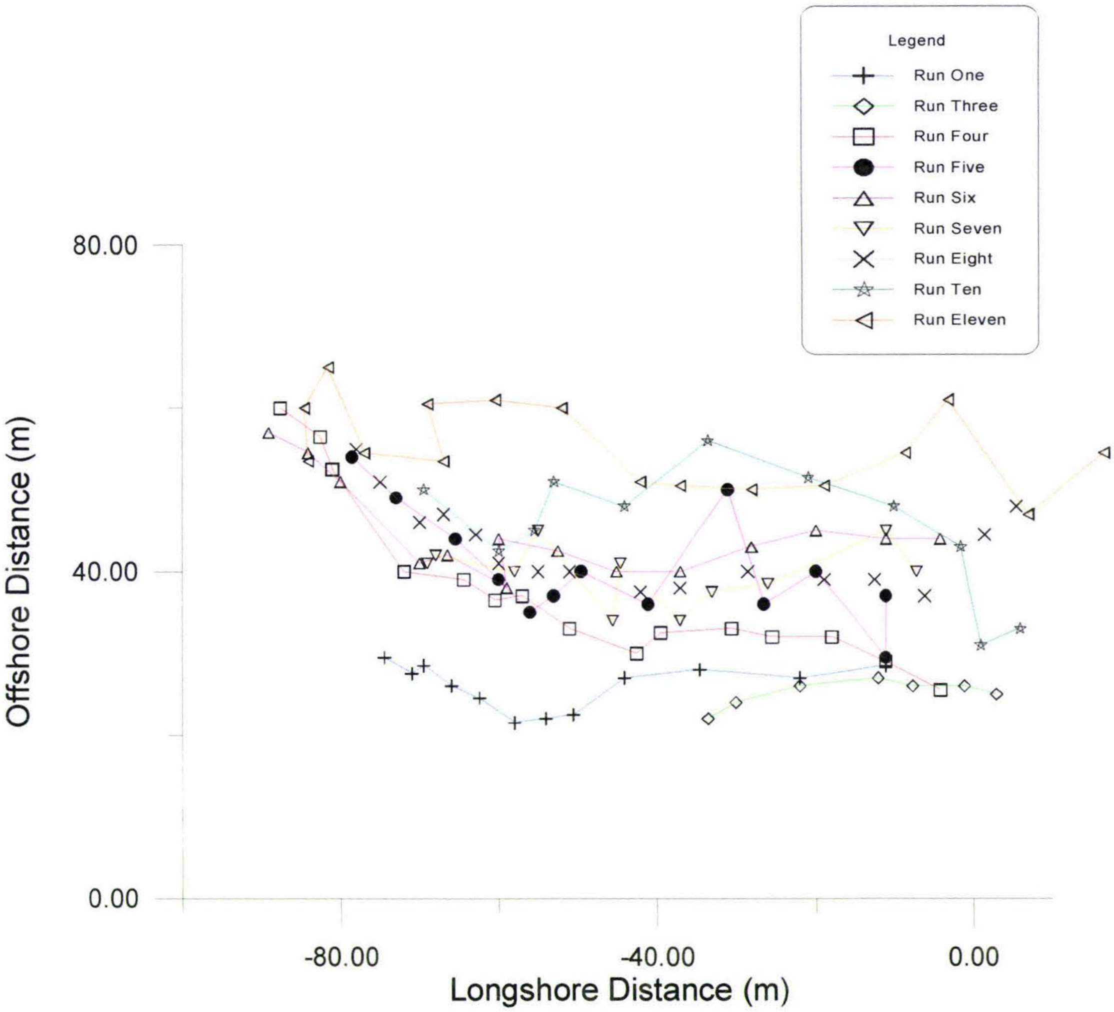


Figure 5.11 Station two (middle): rip float trajectories relative to southern measuring point.

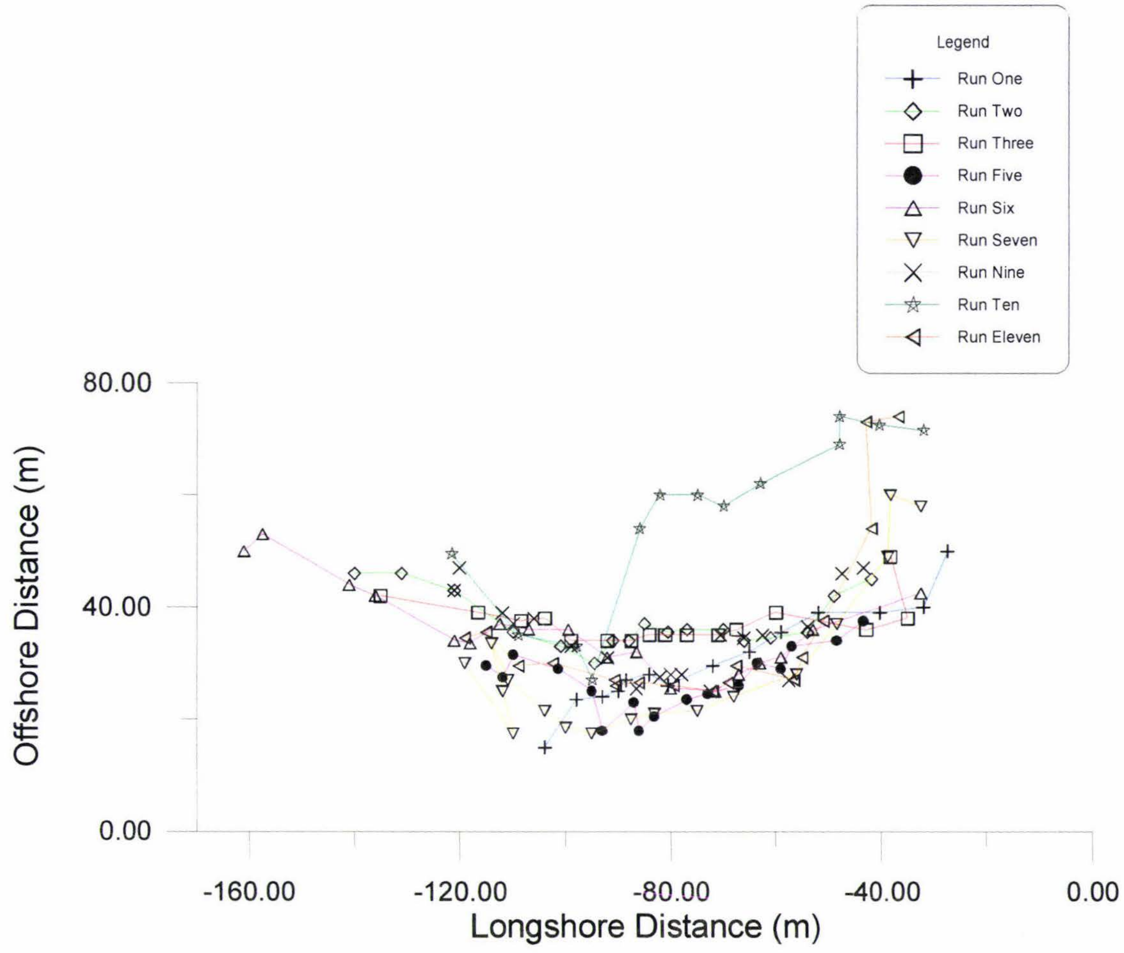


Figure 5.12 Station three (southern) rip float trajectories relative to southern measuring point.

## 5.6 RIP VELOCITY PROFILES

Figure 5.13 illustrates the rip velocity profile for the northern station, which measured rip velocities as the rip turned to exit out of the Gap. The velocity of water flowing within the rip current was highly variable, not only between runs but also within each run, as is illustrated in the rip velocity profile. The highest rip velocity at station one was 4.13ms$^{-1}$ in the sixth run. The lowest rip velocity was 0.36ms$^{-1}$ in the second run. The sixth run had the greatest variance in rip velocities, ranging from a maximum of 4.13 ms$^{-1}$ to a minimum of just 0.40ms$^{-1}$. Run three, nine and eleven were also characterised by highly variable rip velocities with ranges respectively of 0.53ms$^{-1}$ to 2.26ms$^{-1}$, 0.60ms$^{-1}$ to 3.20ms$^{-1}$, and 0.6ms$^{-1}$ to 2.70ms$^{-1}$. In contrast, runs two, ten and five had much smaller variances within the runs, with respective rip velocities ranging from $0.36ms^{-1}$ to $1.13ms^{-1}$, $0.46ms^{-1}$ to $1.46ms^{-1}$, and $0.40ms^{-1}$ to $1.10ms^{-1}$.

The high values for rip velocities, particularly values over $3ms^{-1}$ are particular interesting. Short (1985) suggests that rip current velocities in mega-rips can approach $3ms^{-1}$ but values greater than this are not found in the literature (e.g. Brander *et al.*, 1999; Brander, 1999b; Aagaard *et al.*, 1997; Huntley *et al.*, 1988). However, in this experiment, high velocities were not isolated incidents. In fact, velocities exceeded $3ms^{-1}$ on four occasions, and were greater than $2ms^{-1}$ in a further three cases.

Errors may have occurred due to the large offshore and longshore distances from the measuring points (see Figures 5.18 and 5.19). However this rip was removing the majority of water from the Gap embayment. At the northern end of the Gap, the small inlet, which was fed by two rip currents located in breaches of the Reef, exited into the Gap. The very large volume of water having to leave the Gap embayment may account for the particularly high momentary velocities found in this rip current. The dominance that the topography exerted on this system is also likely to play a role in the unusually high rip velocities found here.

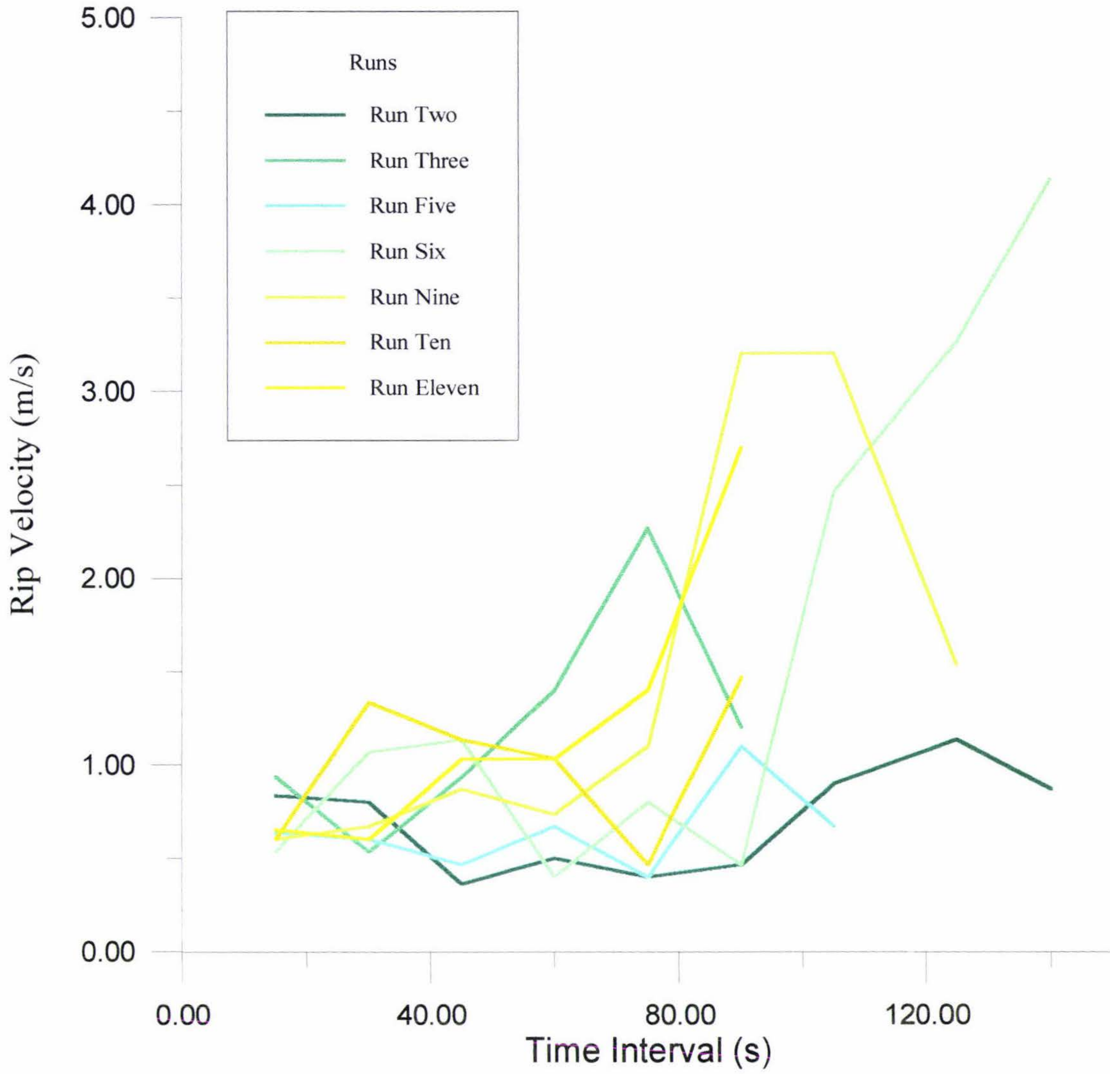


Figure 5.13 Rip velocity profile station one (north).

Figure 5.14 shows the rip velocity profiles for station two, located in the mid portion of the longshore trough. The trough acted as a rip feeder channel for the rip at the northern end of the beach. The velocity of water flowing within the longshore trough was again highly variable, although within a narrower range than was experienced at station one. A maximum rip velocity value of $1.20ms^{-1}$ was obtained in both run ten and run 11. A minimum rip velocity value of $0.20ms^{-1}$ was recorded in run one and run eight.

The runs from station two all tend to have a high degree of variability in velocity throughout each run. However, in comparison with station one, these runs are much more typical of runs two, five and ten, which had small overall variability within the run.

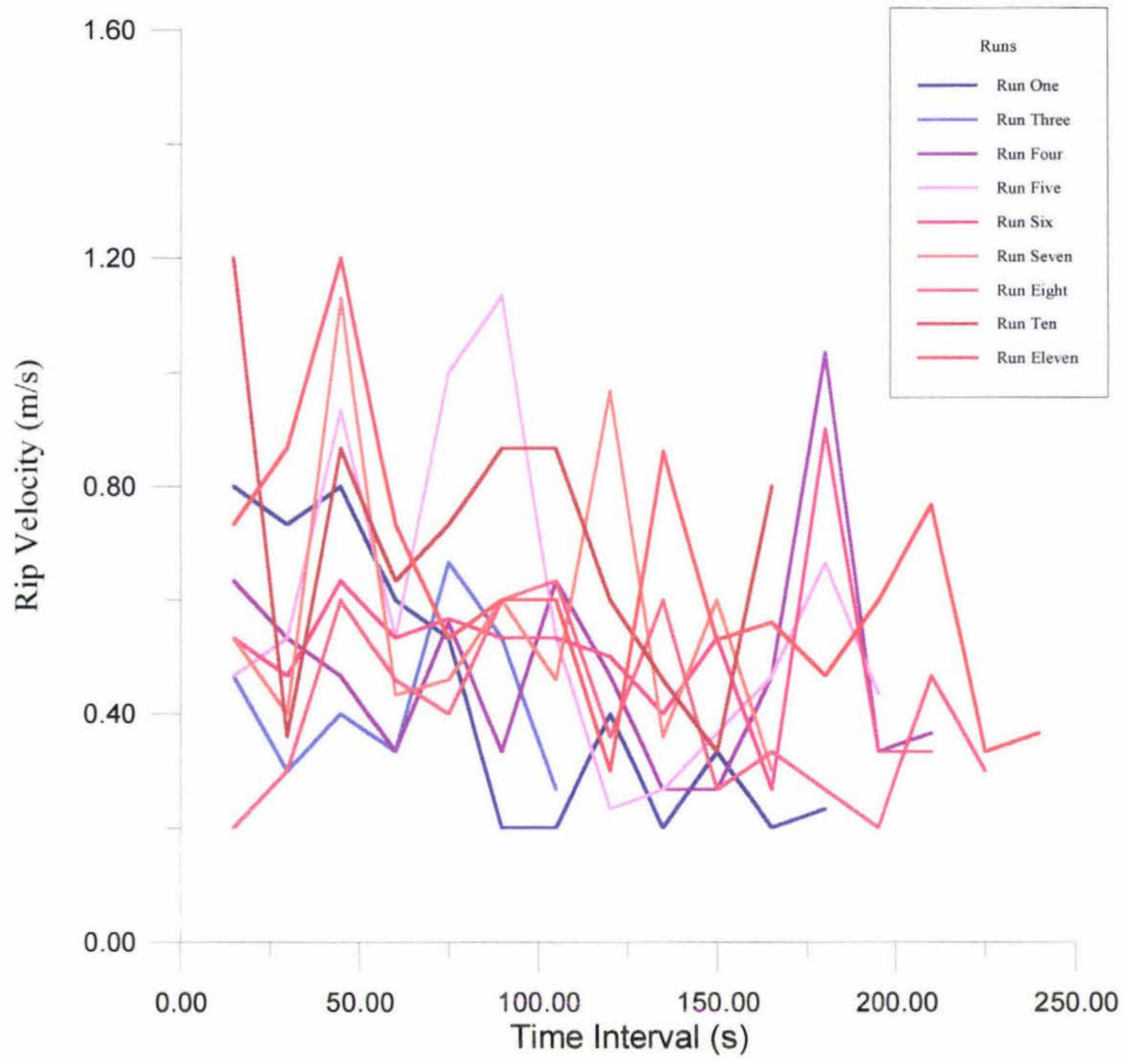


Figure 5.14 Rip velocity profile, station two (middle site).

The station three rip velocity profiles shown in Figure 5.15 are again highly variable. The lowest rip velocity of $0.10ms^{-1}$ for the ninth run was the lowest velocity recorded for any station. The highest rip velocity was recorded on the tenth run, at $1.90ms^{-1}$, closely followed by $1.86ms^{-1}$ on the sixth run. These two runs are also characterised by a greater degree of variability, with rip velocities ranging from $1.90ms^{-1}$ to $0.30ms^{-1}$ for run ten, and $1.86ms^{-1}$ to $0.20ms^{-1}$ for run six. The majority of other rip velocity values are similar to that found at station two both for variability and speed.

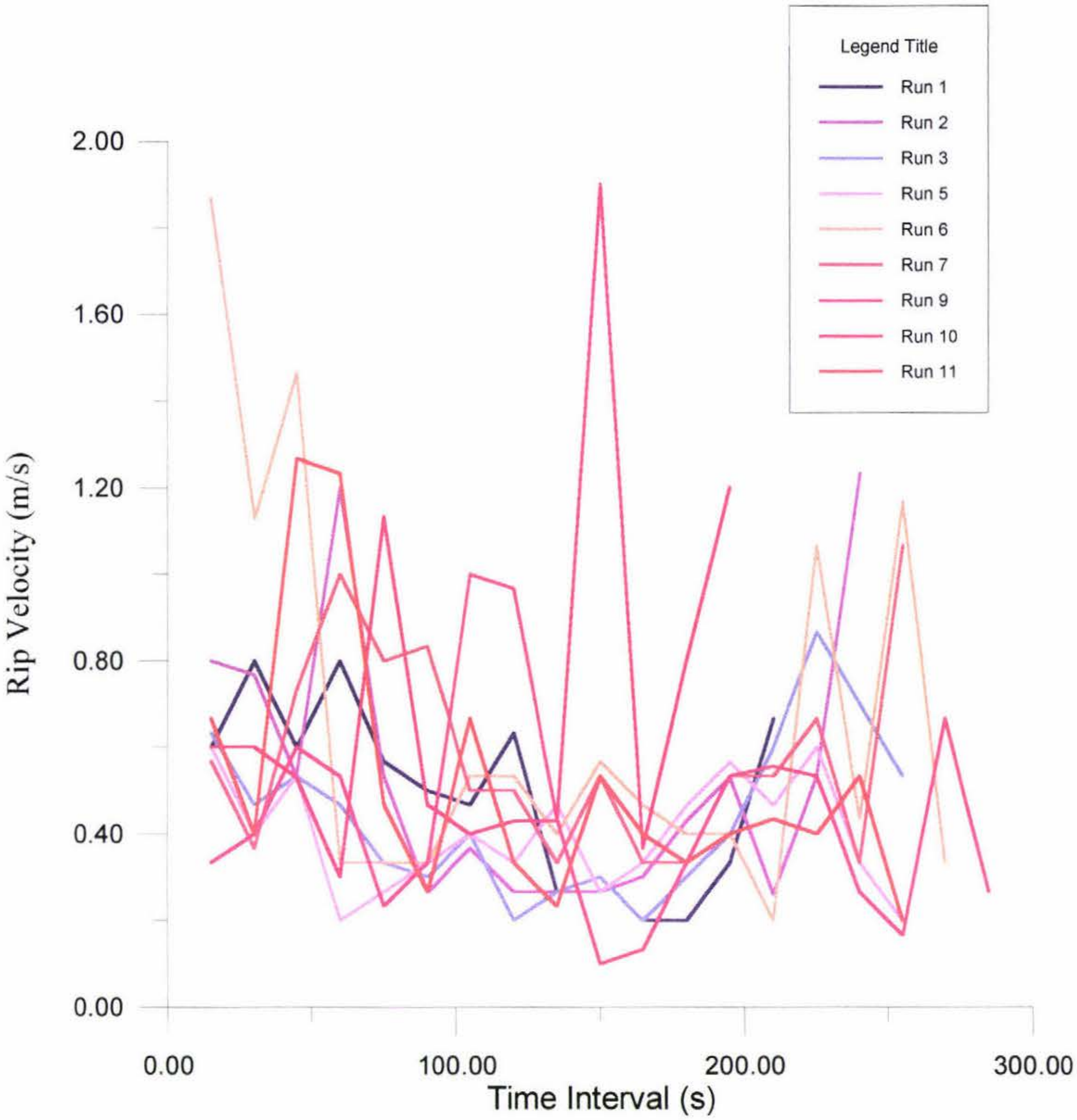


Figure 5.15 Rip velocity profiles at station three (south).

### 5.6.1 Rip Pulsing behaviour

Throughout the series rip velocity profiles, particularly those recorded at stations two and three, rips appear to have a pulsing behaviour. This is likely to be produced either through wave action (i.e. wave periodicity) or wave sets. At station two; runs seven, 10 and 11 show distinct periodic episodes of higher rip current velocity, while runs three and eight show distinct periodic episodes of lower rip current velocities. Runs six and 10 at station three produced distinct high velocity periods, with run nine producing distinct low velocity periods.

The most common time period between pulsing events is 75 seconds. The mean time period between pulses is 89 seconds. This suggests that rip pulsing may be produced by wave sets rather than individual waves, since wave period was estimated to be between eight and 12 seconds.

| STATION TWO | | STATION THREE | |
|---|---|---|---|
| **Run** | **Time between high velocities** | **Run** | **Time between high velocities** |
| 7 | 75 seconds | 6 | 180 seconds |
| 10 | 55 and 65 seconds | 10 | 75 seconds |
| 11 | 90 and 75 seconds | | |
| **Run** | **Time between low velocities** | **Run** | **Time between low velocities** |
| 3 | 60 seconds | 9 | 75 and 105 seconds |
| 8 | 120 seconds | | |

Table 5.2 Pulsing events in the rip velocity profiles.

### 5.7 Mean Rip Velocities And Tidal Modulation

The mean rip velocities of each station over the eleven runs are shown in Figure 5.16. Mean rip velocities ($\bar{x}_r$) for each run were calculated using the equation:

$$\bar{x}_r = (\Sigma\, v_r / n) / 15\text{sec}$$

where $v_r$ is the velocity found for each 15-second interval, and n is the number of intervals.

All three stations had variable mean rip velocity flows, particularly station one, which ranged from a maximum of 1.68ms$^{-1}$ to a minimum of 0.65ms$^{-1}$. Much of this range is due to the fact that runs three, six, nine and 11 were characterised by trajectories where the oranges went much further than the remaining runs, as shown in Figure 5.16. All four runs experienced significantly higher rip velocities than the other runs, where measurements into the outer surf zone were not acquired. However, the remaining three runs still had significantly higher rip velocities than were recorded at stations two or three. The high rip velocities found further out in the rip suggest that this section of the rip was an area of particularly high velocity. This is due to the fact that this area involved the convergence of the majority of the water from the Gap and the northern inlet. The Reef acted as a barrier to the rip current and also worked to accelerate flow through topographic end effects within the Gap embayment.

In contrast, stations two and three had much less variability and far lower mean rip velocities, with little difference in range recorded between the two sites. The maximum mean rip velocities for stations two and three respectively were $0.70ms^{-1}$ and $0.71ms^{-1}$, both in the tenth run. A minimum mean rip velocity of $0.40ms^{-1}$ was gained for station two in the eighth run, while the minimum for station three was $0.39ms^{-1}$ in the fifth run. It is interesting to note the similarity between these two areas of the longshore trough. Although the morphology of the middle site is not as distinct as that of the northern site (Figure 5.7), the channel both through observation and survey was still more defined than the southern site.

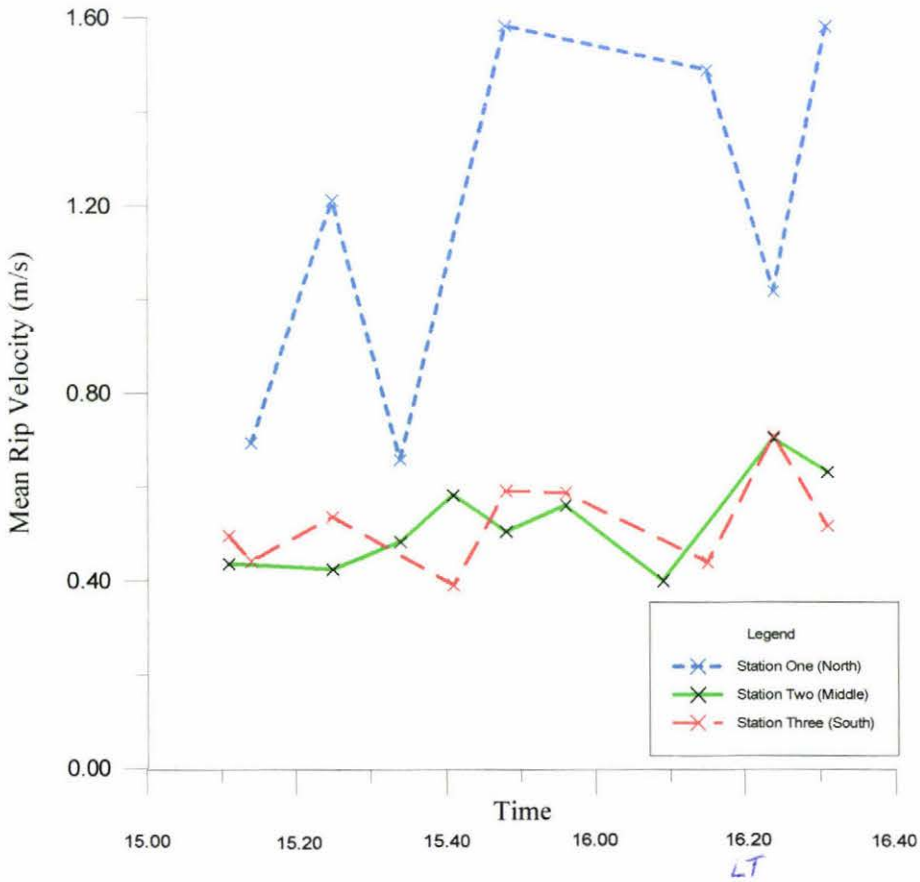


Figure 5.16 Mean rip velocity over time, Castlepoint.

Figure 5.17 indicates the overall trend of mean rip velocity over time. Station one, which tracked rip velocities in the northern end of the rip channel, had a distinctive pattern of rip velocity increasing over time. The trend of increasing rip velocity over time was evident in both the runs that included measurement within the rip channel as it turned to exit the Gap, as well as measurements that took in the longshore trough. This trend coincides to some extent with the tidal regime, as shown in Table 5.1 with low tide occurring at 1616, at a height of 0.5m. However, an extended period of surveying, particularly closer to high tide and across the low tide would have provided some valuable insights into this particular trend since rip velocity values were so variable.

Results from stations two and three are interesting in comparison to station one, with a very different overall pattern occurring. Tidal modulation seems to have little impact within the longshore trough, as compared with the rip current itself. In fact the rip velocities found at these two sites are relatively similar. Station two has a slight trend of increasing rip velocity as low tide was reached, while station three has a relatively stable rip velocity flow over the same time period. Again, the short duration of the experiment reduces the confidence in of any conclusions that can be made about the effect of tidal modulation.

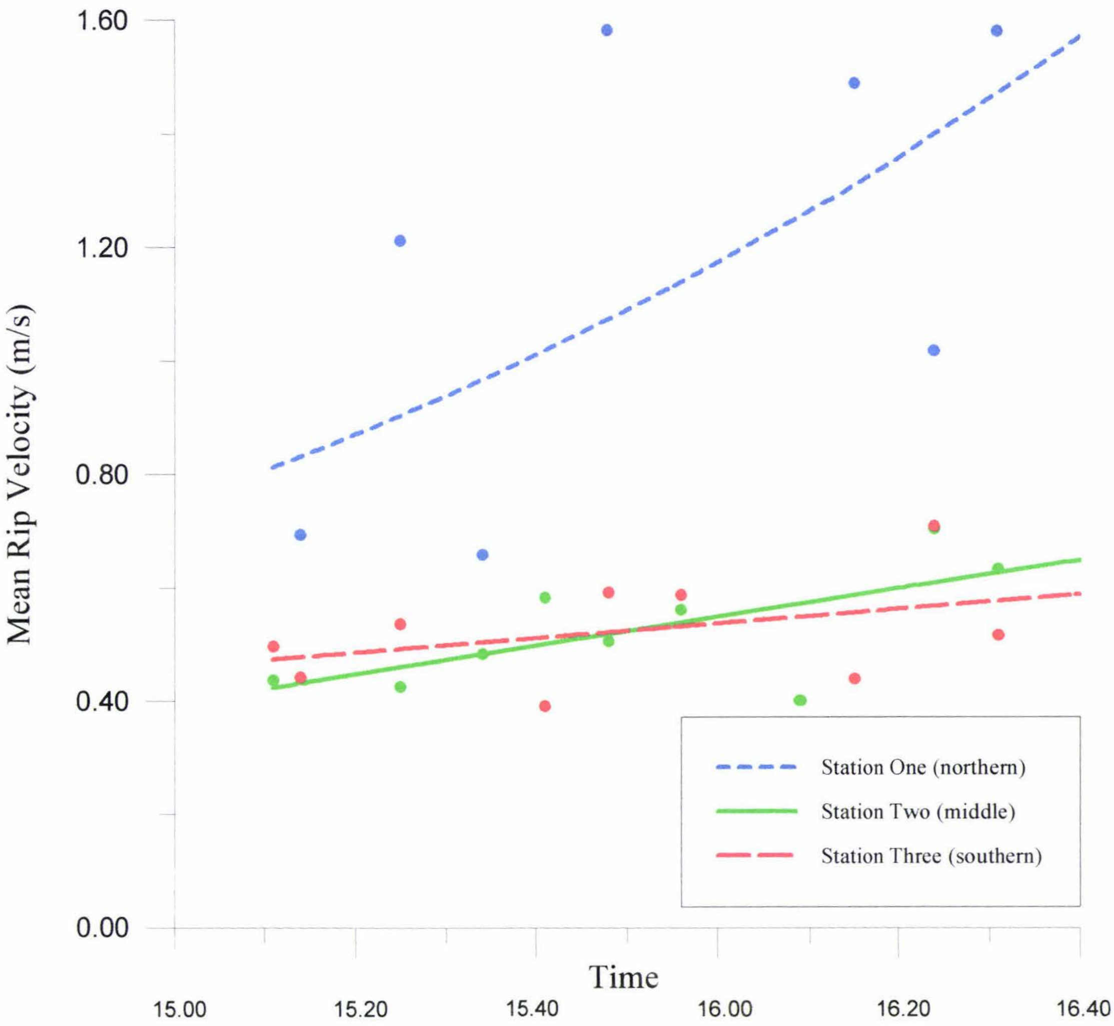


Figure 5.17 Overall rip velocity profiles.

## 5.8 Spatial Patterns Of Surface Flow

The relationship between rip velocity and longshore distance, and rip velocity and offshore distance measured from station one are shown in Figures 5.18 and 5.19. Strong overall trends, where rip velocity increased substantially alongshore and offshore are depicted. This illustrates the significant increase in velocity within the rip current as compared with the convergence area with the feeder current/longshore trough. Comparison with station two and three also indicates that this convergence area is characterised by higher rip velocities than with the longshore trough further south. It is important to note however, that rip velocity is still highly variable both along shore and in offshore directions.

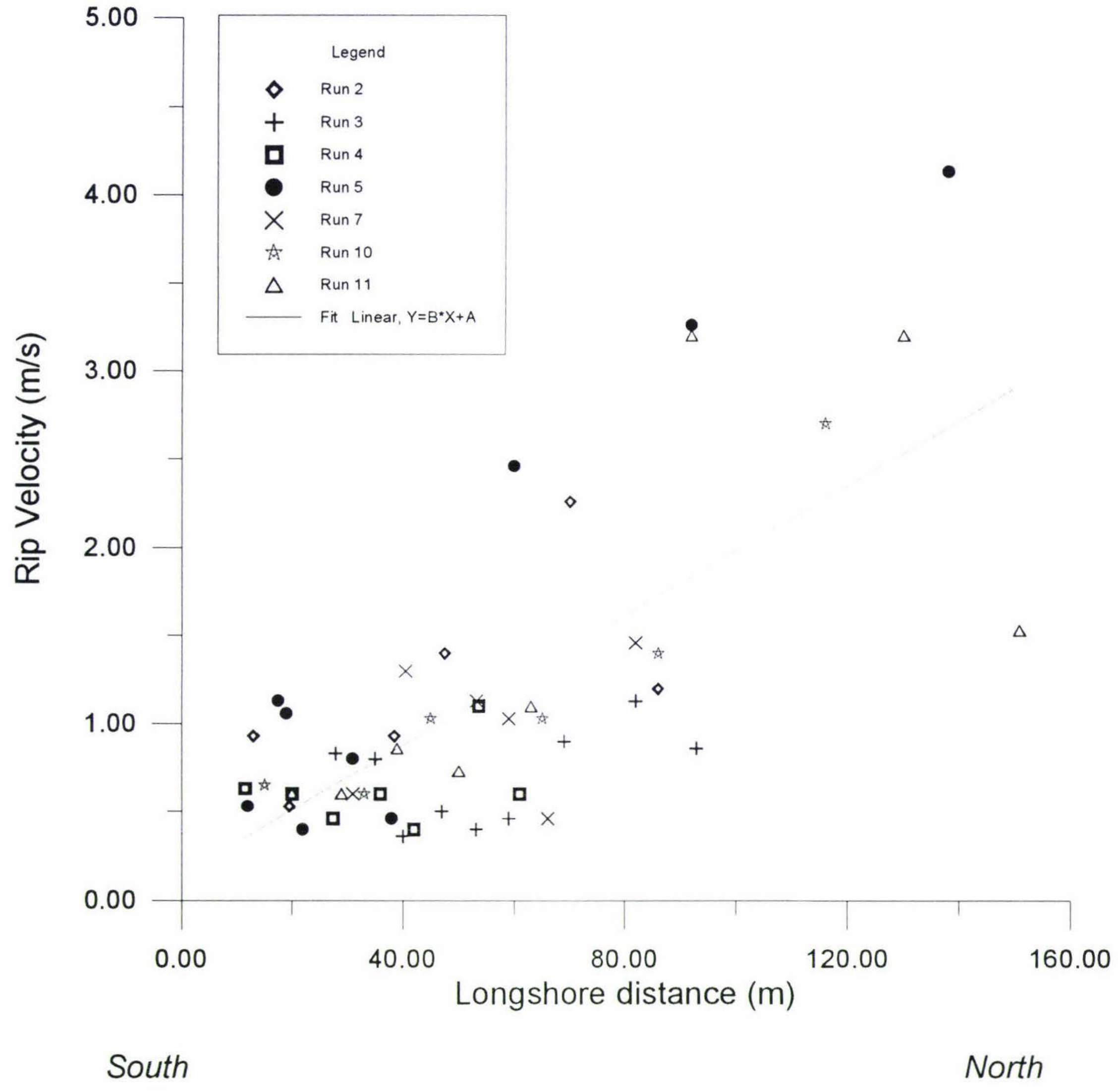


Figure 5.18 Station one rip velocity verses longshore distance.

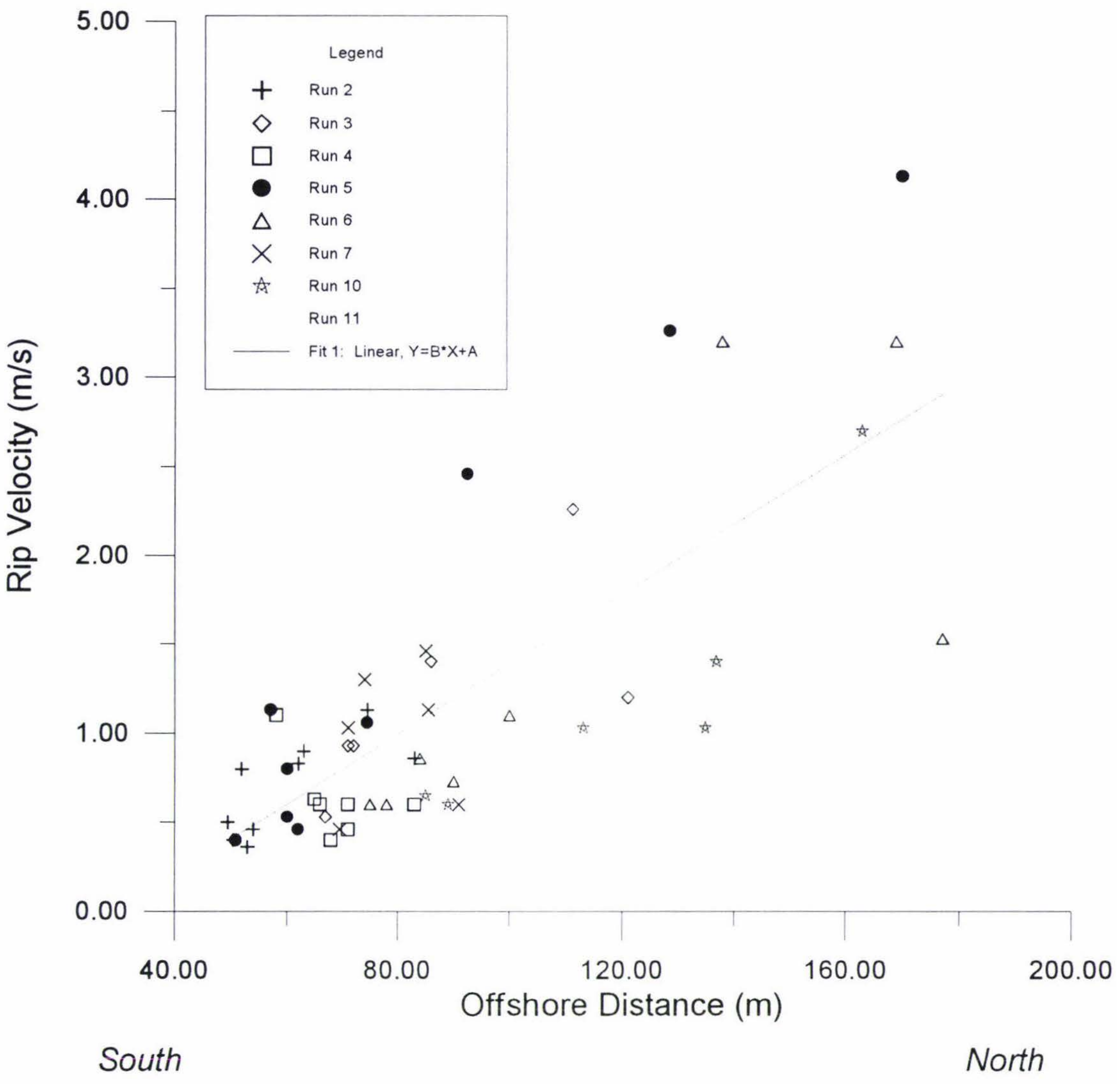


Figure 5.19 Station one rip velocity verses offshore distance.

The relationships between rip velocity and longshore distance, and rip velocity and offshore distance are shown for station two in Figures 5.20 and 5.21, and station three in Figures 5.22 and 5.23. Although there was a wide range in rip velocities for both longshore and offshore extent, general trends are apparent in the data. In the relationship between rip velocity and longshore extent there was a slight trend towards lower rip velocities northward of both stations. Conversely, there was a slight trend for greater velocities with offshore distance.

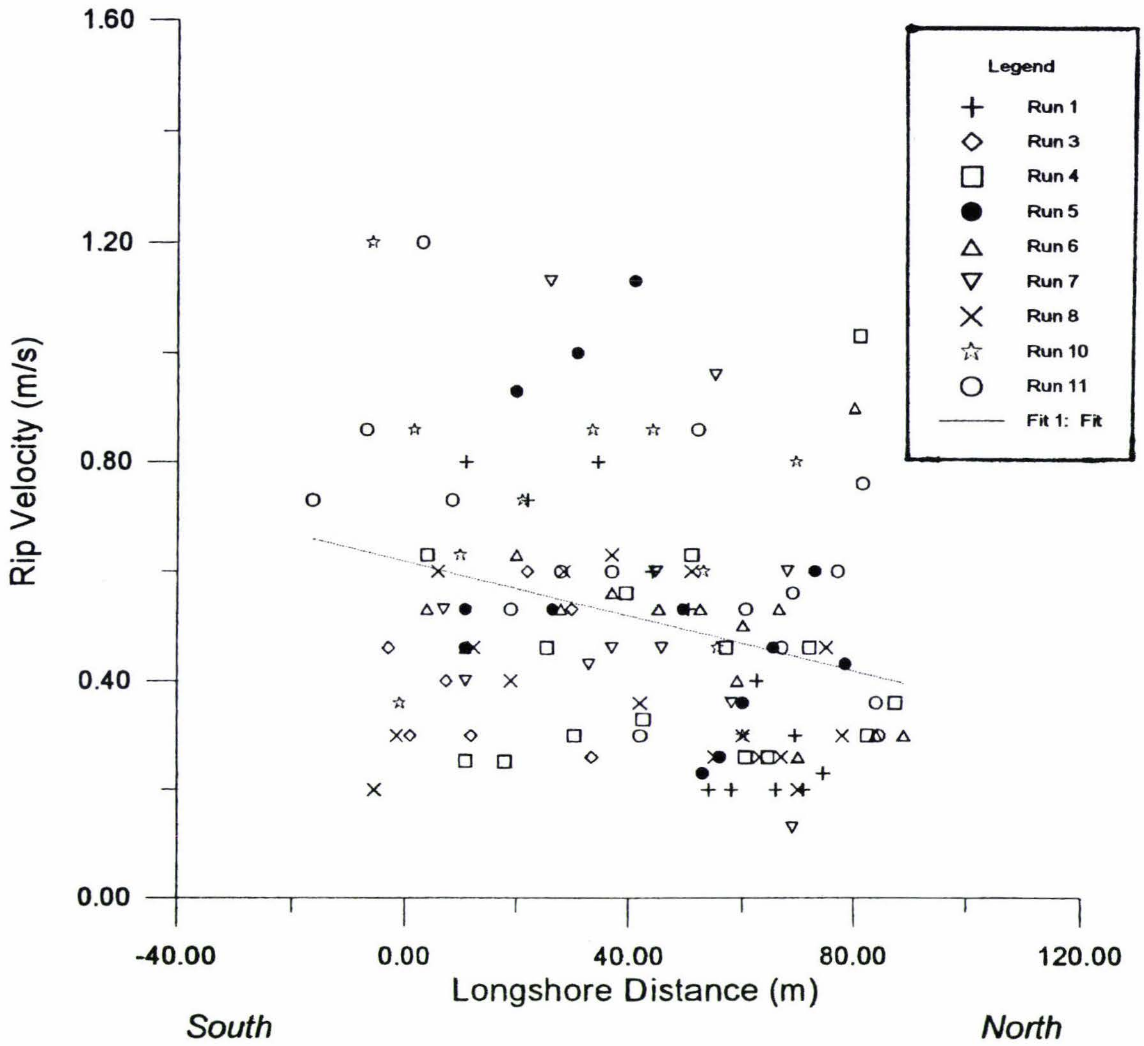


Figure 5.20 Station two longshore distance verses rip velocity.

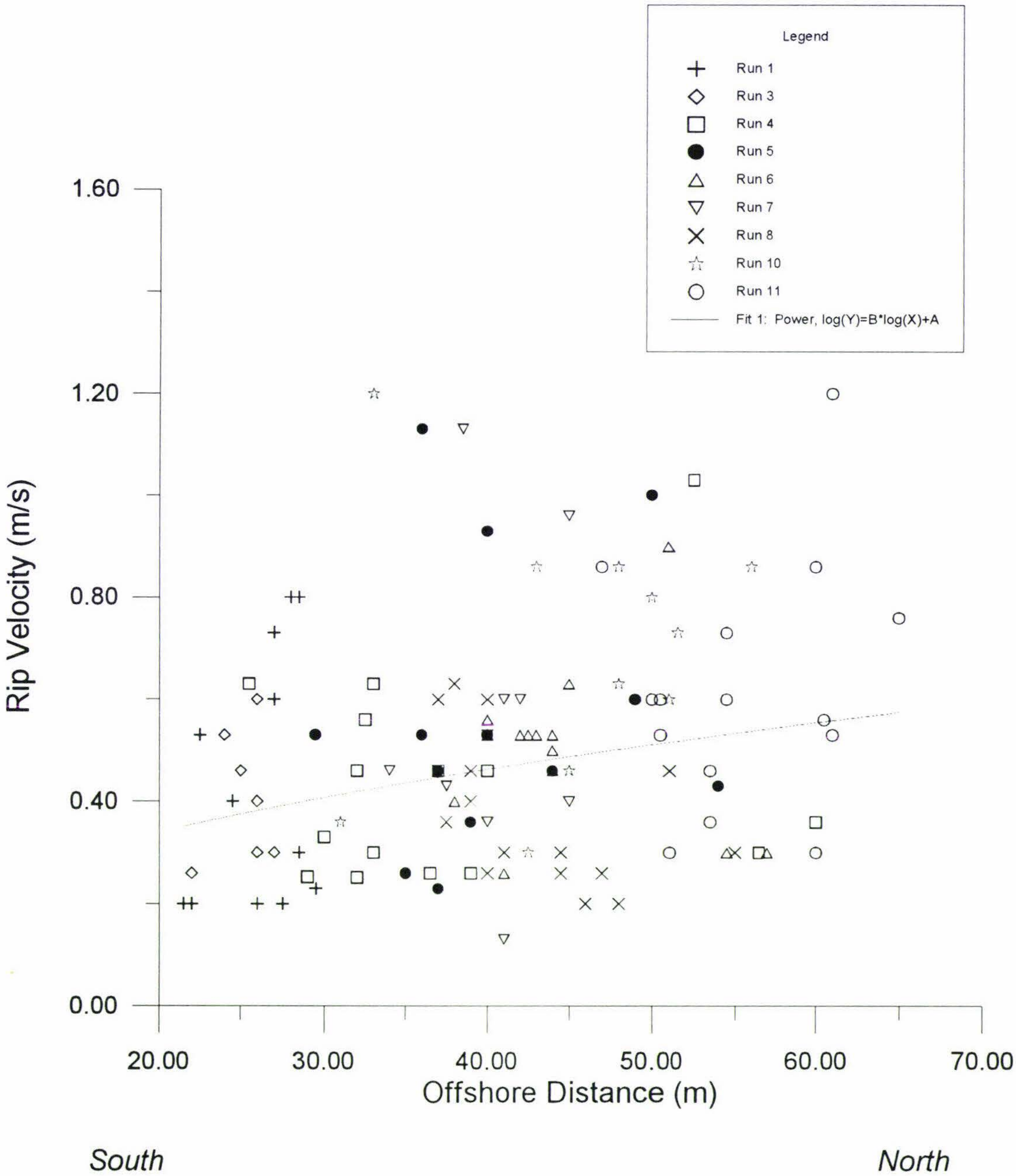


Figure 5.21 Station two rip velocity verses offshore distance.

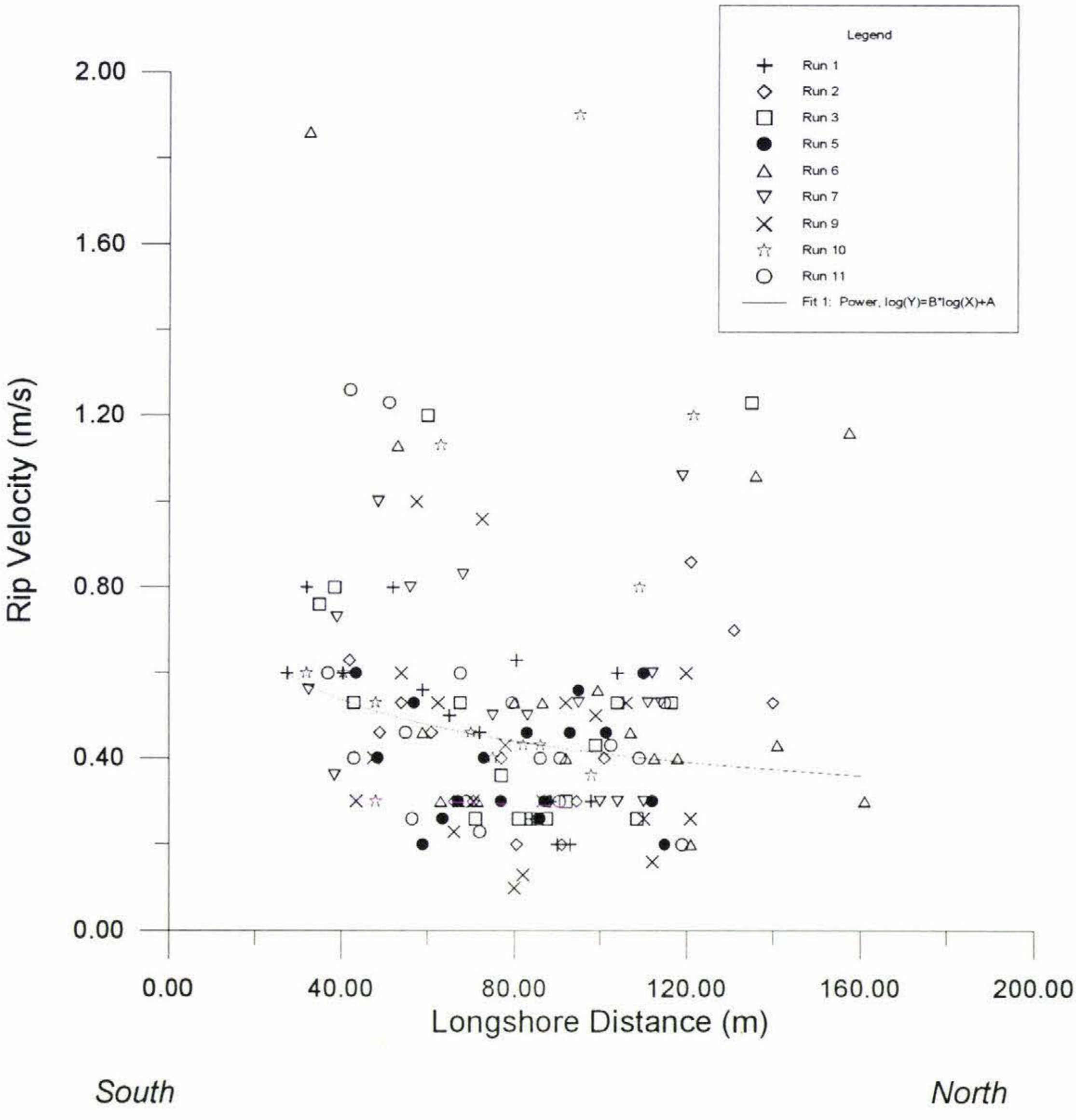


Figure 5.22 Station three, rip velocity verses longshore distance.

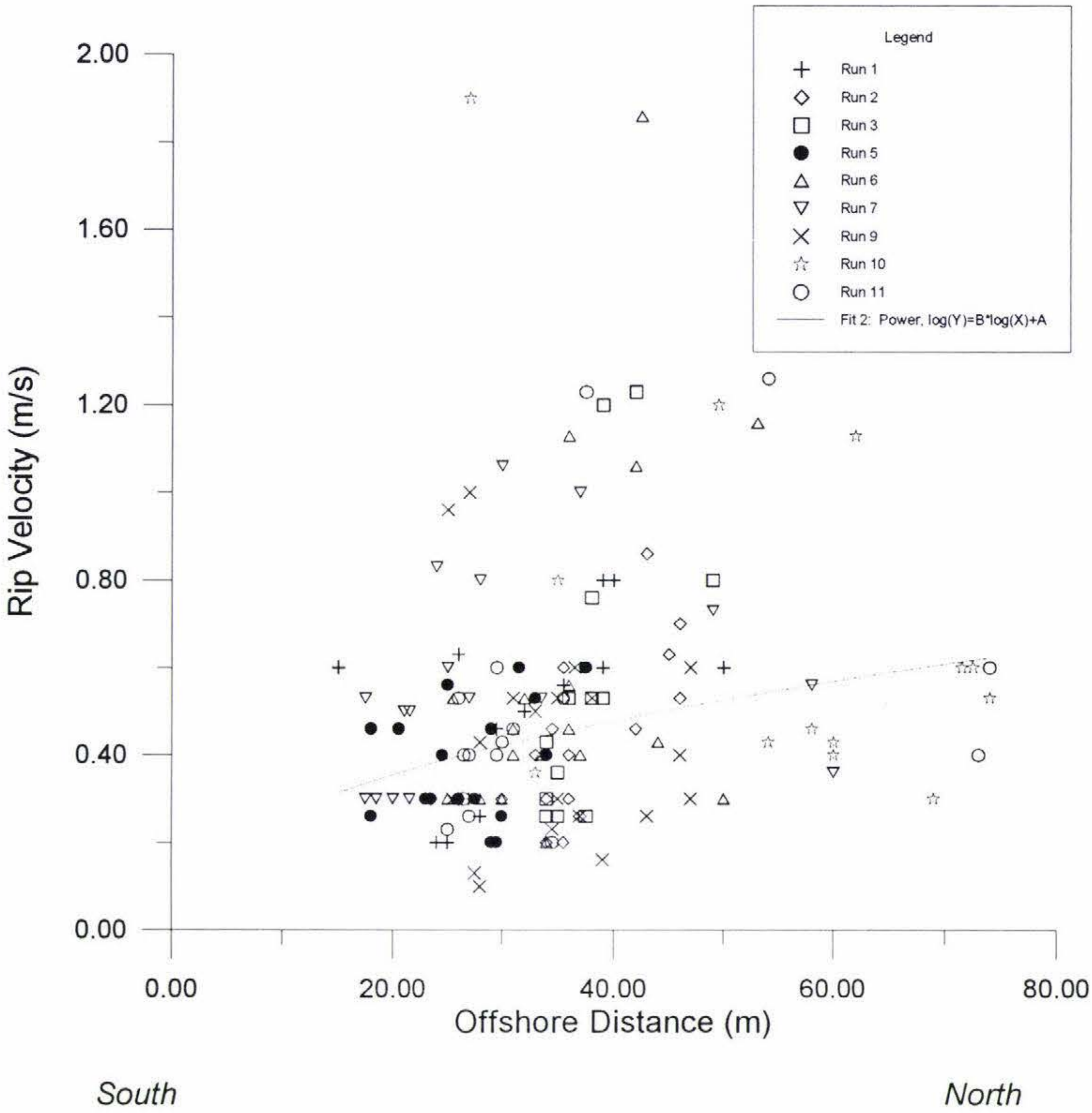


Figure 5.23 Station three, rip velocity verses offshore distance.

## 5.9 RIP DENSITY AND RIP VELOCITY

Because the Gap is an unusual case, in that it is highly topographically controlled, an investigation was also carried out on rip densities in the embayment.

The rip density, or number of rips per kilometre of coastline, can be predicted through the equation found in Chapter 4.2 of this research:

$$Y_r = 1.18X_s + 71.75$$

where $Y_r$ is the spacing between rips, and $X_s$ is the surf zone width. The surf zone width at the Gap was approximately 200 metres. Therefore, it is predicted that the spacing between rips would be 235.70 metres. This value differs markedly from the actual spacing between the two rips at either end of the Gap that was approximately 450 metres.

A second parameter that provides a further perspective on the rip density of the Gap embayment is the non-dimensional embayment scaling predictor proposed by Martens *et al.* (in press, cited in Short, 1999), which predicts the degree of headland impact on surf zone morphology and currents. The scaling parameter δ' is based on the equation:

$$\delta' = S_l^2/100C_lH_b$$

where $S_l$ is the shoreline length, $C_l$ is the embayment width, and $H_b$ is the wave height. The degree of headland impact can be predicted using the non-dimensional embayment scaling predictor δ':

| | |
|---|---|
| $\delta' > 19$ | normal beach circulation |
| $\delta' = 8\text{-}19$ | transitional circulation |
| $\delta' < 8$ | cellular beach circulation. |

Normal beach circulation consists of the micro and macro tidal models proposed by Wright and Short (1984) Short and Aagaard (1993) and Short and Masselink (1993). Transitional circulation occurs when the shape and size of the embayment begins to influence the surf zone circulation. This is initially characterised by longshore currents flowing seaward against each headland, while some normal beach circulation occurs away from the headlands.

Cellular circulation occurs when the topography dominates the circulation of the entire embayment. This results in the pre-dominance of longshore flow within the embayment, and strong, seaward flowing mega-rips (Short, 1985) occurring at one or both ends of the embayment, and in the case of longer embayments also away from the headlands (Short and Masselink, 1999).

In the case of the Gap, wave heights were recorded for the inner and outer surf zone, at 1.5 metres, and 2.0 metres respectively. Shoreline length is approximately 950 metres and embayment width is 400 metres. Therefore, the embayment scaling parameter when wave height equals 1.5 metres is:

$$\delta' = 9502/100\times400\times1.5$$
$$= 15.041667$$
$$= 15.$$

When wave height equals 2.0 metres, the embayment scaling parameter is:

$$\delta' = 9502/100\times400\times2.0$$
$$= 11.28125$$
$$= 11.$$

In both cases the non-dimensional embayment scaling predictor indicates an embayment that is in a transitional circulation system, although the outer surf zone value suggests that the circulation system could tend towards the cellular dominated system rather than a normal beach circulation system.

The fact that the Gap embayment is in a transitional circulation system, where the end effects of the headland begin to influence the surf zone morphology, provides a good indication as to why the surf zone width predictor equation for rip spacing is inaccurate in this case.

Furthermore, for a cellular beach circulation to dominate using the Martens *et al.* (in press) model, the wave height in the Gap embayment must be greater than 2.82 metres. To achieve normal beach circulation the wave height must be less than 1.19 metres.

Two issues emerge from the Martens *et al.* (in press) model. Firstly, how has wave height been determined and therefore where have wave height measurements been taken from. There was a 0.5 metre difference between wave height at the entrance to the Gap and within the Gap. However, it is not clear which wave height value should be used. Secondly, the high rip velocity values may suggest that this rip is in fact a mega-rip (Short, 1985). This leads to the possibility that the Marten's *et al.* (in press) equation may need to be refined through the investigation of a wide range of embayed beaches, to insure that an accurate classification of beach systems is found.

### 5.10 DISCUSSION

The relationship between the morphology of a rip channel and the velocities of a rip are of particular interest. A major feature found in this experiment is the similarity between the middle and southern survey areas. Both had relatively similar rip velocity ranges. However the middle topographical survey indicates a much more defined channel at this location in comparison with the southern survey (Figure 5.4 and Figures 5.7a,b). This result is somewhat surprising, since it is generally expected that a more defined channel would result in significantly greater rip velocities.

In contrast, the northern station, which was located only 50 metres north of the middle station, was distinct from both the middle and southern stations. Rip velocities were significantly higher throughout this area of the rip that was investigated. The channel morphology in particular is more defined. The northern station encompassed the area of the rip where it began to exit the Gap. The effect of the enclosure provided by the Reef, and the fact that at this point the majority of the water was exiting both from the Gap and the smaller northern inlet contributed to the increased velocity of the rip current. The topographic controls and shear volume of water being driven at this point also contribute to the creation of such a well-defined trough.

The density of rips within the embayment may also provide some explanation for the significantly high rip velocities found here. A value of 236 metres was calculated for the predicted rip spacing based on surf zone width. This suggests that there should have been three rips within the embayment, rather than just two. The Martens *et al.* (in press) predictor for the degree of headland influence suggests that the Gap was in a transitional circulation phase. This may imply that under normal conditions the amount of water exiting the Gap through the rip at the northern end of the beach would exit through two separate rips. Therefore, rip velocities were high due to the shear volume of water that was forced to exit through this one rip current.

Because of the short nature of the experiment, it is uncertain whether there is a significant effect from tidal modulation on this particular rip system. Investigation over a longer period of the tidal cycle is needed to confirm any results related to tidal modulation found here.

## 5.11 CONCLUSION

The Gap embayment is an example of beach that is affected on a regular basis by the control of end effects from the prominent headlands that are present. During this investigation, the Gap was in a transitional state (Martens *et al.*, in press) where end effects exerted increasing controls on the morphology of the surf zone.

High periodic rip velocities were recorded at the northern end of the embayment, where a major rip exited the Gap. Velocities within the rip current exceeded $3ms^{-1}$ on four occasions, and were greater than $2ms^{-1}$ at three further times. Short (1985) has stated that the velocity of currents within mega-rips can reach $3ms^{-1}$, however, the Gap is not considered to be a mega-rip under the Martens *et al.* (in press) classification.

The assumption that mega-rip current velocities peak around $3ms^{-1}$ is based on anecdotal evidence. This research suggests that this value is likely to be an under-estimate, and therefore, further field investigations are needed to assess the true nature of rip and mega-rip current velocities.

# CHAPTER SIX: RIP CURRENTS AT THE MODERATE TO HIGH ENERGY TARANAKI COASTLINE

## 6.1 INTRODUCTION

The investigation in Chapter Four produced a range of interesting, and at times, surprising outcomes. A number of the results, particularly those involving wave climate, produced very poor relationships. These outcomes are, to some extent, due to temporal variability of wave height and period on beaches. Actual values for these parameters were unknown for beaches displaying rip channels/currents in the aerial photographs that were analysed. Therefore, the author endeavoured to obtain field data from a range of beaches around the New Zealand coastline, in an attempt to gain a better understanding of some of the relationships found in Chapter Four. A second focus for this investigation was to explore the interactions between the spacing and morphology of rip currents, and the velocity of water flowing within rip currents. Although investigations carried out at Taranaki were successful, attempts to examine rip currents at Tairua and Piha beaches failed. Clarification on the difficulties faced at these sites is elaborated in Chapter One.

## 6.2 THE SITES

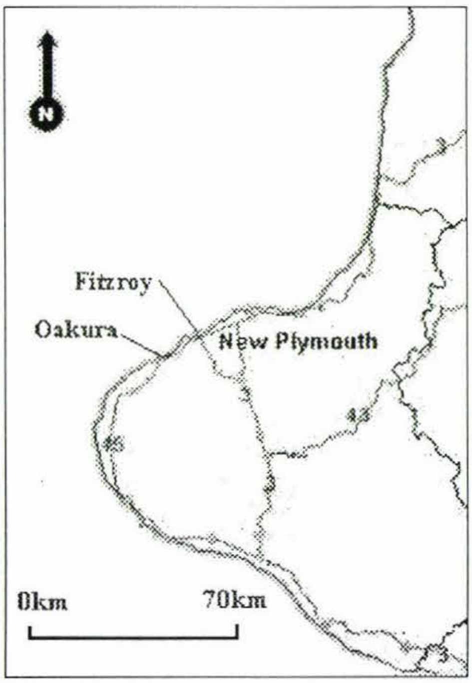


Figure 6.1 Taranaki location map.

Two beaches were investigated along the Taranaki coastline: Fitzroy, a popular surf beach adjacent to the city of New Plymouth; and Oakura, which is located approximately 15 minutes south of New Plymouth (Figure 6.1). The average wave height for both beaches is 1.5 metres (Hesp and O'Dea, 1999b). The sediment is typical of most of the west coast of the North Island, with particularly high concentrations of dense titanomagnetite sands dominating the sediment composition of the beaches.

Fitzroy is a high-energy mesotidal beach. The bathymetry of this beach is complex with predominant reef and channel structures of inter-bedded lahar deposits (McComb *et al.,* 1997). The substrate is intermittently overlain with sand, gravels and boulders (Arron and Mitchell, 1984), which were observed to control the morphology and location of the rip currents to some extent during the investigation (Figure 6.2). On the 16th of September 2000 the beach was in a single bar, transverse bar and rip system with waves of approximately one metre in height. The mean sand grain size was found by Hesp and O'Dea (1999a) to be 2.27 phi, indicating a relatively fine-grained sand. The sediment fall velocity for the Fitzroy beach sediment is $0.03ms^{-1}$ (Hesp and O'Dea, 1999a).

Figure 6.2 Fitzroy Beach: location of study site displaying boulders that controlled the rip morphology to some extent.

Oakura beach is a moderate to high energy mesotidal beach (Figure 6.3 and 6.4). On the 17th of September 2000 the beach was in a two bar system, with an inner, rhythmic bar and beach type, and a dissipative outer bar. The wave height was approximately 1.5 metres. The mean grain size is 0.99 phi (Hesp and O'Dea, 1999a), indicative of a coarse to medium sand grain size. The sediment fall velocity is $0.06 ms^{-1}$ (Hesp and O'Dea, 1999a).

Figure 6.3 The Oakura beach site, taken from the foredune.

The tidal regime for the Taranaki Coastline on the 16th and 17th of September is shown in Table 6.1. The tidal range was between 3.1 and 3.2 metres during the period of investigation.

| | 16th September | | 17th September | |
|---|---|---|---|---|
| | Time | Height | Time | Height |
| Low | 0432 | 0.3m | 0507 | 0.3m |
| High | 1040 | 3.4m | 1113 | 3.5m |
| Low | 1648 | 0.3m | 1723 | 0.3m |
| High | 2252 | 3.5m | 2326 | 3.5m |

Table 6.1 Tidal Regime for the Taranaki Coast (Ministry of Transport, 2000).

6.4 Oakura Beach, photograph is taken while standing on the inner bar at low tide.

## 6.3 General Rip Characteristics

The rips studied at Fitzroy and Oakura Beach exhibited highly variable characteristics. Both rips were sporadic in both strength and location. This could be partially accounted for at Fitzroy due to the affects of the sub-aqueous boulders. Sediment was scoured from around the rocks. This produced topographic depressions in the bar, resulting in more advantageous locations for rips to occur.

Three rip currents were observed at the Oakura site during the investigation. The occurrence of rips at Oakura was highly variable, with dominance of each rip current fluctuating between the three locations over a matter of minutes. Due to the rhythmic bar and beach type of the inner bar, longshore flows within rip feeder currents were more evident at Oakura than at Fitzroy. The direction of longshore flow was just as variable as the location of the rip currents, and depended on which rip was dominating at the time.

An objective of this research was to gain rip velocity measurements over a tidal cycle. However, the high degree of variability for rip location and strength at both sites resulted in only two complete rip velocity measurements, one for each site. It was also observed that at low tide on both beaches, the inner bars that produced the rip currents were completely out of the water. However, an increase in rip velocity at low tide has been observed on many occasions at both beaches (A. Flynn, Pers. Obs.).

## 6.4 RIP SPACING

The spacing between rips was measured at Fitzroy and Oakura beach by pacing out the distance between each rip along the beach. These measurements were confirmed through the use of paced measurements of objects, such as the distances between two bridges or surf life saving clubhouses. These were then compared with actual distances on the relevant topographical map to establish distances in metres.

The mean spacing between rips on Fitzroy Beach was 133.90 metres, with a standard deviation of 35.20 metres and a range from 79.30 metres to 200.20 metres. The mean spacing between rips on Oakura Beach was 172.38 metres, with a standard deviation of 56.12 metres and a range from 97.50 metres to 247 metres.

## 6.5 TOPOGRAPHICAL SURVEYS

A topographical survey was carried out at both beaches. Figure 6.5 shows the Digital Elevation Model and contour map for Fitzroy Beach. The survey was carried out where a rip trajectory and velocity profile was obtained. The lack of a defined rip channel provides an explanation for the difficulty in obtaining a series of rip velocity profiles over a tidal cycle.

The Digital Elevation Model and contour map for Oakura Beach is shown in Figure 6.6. This survey shows a more defined series of holes in the surf zone. The inner bar is present at approximately 130 metres, horizontal distance. A survey of the outer bar was not made due to difficulties reaching it in the surf conditions.

Rip current location and velocity is highly variable (Huntley *et al.*, 1988). Rips at both Oakura and Fitzroy were observed to be unsteady and episodic. The lack of a defined rip channel at these beaches, particularly Fitzroy, provides some explanation for the difficulties incurred when attempting to measure rip current velocity. Smith and Largier (1995) observed similar, unsteady, episodic rip currents that reoccurred periodically. They proposed that the unsteady nature of the rip currents suggested that the offshore 'burst' depleted the nearshore energy reservoir, which in their case was stored up in the longshore flow, and the system was reset.

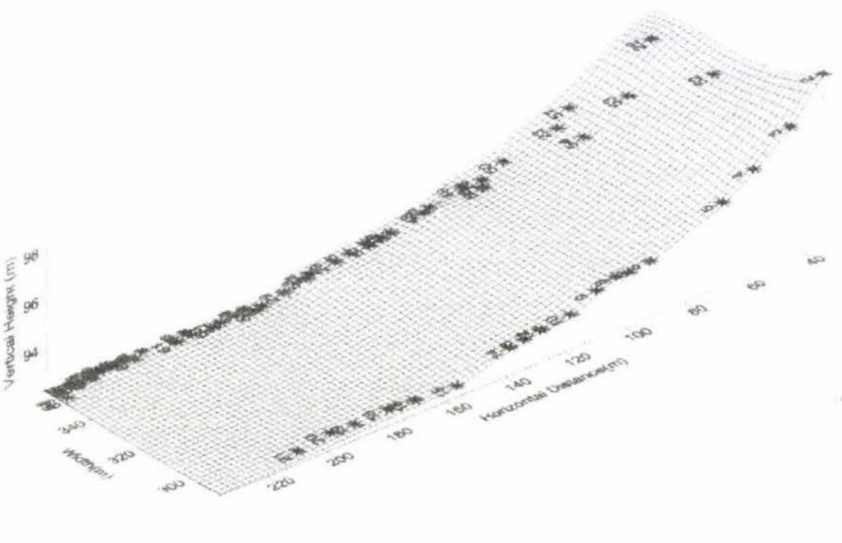

Figure 6.5a Digital Elevation Model of the location of the rip current in the Fitzroy Beach surf zone.

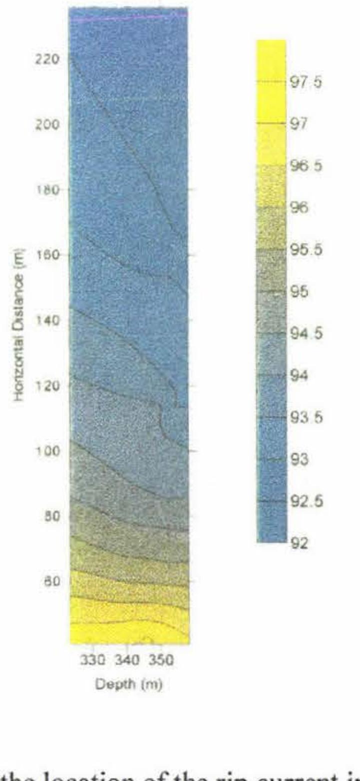


Figure 6.5b Contour map of the location of the rip current in the Fitzroy Beach surf zone.

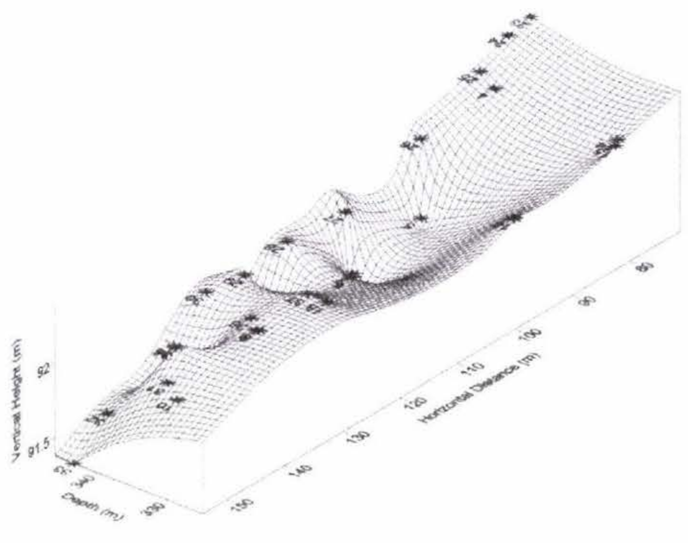


Figure 6.6a Digital Elevation Model of the location of the rip current in the Oakura Beach surf zone.

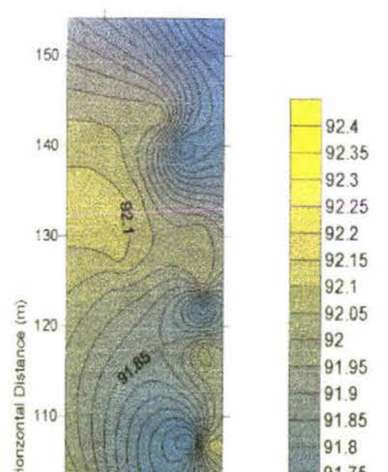


Figure 6.6b Contour map of the site of the rip in the Oakura Beach surf zone.

## 6.6 RIP TRAJECTORIES

Rip float experiments were conducted to determine lagrangian rip velocity flows. This involved the use of the method described by Short and Hogan (1994), which utilised human floaters (Brander *et al.*, 1999), who floated freely in the rip current. Their trajectories were tracked using two compasses at a known distance apart. The position of the rip float was recorded every 15 seconds, with measurements taken from the float's head. Human rip floats were used owing to difficulties in distinguishing the oranges because of the impacts of breaking waves.

Figure 6.7 illustrates the trajectory of the rip current at Fitzroy Beach. This trajectory is characterised by a relatively straight course through the surf zone, characteristic of a rip in the transverse bar and rip state. The effects of waves on the human float are evident, particularly at approximately 130 metres and 160 metres from the survey location, where the rip float is pushed towards the shore. Measurements cease at around 225 metres seawards due to difficulties in observing the rip float. However, it is noted that the rip float actually traveled approximately 100 metres further out to sea from this point. There was no evidence of any substantial return flow.

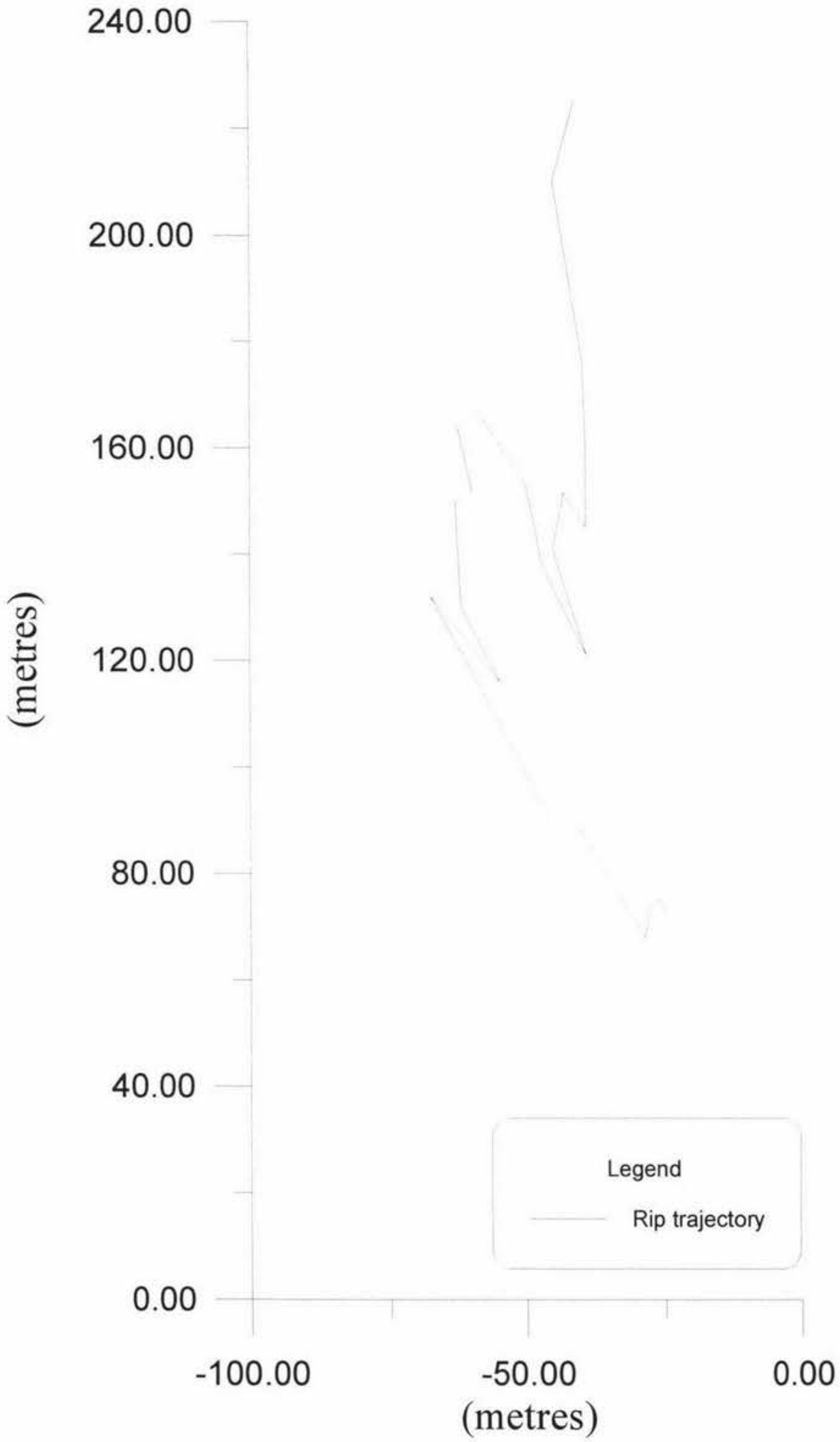


Figure 6.7 Rip current trajectory at Fitzroy Beach, Taranaki.

In contrast, the trajectory of the rip at Oakura Beach, as shown in Figure 6.8 is very different. A distinct circulatory system was observed at this location. The rip float was moved initially in a cross-shore direction (Rip I). As he/she went further into the surf, breaking waves played a significant role at times, pushing the rip float back towards the shore.

The outer bar played a substantial role in the nature of this particular rip current. Instead of the rip exiting the surf zone as observed at Fitzroy, the outer bar acted as a barrier. The rip float travelled in a shoreward direction (return flow). This could be attributed to a return flow of the rip current, the influence of waves pushing the rip float towards the shore, or a combination of the two mechanisms. This flow was then shown to return back to the initial exiting rip current, although it seems to have moved approximately 30 metres to the left of the original location (Rip II).

Another interesting feature of the rip at Oakura is the pulsing nature it exhibits. The rip float passes through the rip current on three occasions. The lack of any substantial effect from the rip current (i.e. the rip float is not caught in the rip) indicates that the rip was relatively inactive at these times. This is indicative of rip pulsing occurring.

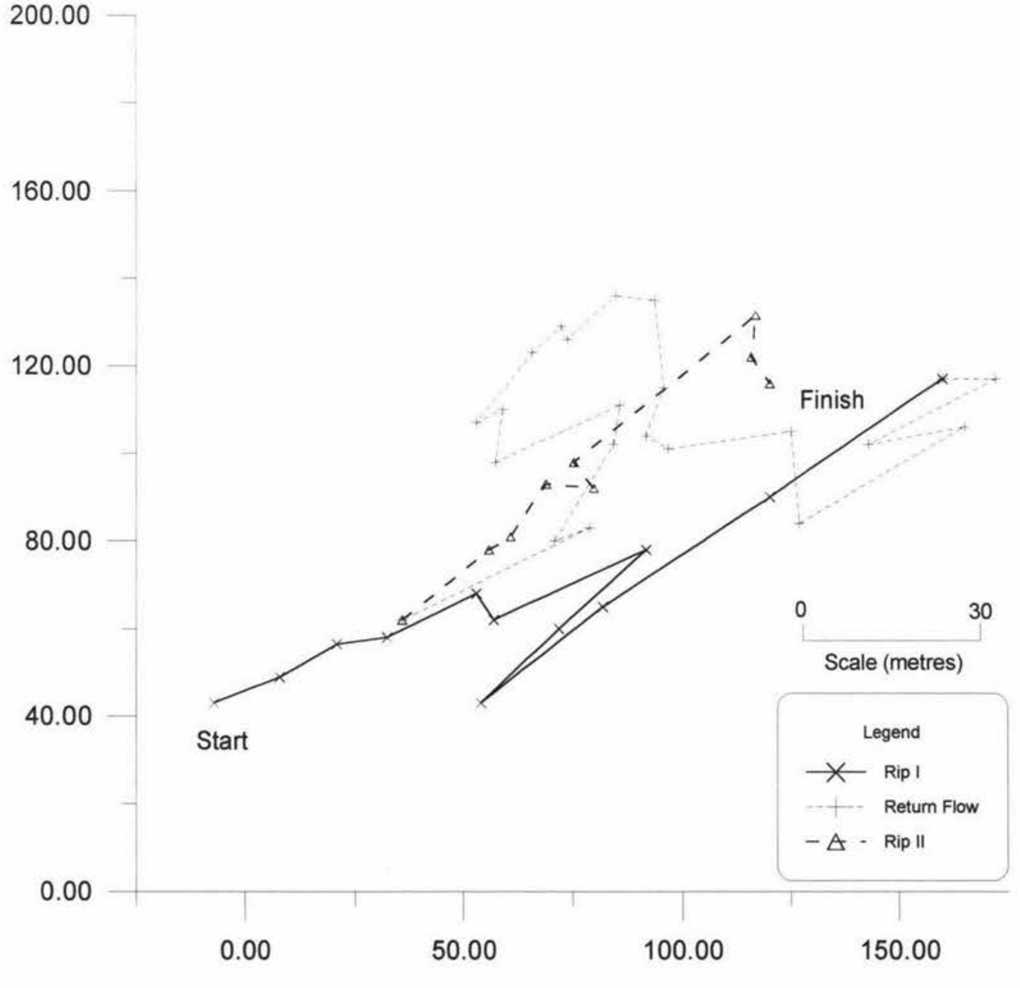


Figure 6.8 Rip current trajectory for Oakura Beach.

## 6.7 RIP VELOCITY

Rip velocity ($v_r$) was found by taking the distance of each 15-second interval and dividing it by 15 to get the distance travelled per second ($ms^{-1}$). Mean rip velocities ($\bar{x}_r$) for each run were calculated using the equation:

$$\bar{x}_r = (\Sigma\ v_r / n) / 15sec$$

where $v_r$ is the velocity found for each 15 second interval, and n is the number of intervals.

The rip velocity profile for Fitzroy Beach is shown in Figure 6.9. The flow of the rip current displays a strong pulsing nature. The mean rip velocity was 0.93 $ms^{-1}$, with a standard deviation of 0.54 $ms^{-1}$. The lowest velocity was 0.13 $ms^{-1}$, prior to the rip float getting caught in the rip current. The maximum rip velocity was 1.57$ms^{-1}$ as the rip float went through the surf zone. Although rip velocities peaked as the float went through the surf zone, the influence of waves was significant at times, particularly between 170 and 240 seconds.

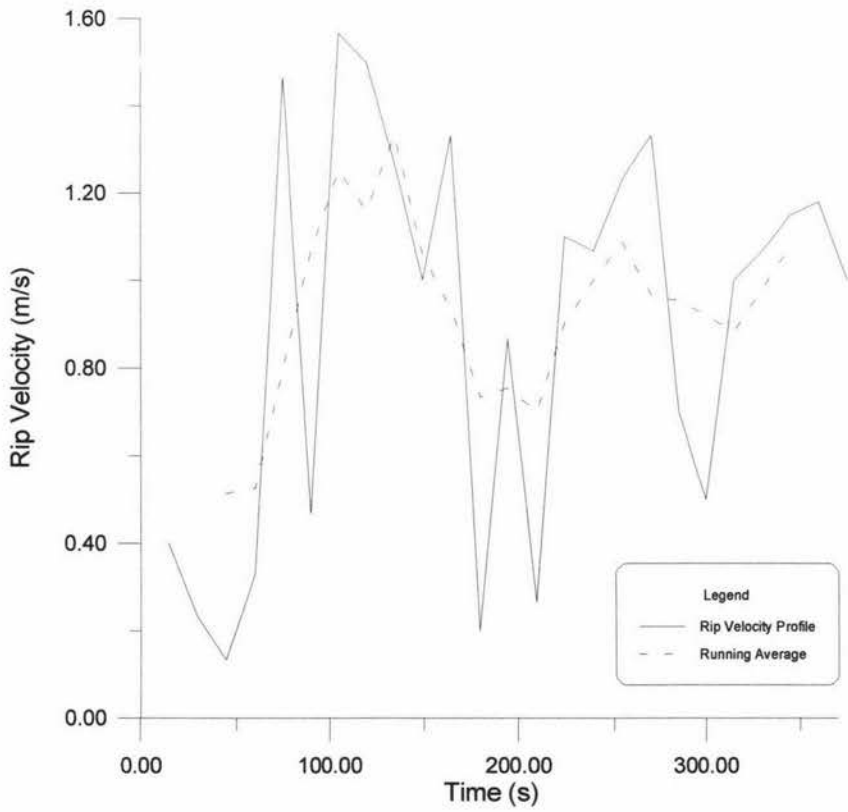


Figure 6.9 Rip velocity profile for Fitzroy Beach, run two.

The rip velocity profile for Oakura Beach is shown in Figure 6.10. The mean rip velocity for the Oakura Beach run was $1.03ms^{-1}$, with a median of $0.80ms^{-1}$. The rip trajectory shows that measurements of the rip current were taken twice as the rip went over the first bar, with only one return flow recorded. This may provide some explanation for the relatively large differences between median and mean rip velocity values. A standard deviation of $0.69ms^{-1}$ was established. A minimum value of $0.15ms^{-1}$ was found when the rip float was moving in a landward direction. Rip velocities below $0.50ms^{-1}$ occurred throughout the run, however they were more common as the rip float moved towards the beach. A maximum rip velocity of $2.68ms^{-1}$ occurred as the rip float was taken through the surf zone for the second time. Speeds of greater than $2ms^{-1}$ occurred on five occasions, as the rip float was moving in a seaward direction.

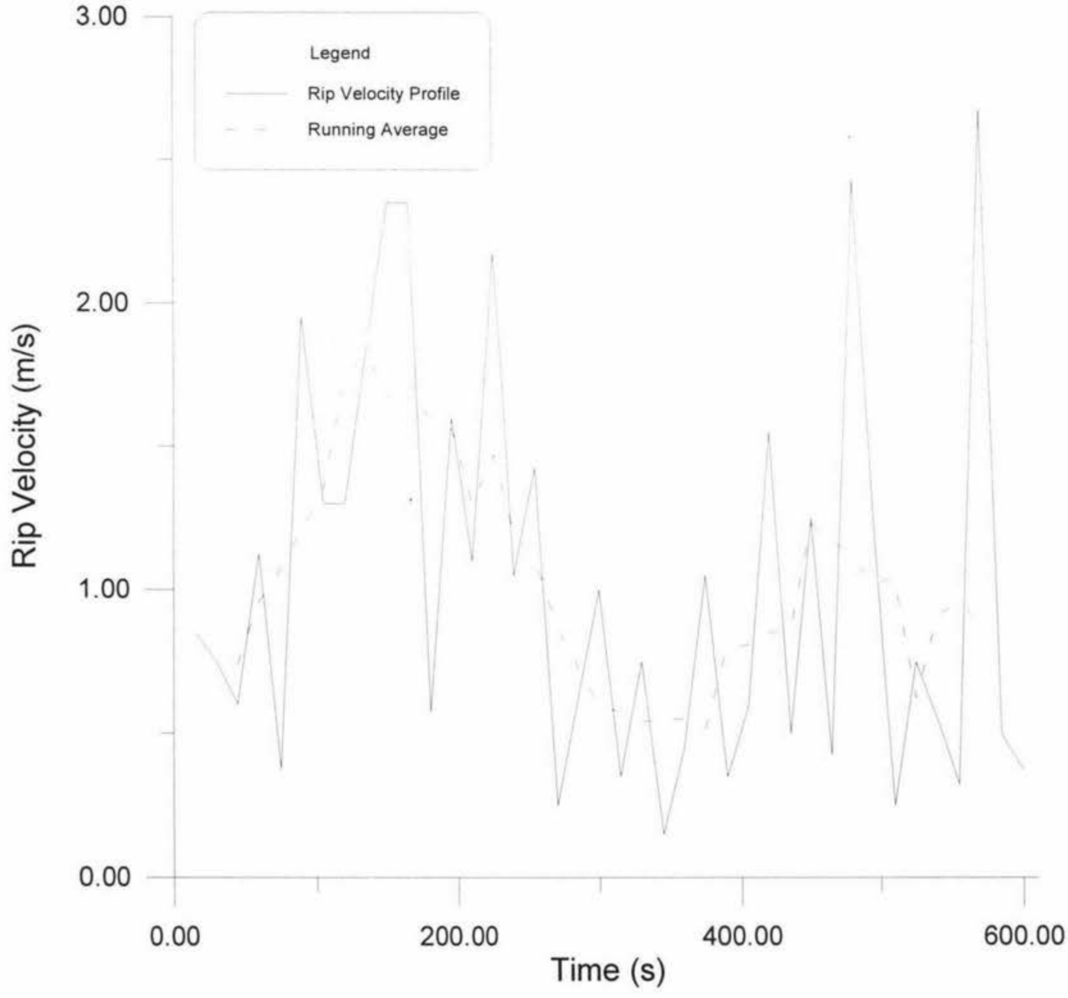


Figure 6.10 Oakura Beach rip velocity profile run two.

## 6.8 Comparison With Other Rip Velocity Measurements

Table 6.2 shows a comparison of the Fitzroy and Oakura rip velocity measurements with those from the literature. The mean rip velocities from Fitzroy and Wright and Short's (1983) transverse bar and rip (TBR) example are quite similar and are also characterised by similar wave height values. However, the rip velocity and wave height values obtained from Fitzroy are twice that of Huntley's *et al.* (1988) example. Mean rip spacing is also smaller for Fitzroy Beach in comparison.

The mean rip velocity and wave height found for Oakura are similar to that found by Wright and Short's (1983) rhythmic bar and beach (RBB) example. Rip velocities for the example from Aagaard *et al.* (1997) are lower than Oakura's outcome, but the example is also characterised by a smaller wave height.

| Source | Beach Type | Wave Height | Mean Rip Spacing | Mean Rip Velocity | Maximum Rip Velocity |
|---|---|---|---|---|---|
| Fitzroy | TBR | 1.0m | 134m | $0.9ms^{-1}$ | $1.57ms^{-1}$ |
| Oakura | 2 bar, inner RBB | 1.5m | 172m | $1.0ms^{-1}$ | $2.67ms^{-1}$ |
| The Gap, Castlepoint | LBT topo-controlled | 1.5-2m | 450m | $1.7ms^{-1}$ | $4.13ms^{-1}$ |
| Wright and Short (1983) | RBB | 1-1.5m | Unknown | $0.9ms^{-1}$ | Unknown |
| Wright and Short (1983) | TBR | 1.0m | Unknown | $1.0ms^{-1}$ | Unknown |
| Brander et al. (1999) | LBT | 1.5-2.5m | 750m | $0.6\text{-}0.8ms^{-1}$ | $1\text{-}1.4ms^{-1}$ |
| Aagaard et al. (1997) | 2 Bar, inner RBB | 1.3m | Unknown | $0.6ms^{-1}$ | Unknown |
| Huntley et al. (1988) | TBR pocket beach | 0.47m | 200m | $0.4ms^{-1}$ | $0.65ms^{-1}$ |

Table 6.2 Comparison between wave height, rip spacing and rip velocity measurements at Fitzroy, Oakura and The Gap beaches with values found in the literature.

## 6.9 CONCLUSION

The rip currents investigated at Fitzroy and Oakura beach provide quantitative information on unsteady, episodic rip currents. At both locations, rip current channels were poorly defined.

The single bar, transverse bar and rip morphology observed at Fitzroy produced a relatively straight rip trajectory, with the rip float travelling at least 300 metres in a seawards direction. The double bar, rhythmic bar and beach inner bar, and dissipative outer bar morphology at Oakura produced a particularly interesting spatial pattern for the rip trajectory. The outer bar acted as a barrier to the rip current, forcing the rip to stay within the surf zone. A possible combination of return flow from the rip current and the effect of incoming waves resulted in a circulatory system being evident at Oakura.

Mean rip velocities are within the range stated in the literature (i.e. Shepard *et al.*, 1941; Ingle, 1966; Cook, 1970; Reimintz, 1971; Wright and Short, 1984; Brander, 1999a) with mean rip velocities of $0.93ms^{-1}$ and $1.03ms^{-1}$ at Fitzroy and Oakura beach respectively. Maximum rip velocities at both sites were higher, with $1.57ms^{-1}$ at Fitzroy, and $2.68ms^{-1}$ at Oakura.

# CHAPTER SEVEN: CONCLUSION

## 7.1 SHORT AND BRANDER'S (1999) RIP SCALING HYPOTHESIS IN THE NEW ZEALAND CONTEXT

Short and Brander (1999) suggested that a scaling relationship exists between rip current densities (i.e. the number of rips per kilometre of coastline) based on five global wave climate regimes originally proposed by Davies (1980). Utilising this classification, New Zealand can be characterised by two regional wave climates, west coast swell and east coast swell for west and east coasts respectively. Short and Brander proposed that there is a scaling relationship between east coast and west coast swell rip densities of 2.5, with 2.5 times as many rips on east coast swell beaches compared to west coast swell beaches. It was also suggested that other rip morphometric parameters, such as rip width and rip length, have a similar scaling relationship.

The present investigation found that in no case was a rip density scaling relationship resembling 2.5 found between west coast swell and east coast swell beaches in New Zealand. A scaling relationship of 1.44 for rip spacing was the largest difference between the two regional wave climates. The rip morphometric parameters of rip length and rip width had a scaling relationship of 1.41 and 1.38 respectively, while surf zone width had the smallest difference at 1.35.

A second factor contributing to the rejection of Short and Brander's hypothesis is the overall regression coefficients for a range of not only rip and surf zone morphometric parameters, but also sediment and wave climate variables. The data set was analysed in terms of the respective regional wave climate and the total data. The total data set which included all beaches (i.e. WCS and ECS) in every case provided higher correlation coefficient values, and therefore more statistically significant relationships, than the outcomes based solely on separating the respective regional wave climates (WCS and ECS). This suggests that regional wave climate is not a suitable classification system on which to predict rip spacing for the New Zealand coastline.

Furthermore, the use of significant wave height as a predictor for rip spacing provided one of the poorest outcomes in the data set, with a regression coefficient value of 0.06 and a p-value of 0.96, suggesting that there is no relationship between significant wave height and the spacing between rips. In contrast, the relationship between sediment size and rip spacing produced the strongest relationship in this data set, with a regression coefficient value of 0.61 and a p-value of $<0.01$.

A further implication from these findings is that the use of one factor which influences rip spacing and rip morphology in general, such as wave climate, is too simplistic on which to base predictions of rip spacing. Rips by their very nature are the outcome of complex interactions between a range of dynamic factors, wave climate being just one. To suggest that the spacing between rips can be classified under its regional wave climate ignores the relatively strong influence that additional factors such as sediment size and type may exert on rip spacing.

## 7.2 MURIWAI BEACH AS A REPRESENTATIVE EXAMPLE OF A NEW ZEALAND WCS BEACH SYSTEM

The dataset utilised by Short and Brander (1999) employed 21 beaches, with 15 examples from six locations for the WCS regional wave climate, and 35 examples from 10 locations for the ECS regional wave climate. Muriwai Beach is classified as a WCS beach, and is the only example taken from the New Zealand coastline in Short and Brander's investigation. Muriwai Beach in both Short and Brander's and this current research is typically in an oblique wave state, producing a longshore bar and trough system, with the trough acting as a long-shore directed rip current.

However, when analysis was undertaken, Muriwai Beach was shown to be a significant outlier, particularly with regard to the relationships between rip spacing and surf zone width, rip spacing and rip length, and rip width and rip length. Therefore, it is concluded that Muriwai Beach is atypical of not only WCS beaches in New Zealand, but of most beaches found along the New Zealand coastline, and its sole use as a representative New Zealand WCS beach in Short and Brander's investigation is called into question. Furthermore, if Muriwai Beach is not a characteristic New Zealand WCS beach, an investigation into how appropriate other beach examples were within Short and Brander's research for their respective wave climate may be of interest.

## 7.3 Rip Spacing And The Relationship Between Sediment Size And Sediment Fall Velocity

Analysis of the correlation between rip spacing and sediment size proved to be the strongest relationship of the entire data set, with a correlation coefficient value of 0.61 and a p-value of $<0.01$. In contrast, sediment fall velocity, which is a variable utilised in a wide range of models including Huntley and Short's (1992) rip spacing predictor and a range of morphodynamic beach state model's (i.e. Wright and Short, 1984; Short and Aagaard, 1993; Masselink and Short, 1983) produced no statistically significant relationship, with a correlation coefficient value of 0.04 and a p-value of 0.29.

Both variables were calculated from the same sediment samples and subsequent analysis showed that there was a moderately strong relationship between these two parameters. Some differences occurred based on the effects of the denser titanomagnetite sands of the North Island's west coast, in comparison to the lighter quartzo-feldspathic sands of the east coast. This assessment indicated that it is unlikely that there were major errors in the measurement of the sediment fall velocity.

The results suggest that sediment fall velocity is not an adequate sediment parameter to use as a basis for predicting rip spacing. This outcome may also suggest that the reliance on sediment fall velocity as the parameter on which to include sediment characteristics in surf zone morphodynamic models may not provide as satisfactory an outcome as sediment size, and thus indirectly, beach gradient. This may be particularly important when beach sediments are made up of denser heavy minerals, as compared with the quartose Australian beaches, which the classic Short and Wright (1994) model is based on.

## 7.4 Topographic Controls On Rip Currents At The Gap, Castlepoint

The Gap embayment at Castlepoint was an example of a beach in a transitional state (Martens *et al.*, in press), where the end effects of the prominent headlands exerted increased controls on the morphology of the surf zone. Two rips were present, a particularly small rip current at the southern end of the beach, and a major rip current, removing the majority of the water from the bay at the northern end of the beach, which was the focus of the investigation.

Short (1985) has stated that the velocity of currents within mega-rips can reach $3ms^{-1}$. However, periodic rip velocities measured within the Gap rip exceeded $3ms^{-1}$ on four occasions, and surpassed $2ms^{-1}$ in a further three instances. Although this rip experienced a high degree of topographic control it could not be classed as a mega-rip under Marten's *et al.* (in press) classification system. It can be concluded from this outcome that our definitions of how fast rip currents can travel, particularly in mega-rip conditions, needs to be re-defined. The assumption that rip currents have peak velocities of around $3ms^{-1}$ is based on anecdotal evidence rather than actual rip velocity measurements. This current body of research not only suggests that rip currents can pulsate at faster speeds than was earlier thought, but also that there is a need for further research to assess the true nature of rip current velocities in a wide range of topographic environments.

## 7.5 Taranaki Coastline Rips

Although the data gained during experiments at Fitzroy Beach and Oakura Beach on the Taranaki coastline were limited, this research provides further quantitative information on rip current spacing and velocity.

The investigation along the Taranaki coastline showed that the beach state played an important role in the trajectory of the rip currents. The single bar, transverse bar and rip morphology of Fitzroy Beach produced a relatively straight rip trajectory. Rip velocities were fastest as the rip went through the surf zone. The double bar, rhythmic bar and beach inner bar and dissipative outer bar morphology at Oakura produced a particularly interesting rip trajectory spatial pattern. The outer bar controlled the rip by inhibiting its exit from the surf zone, thus contributing to the operation of a possible circulatory system.

Mean rip velocities at both sites fell within the general rip velocity range of between 0.35 and 1.5 $ms^{-1}$ suggested in the literature (Shepard *et al.*, 1941; Ingle, 1966; Cook, 1970; Reimintz, 1971; Wright and Short, 1984; Brander, 1999a). Velocities at both beaches were similar to the velocities found by Wright and Short (1983) for rips in similar beach states and wave climate conditions. However, maximum rip velocities at both sites were higher than those found in the literature, with $1.57ms^{-1}$ at Fitzroy and $2.68ms^{-1}$ at Oakura. The lack of quantitative investigations within the literature, particularly the lack of rip spacing measurements, resulted in an inability to seriously investigate the relationship between rip velocity and the spacing between rip currents.

## 7.6 Future Research

The results obtained in this research suggest a number of directions for future research.

1. Further investigate the relationship between rip spacing and rip velocity. A longer time frame and a wider range of beaches would be invaluable and would contribute to gaining a greater understanding of rip current processes.

2. Continue to investigate the relationship between rip spacing and other rip morphometric parameters, and the relationship between wave climate over a wide range of beaches and beach types. Results from this current body of research indicate that there was no relationship between significant wave height and the spacing between rips. However, the quality and accuracy of the wave climate data is variable, and previous investigations of single beach systems suggest that there is a strong relationship between rip spacing and wave height.

3. In Chapter Four an interesting relationship between rip spacing, sediment size and sediment fall velocity was identified. Further investigation into sediment characteristics is warranted, particularly the use of the sediment fall velocity parameter in a range of widely accepted morphodynamic models. An additional area to explore is the effect of denser titanomagnetite sediment when utilising the sediment fall velocity parameter in an array of models.

4. It was found at Piha Beach that although a visual assessment of the surf zone concluded that rip channels were present the *currents* were, in fact, inactive. The monitoring of rip current evolution and dynamics has recently been enhanced by the use of video camera techniques. However, this innovative technique cannot assess whether the rip is actually functioning or not. This may be an interesting area to scrutinise, in an attempt to increase the accuracy of research gained from video imaging techniques.

5. Further research is needed to gain actual quantitative data on rip velocity, and its relationship to rip and surf zone morphology, beach size and rip density. There is a lack of quantitative information on rip currents within the literature.

# REFERENCES


Aagaard, T., 1990, Infragravity waves and nearshore bars in protected, storm -dominated coastal environments. *Marine Geology,* 94: 181-203.

Aagaard, T and Masselink, G., 1999, *In* A.D. Short, *Handbook of Beach and Shoreface Morphodynamics,* John Wiley and Sons Ltd, New York, 72-113.

Aagaard, T., Greenwood, B. and Neilsen, J., 1997, Mean currents and sediment transport in a rip channel. *Marine Geology,* 140: 25-45.

Al-Ghadban, A.N., 1990, Holocene Sediments in a Shallow Bay, Southern Coast of Kuwait, Arabian Gulf. *Marine Geology*, 92: 237-254.

Arron, E.S. and Mitchell, J.S., 1984, *Distribution and depth of nearshore sediments, Port Taranaki to the Waiwakaiho River.* New Zealand Oceanographic Institute, DSIR.

Bogle, J.A., Bryan, K.R., Black, K.P., Hume, T.M. and Healy, T.R., 1999, Observations of geomorphic Parameters Using Video Images. *Proceeding of the 14th Australasian Coastal and Ocean Engineering Conference and the 7th Australasian Port and Harbour Conference*, 14-16th April, 1999, Perth. 70-75.

Bogle, J.A., Bryan, K.R., Black, K.P., Hume, T.M. and Healy, T.R., (in press) Video Observations of Rip Formation and Evolution. Submitted to the *Journal of Coastal Research.*

Bowen, A.J., 1969, Rip Currents, 1: Theoretical Investigations. *Journal of Marine Research,* 74: 5468-5478.

Bowen, A.J., 1980, Simple models of nearshore sedimentation: beach profiles and long-shore bars. *In* S.B. McCann (Ed.) *The Coastline of Canada.* Geological Survey Canada, Ottawa, Ontario, Paper 80-10: 1-11.

Bowen, A.J. and Inman, D.L., 1969, Rip Currents, 2: Laboratory and Field Observations. *Journal of Geophysical Research,* 74: 5479-5490.

Bowen, A.J. & Guza, R.T., 1978, Edge Waves and Surf Beats. *Journal of Geophysical Research,* 83: 1913-1920.

Bowman, D. and Goldsmith, V., 1983, Edge waves and surf beat. *Journal of Geophysical Research,* 83: 1913-1920.

Brander, R.W., 1999a, Sediment Transport in Low-Energy Rip Current Systems. *Journal of Coastal Research,* 15 (3): 839-849.

Brander, R.W., 1999b, Field observations on the morphodynamic evolution of a low -energy rip current system. *Marine Geology,* 157: 199-217.

Brander, R.W., 1997, *Field observations on the morphodynamics of rip currents*. PhD Thesis, Department of Geography, University of Sydney, Australia.

Brander, R.W., Short, A.D., Osbourne, P.D., Hughes, M.G. and Mitchell, D.M., 1999, Field measurements of a large-scale rip current system. *Coastal Sediments '99,* 562-575.

Cook, D.O., 1970, The occurrence and geologic work of rip currents of southern California. *Marine Geology,* 9: 173-186.

Cowell, P.J. and Thom, B.G., 1994, Morphodynamics of coastal evolution. *In* R.W.G. Carter and C.D. Woodroffe (eds), *Coastal Evolution: Late Quaternary Shoreline Morphodynamics,* Cambridge University Press, Cambridge, 33-86.

Carter, R.W.G., 1988, *Coastal Environments.* Academic Press, San Diego.

Dalrymple, R.A., 1975, A Mechanism for Rip Current Generation on an Open Coast. *Journal of Geophysical Research,* 80: 3485-3487.

Dalrymple, R.A and Lozano, C.J., 1978, Wave-current Interaction Models for Rip Currents. *Journal of Geophysical Research,* 83: 6063-6071.

Davidson-Arnott, R.G.D. & Greenwood, B., 1974, Bedforms and structures associated with bar topography in the shallow-water environment, Kouchibouguac Bay, New Brunswick, Canada. *Journal of Sedimentary Petrology,* 44: 698-704.

Davies, J.L., 1964, A morphogenic approach to world shorelines. *Zeitschrift fur Geomorphologie,* 8: 127-142.

Davies, J.L., 1980, *Geographical Variation in Coastal Development 2nd Ed,* London, Longman.

Davis, R.A. & Fox, W.T., 1972, Coastal processes and nearshore sandbars. *Journal of Sedimentary Petrology,* 42: 401-412.

Dean, R.G., 1973, Heuristic models of sand transport in the surf zone. *Proceedings of the Conference of Engineering Dynamics in the Surf Zone, Sydney, NSW,* 208-214.

Dean, R.G., 1977, *Equilibrium beach profiles: US Atlantic and Gulf Coasts.* Engineering Report 12. Department of Civil Engineering, University of Delaware.

Dolan, R., 1971, Coastal landforms: crescentic and rhythmic. *Bulletin of the geological society of America,* 82: 177-180.

Dubois, R.N., 1985, Development of a shoreline rhythm, outer banks of North Carolina. *Marine Geology,* 62: 31-53.

Flint, S.B., 1998, *Sediment Trapping in the Nearshore Coastal Environment.* Department of Earth Science, University of Waikato Unpublished MSc (Tech) Thesis.

Folk, R.L., 1974, *Petrology of Sedimentary Rocks.* Hemphills, Austin, Texas.

Goldsmith, V., Bowen, D. and Kiley, K., 1982, Sequential development of crescentic bars: Hahoterim beach, southern Mediterranean. *Journal of Sedimentary Petrology,* 52: 233-249.

Gourley. M.R., 1974, Wave set-up and Wave Generated Currents in the Lee of a Breakwater or Headland. *Proceedings of the 14th Coastal Engineering Conference, American Society of Civil Engineers.* 1976-1995.

Gourley, M.R., 1976, Non-uniform Alongshore Currents. *Proceedings of the 15th Coastal Engineering Conference, American Society of Civil Engineers.* 701 -720.

Greenwood, B, and Davidson-Arnott, R.G.D., 1979, Sedimentation and equilibrium in wave-formed bars: a review and case study. *Canadian Journal of Earth Sciences,* 16: 312-332.

Gruszczynski, M., Rudowski, S., Semil, J., Slominski, J. and Zrobek, J., 1993, Rip currents as a geological tool. *Sedimentology,* 40: 217-236.

Guza, R.T. and Thornton, E.B., 1982, Swash oscillations on a natural beach. *Journal of geophysical research,* 81(C1): 483-491.

Guza, R.T. and Inman, D.L., 1975, Edge Waves and Beach Cusps. *Journal of Geophysical Research,* 80: 2998-3012.

Hesp, P. and O'Dea, T., 1999, *Analysis of Selected New Zealand Beach Sediments.* Geography Programme, School of Global Studies, Massey University, Miscellaneous Publication Series 99/1.

Hesp, P. and O'Dea, T., 1999, *Surf Life Saving New Zealand, Summer 1997-1998 Club Statistics, Surf Conditions and Weather.* Geography Programme, School of Global Studies, Massey University, Miscellaneous Publication Series 99/2.

Hesp, P.A., Shepherd, M.J. and Parnell, K., 1999, Coastal Geomorphology in New Zealand, 1989-99. *Progress in Physical Geography,* 23(4): 501-524.

Hino, M., 1974, Theory on Formation of Rip Current and Cuspidal Coast. *Proceedings of the 14th Coastal Engineering Conference, American Society of Civil Engineers,* 901-919.

Holman, R.A., 1983, Edge waves and the configuration of the shoreline. In P.D. Komar (ed.) *CRC handbook of Coastal Processes and Erosion,* CRC Press, Boca Raton, Florida, 21-33.

Holman, R.A. and Bowen, A.J., 1982, Bars, bumps, and holes: models for the generation of complex beach topography. *Journal of Geophysical Research,* 87: 457-468.

Holman, R.A., and Bowen, A.J., 1984, Longshore structure of infragravity wave motions. *Journal of Geophysical Research,* 89: 6446-6452.

Holman, R,A, and Lippmann, T.C., 1987, Remote sensing of nearshore bar systems: making morphology visible. *Proceedings of Coastal Sediments 87'* (ASCE), 927-944.

Holland, K.T., Holman, R.A., Lippman, T.C., Stanley, J., and Plant, N., 1997, Practical use of Video Imagery in Nearshore Oceanographic Field Studies. *IEEE Journal of Oceanic Engineering*, 22(1): 81-92.

Hom-ma, M. and Sonu, C., 1962, Rhythmic patterns of longshore bars related to sediment characteristics. *Proceedings of the 8th Conference on Coastal Engineering,* Council on Wave Research, 248-278.

Huntley, D.A., Hendry, M.D., Haines.J., and Greenridge, B., 1988, Waves and rip currents on a Caribbean Pocket Beach, Jamaica. *Journal of Coastal Research,* 4 (1): 69-79.

Huntley, D.A. and Short, A.D., 1992, On the Spacing between observed rip currents. *Coastal Engineering,* 17: 211-225.

Ingle, J.C. Jr., 1966, *The movement of Beach Sand, Developments in Sedimentology. Vol 5.* Elsevier, Amsterdam.

Inman, D.L and Quinn, W.H., 1952, Currents in the surf zone. *Proceedings n the 2nd Conference of the Coastal Engineering Council on Wave Research,* 24-36.

Iwata, N., 1976 Rip Current Spacing. *Journal of Oceanographical Society of Japan,* 32: 1-10.

Johnston, M.R., 1972, Geology of Castlepoint headland and reef, Wairarapa, New Zealand. *New Zealand Journal of Geology and Geophysics,* 16 (4): 909-916.

Komar, P.D., 1998, *Beach Processes and Sedimentation,* 2nd Edition, Prentice and Hall, New Jersey.

Komar, P.D., 1971, Nearshore cell circulation and the formation of giant cusps. *Bulletin of the Geological Society of America,* 82: 2643-2650.

Komar, P.D., 1983a, Rhythmic shoreline features and their origins. *In*: R. Gardiner and H. Scoging (ed.) *Mega-Geomorphology,* Claredon press, Oxford, 22-112.

Komar, P.D., 1983b, Beach processes and erosion. *In*: P.D. Komar (ed), *CRC Handbook of Coastal Processes and Erosion,* Boca Raton, FL, CRC Press, 1-20.

Komar, P.D. and Holman, R.A., 1986, Coastal processes and the development of shoreline erosion. *Annual Review of Earth and Planetary Science,* 14: 237 -265.

Lippman, T. and Holman, R., 1990, The spatial and temporal variability of sand bar morphology. *Journal of Geophysical Research,* 94: 995-1011.

Longuet-Higgins, M.S. & Stewart, R.W., 1964, Radiation stress in water waves: a physical discussion with applications. *Deep-sea Research.,* 11: 529-563.

Martens, D., Williams, T., and Cowell, P.J., (in press) Mega-rip dimensional analysis on the Sydney Coast, Australia, and implications for beach-state recognition and prediction. *Journal of Coastal Research.*

Masselink, G. and Hegge, B., 1995, Morphodynamics of meso- and macrotidal beaches: examples from central Queensland, Australia. *Marine Geology,* 129: 1-23.

Masselink, G. and Short, A.D., 1993, The effect of tide range on beach morphodynamics and morphology: a conceptual beach model. *Journal of Coastal Research,* 9: 785-800.

McComb, P.J., Black, K.P., Atkinson, P.N., Bell, R.G. Healy, T.R., 1997, High-resolution wave transformation on a coast with complex bathymetry. *Combined Australasian Coastal Engineering and Ports Conference Proceedings*, Christchurch, 995-1000.

McKenzie, P., 1958, Rip-current systems, *Journal of Geology,* 66: 103-113.

Mei, C.C. and Lui, P.L., 1977, Effects of Topography on the Circulation in and near the Surf Zone- Linear Theory. *Journal of Estuary Coastal Marine Sciences,* 5: 25-37.

Michel, D. and Howa, H.L., 1999, Short-term morphodynamic response of a ridge and runnel system on a mesotidal sandy beach. *Journal of Coastal Research,* 15(2): 428-437.

Miller, C. and Barcillon, A., 1978, Hydrodynamic Instability in the Surf Zone as a Mechanism for the Formation of Horizontal Gyres. *Journal of Geophysical Research,* 83: 4107-4116.

Ministry of Transport, 2000. *New Zealand Nautical Almanac; prepared in the office of the New Zealand Nautical Advisor, Marine Division Ministry of Transport.* Wellington, New Zealand.

Moore, D.S. and McCabe, G.P., 1993, *Introduction to the Practice of Statistics, Second Addition*, W.H. Freeman and Company, New York.

Nafaa, M.G. and Frihy, O.E., 1993, Beach and Nearshore features along the dissipative coastline of the Nile Delta, Egypt. *Journal of Coastal Research,* 9(2): 423-433.

Noda, E.K., 1974, Wave induced nearshore circulation. *Journal of Geophysical Research,* 79: 4097-4106.

O'Dea, T. and Hesp, P., 1999, *Surf Life Saving New Zealand Summer 1997-98, Club Statistics.* Geography Programme, School of Global Studies, Massey University, Miscellaneous Publication Series, 99/4.

O'Dea, T. and Hesp, P., 2000, *Wave Height Data for the New Zealand Coast.* Geography Programme, School of Global Studies, Massey University, Miscellaneous Publication Series 00/2.

O'Dea, T. and Hesp, P., 2000, *Surf Life Saving NZ Summer 1997-98, Club Statistics, Further Analysis.* Geography Programme, School of Global Studies, Massey University, Miscellaneous Publication Series 00/3.

Oltman-Shay, J. and Guza, R.T., 1987, Infragravity edge wave observations on Two California beaches. *Journal of Physical Oceanography,* 17: 644-663.

Pattiaratchi, C., Hegge, B., Gould, J. and Eliot, I., 1997, Impact of sea-breeze activity on nearshore and foreshore processes in southwestern Australia. *Continental Shelf Research,* 17(13): 1539-1560.

Pickrill, R.A. and Mitchell, J.S., 1979, Ocean wave characteristics around New Zealand. *New Zealand Journal of Marine and Freshwater Research,* 13(4): 501-520.

Putman, J.A., Munk, W.H., & Traylor, M.A., 1949, The Predictions of Longshore Currents. *Transactions of the American Geophysical Union,* 30: 338-345.

Ranasinghe, R., Symonds, G., and Holman, R., 1999a, Quantitative Characterisation of Rip Dynamics via video imaging. *Coastal Sediments '99* 3: 987-1002.

Ranasinghe, R., Symonds, G., and Holman, R., 1999b, Video Imaging: A new technique for coastal zone management. *Coasts and Ports '99: challenges and directions for the new century, proceedings of the 14th Australasian Coastal and Ocean Engineering Conference, 7th Australasian Port and Harbour Conference*, Perth, Western Australia, 14-16 April 1999.

Reimintz, E., 1971, Surf-beat origin for pulsating bottom currents in the Rio Balas Submarine Canyon, Mexico. *Bull. Geol. Soc. Am.,* 82: 81-90.

Reimintz, E., Toimil, L.J., Shepard, F.P. and Gutierrez-Estrana, M., 1976, Possible rip current origin for bottom ripple sones to 30m depth. *Geology,* 4: 395-400.

Sasaki, T., 1983, *Three-dimensional Topographic Changes on the Foreshore Zone of Sandy Beaches.* University of Tsukuba: Institute of Geoscience, Science Report (a), 4: 69-95.

Sasaki, T., 1975, Simulation on Shoreline and Nearshore Current. *Proceedings of the Specialty Conference III, Civil Engineering in the Ocean, Amer. Soc. Civil Engrs., 179-196.*

Sasaki, T., 1977, Field investigation of nearshore currents on a gently sloping bottom. *Nearshore Environmental Research Centre TR 77-2,* Nearshore Environmental Research Centre, Tokyo.

Sasaki, T. and Horikawa, K., 1975, Nearshore current systems on a gently sloping bottom. *Coastal Engineering in Japan,* 19: 123-142.

Sasaki, T.O., Igarashi, H. and Harakai, S., 1981, Nearshore currents on a partially rocky shore. *Proceedings of the 17$^{th}$ Coastal Engineering Conference, Sydney, NSW,* 1071-1090.

Schaffer, H.A. and Jonsson, I.G., 1992, Edge waves revisited. *Coastal Engineering,* 16: 349-368.

Shaw, J., 1985 Morphodynamics of an Atlantic coast embayment: Runkerry Strand, County Antrim. *Irish Geography,* 18: 51-58.

Shepard, F.P., Emery, K.O. & LaFond, E.C., 1941, Rip currents: a process of geological importance. *Journal of Geology.,* 49: 337-369.

Shepard, F.P. & Inman, D.L., 1950a, Nearshore circulations related to bottom topography and refraction. *Trans. Am. Geophysics. Un.,* 31: 555-565.

Shepard, F.P & Inman, D.L., 1950b, Nearshore Circulation. *Proceedings of the 1$^{st}$ Coastal Engineering Conference, Amer. Soc. Civil Engrs., 50-59.*

Shepherd, M.J. and Hesp, P.A. (in press) New Zealand coastal barriers and dunes Chapter Eight. *In:* H. Rouse, J. Goff and S. Nicol (Eds.) *The New Zealand Coast: Te Tai O Aotearoa,* Lincoln University Press in association with Daphne Brasell assoc., Lincoln.

Short, A.D., 1979, Three Dimensional beach stage model. *Journal of Geology,* 87: 553-571.

Short, A.D., 1984, Beach and nearshore, facies: southeast Australia. In: B. Greenwood and R.A. Davies Jr., (Eds.), Hydrodynamics and Sedimentation in Wave-Dominated Coastal Environments. *Marine Geology,* 60: 261-282.

Short, A.D., 1985, Rip Current Type, Spacing and Persistence, Narrabeen Beach, Australia. *Marine Geology* 65: 47-71.

Short, A.D., 1992, Beach systems of the central Netherlands Coast: Processes, morphology and structural impacts in a storm driven multi-bar system. *Marine Geology,* 107: 103-137.

Short, A.D. and Aagaard, T., 1993, Single and multi-bar beach change models. *Journal of Coastal Research, SI 15: 141-157.*

Short, A.D. and Brander, R.W., 1999, Regional Variations in Rip Density. *Journal of Coastal Research.* 15(3): 813-822.

Short, A.D. and Brander, R.W., 1999, Rip scaling in low-to high-energy wave environments. *Coastal Sediments, '99* 551-562.

Short, A.D. and Hesp. P.A., 1982, Wave, beach and dune interaction in Southern Australia. *Marine Geology,* 65: 47-71.

Short, A.D. and Hogan, C.L., 1994, Rip currents and beach hazards: their impact on public safety and implications for coastal management. *Journal of Coastal Research,* SI 12: 197-209.

Short, A.D. and Masselink, G., 1999, Embayed and Structurally Controlled Beaches. *In*: A.D. Short, (ed), *Handbook of Beach and Shoreface Morphodynamics,* John Wiley and Sons Ltd, New York.

Short, A.D. and Wright, L.D., 1981, Beach Systems of the Sydney Region. *Australian Geographer,* 15: 8-16.

Smith, J.A. and Largier, J.L., 1995, Observations of nearshore circulation: Rip Currents. *Journal of Geophysical Research,* 100 (c6): 10,967-10,975.

Sonu, C.J., 1972, Field observations of nearshore circulation and meandering currents. *Journal of Geophysical Research,* 77: 3232-3247.

Stephens, S.A., Healy, T.R., Black, K.P. and de Lange, W.P., 1999, Arcuate Duneline Embayments, Infragravity Signals, Rip Currents and Wave Refraction at Waihi Beach, New Zealand. *Journal of Coastal Research,* 15(3): 823-829.

Sunamura, T., 1988, Beach morphologies and their change. In K. Horikawa (ed.), *Nearshore Dynamics and Coastal Processes.* University of Tokoyo Press, 133-166.

Swift, D.J.P., 1975, Barrier island genesis: Evidence from central Atlantic Shelf, Eastern USA. *Sedimentary Geology,* 14: 1-43.

Symonds, G., Holman, R.A., and Bruno, B., 1997, Rip currents. *Proceedings of Coastal Dynamics '97,* ASCE, 584-593.

Trenhaile, A.S., 1997, *Coastal Dynamics and Landforms.* Clarendon Press, Oxford.

Wright, L.D., 1982, Field observations of long-period surf zone oscillations in relation to contrasting beach morphologies. *Australian Journal of Marine and Freshwater Research,* 33: 181-201.

Wright, L.D. and Short, A.D., 1983, Morphodynamics of beaches and surf zones in Australia. *In*: P.D. Komar (ed), *CRC Handbook of Coastal Processes and Erosion,* CRC Press, Boca Raton, FL, 35-64.

Wright, L.D. and Short, A.D., 1984 Morphodynamic variability of surf zones and beaches: a synthesis. *Marine Geology,* 56: 93-118.

Wright, L.D., Chappell, J., Thom, B.G., Bradshaw, M.P. and Cowell, P., 1979, Morphodynamics of reflective and dissipative beach and inshore systems: Southeastern Australia. *Marine Geology,* 45: 41-62.

Wright, L.D., Coffey, F.C. and Cowell, P.J., 1980, *Nearshore Oceanography and Morphodynamics of the Broken Bay-Palm beach Region, NSW: Implications for Offshore Dredging.* Coastal Studies Unit, University of Sydney, Technical Report NO 80/1.

Wright, L.D., Neilsen, P., Short, A.D., Coffey, F.C. and Green, M.O., 1982a, *Nearshore and Surf Zone morphodynamics of a Storm Wave Environment: Eastern Bass Strait, Australia.* Coastal Studies Unit, University of Sydney, Technical Report, 82/3.

Wright, L.D., Neilsen, P., Short, A.D. and Green, M.O., 1982b Morphodynamics of a macrotidal beach. *Marine Geology,* 56: 93-118.

Wright, L.D., Short, A.D. and Green, M.O., 1985, Short-term changes in morphodynamic state of beaches and surf zones: an empirical predictive model. *Marine Geology*, 62: 339-364.

# APPENDIX I

| MU Data # | Rip ID Data : | Sheet # | Name | Reference |
|---|---|---|---|---|
| | 1 | N166/3 | FLAT POINT | 1ST SEPT 44 |
| 804 | 2 | S23/9 | FOULWIND | 1ST MARCH 51 |
| 914 | 3 | S172/2 | HENLEY | 1ST MARCH 49 |
| 914 | 4 | S172/2 | HENLEY | 1ST MARCH 49 |
| 909 | 5 | S164/7 | ST KILDA | 2ND APRIL 71 |
| | 6 | N1/9 | TE PAKI | 1ST |
| | 7 | N2/5 & N2/8 | OHAU/NORTH CAPE | 1ST |
| 28 | 8 | N2/8 | OHAU | 1ST |
| 28 | 9 | N2/8 | OHAU | 1ST |
| | 10 | N6/3 | CAMEL | 1ST |
| | 11 | N9/9 & N13/3 | HEREKINO | 1ST |
| | 12 | N13/3 | WHANGAPAE | 1ST |
| | 13 | N55/2 | WAIKARETU | 1ST |
| | 14 | N55/8 | CARTER | 1ST APRIL |
| | 15 | N55/5 | WAIMAI | 1ST NOV |
| | 16 | N64/5 | KARIOI | 1ST NOV |
| 243 | 17 | N58/8 | GATE PA | JAN NOV 59 |
| | 18 | N72/4 | RUATORIA | 1ST APRIL |
| 43 | 19 | N11/2 | TAKOU | 1ST OCT |
| | 20 | N30/9 | PT WHANGAPARA | 1ST APRIL |
| | 21 | N30/9 | PT WHANGAPARA | 1ST |
| | 22 | N40/7 | WHANGAPOUA | 1ST |
| | 23 | N44/9 | TAIRUA | 1ST |
| 1 | 24 | N82/1 &N82/4 | KANOHAKU | 1ST |
| 1 | 25 | N82/1 &N82/4 | KANOHAKU | 1ST |
| | 26 | N99/9 | URUTI | 1ST |
| | 27 | N107/1 | TAKARANGI | 1ST APRIL |
| 302 | 28 | N116/1 | WAIROA | EAST WAIROA |
| 412 | 29 | N135/7 | HAUPOURI | 1ST APRIL |
| | 30 | S164/5 | OTAKOU | 2ND APRIL 71 |
| | 31 | S164/2 | TAIAROA | 1ST MARCH |
| | 32 | S155/8 | PUKETERAKI | 1ST FEB |
| | 33 | S146/9 | SHAG POINT | 1ST APRIL |
| | 34 | S185/8 | WAIKAWA | 1ST APRIL |
| 910 | 35 | SN8479 I44 26 | DUNEDIN | 1ST F/15 |
| 912 | 36 | SN8479 I44 26 | DUNEDIN | 1ST F/13 |
| 911 | 37 | SN8479 I44 26 | DUNEDIN | 1ST F/13 |
| 916 | 39 | SN8542 F47 2( | TOKANUI | 1ST F/11 |
| 412 | 40 | SN5761 W22 2 | WAIMARAMA | 2ND N/21 |
| 4 | 41 | SN5479 R14 2( | RAGLAN | 2ND D/1 & E/1 |
| 10 | 43 | SN5789 Q11 2( | WAITAKERE | 2ND P/1 |
| 17 | 44 | SN5924 Q10 2( | HELENSVILLE | 2ND P/5-D/10 |
| 16 | 45 | SN5924 Q10 2( | HELENSVILLE | 2ND D/1-D/13 |
| 14 | 46 | SN5783 Q11 2( | WAITAKERE | 2ND O/1 |
| 11 | 47 | SN5789 Q11 2( | WAITAKERE | 2ND P/1 |
| 6 | 48 | SN8772 R12 2( | PUKEKOHE | 1ST 1980 |
| 16 | 49 | SN8772 Q10 2( | HELENSVILLE | 2ND M1-10 |
| 240 | 50 | SN8626 U13 2( | WAIHI BEACH | 1ST A/5-A/7 |
| 242 | 51 | SN9383 U14 2( | TAURANGA | 2ND F/5 |
| 243 | 52 | SN9383 U14 2( | TAURANGA | 2ND E9 |
| 253 | 53 | SN11596 W15 | WHAKATANE | 2ND F/1 |

| MU Data # | Rip ID Data : | Sheet # | Name | Reference |
|---|---|---|---|---|
| 305 | 54 | SN5922 Y19 2( | WHARERATA | 2ND B/2-B/5 |
| 703 | 55 | SN5310 U26 2( | CASTLEPOINT | 2ND C/30-C/31 |
| 803 | 56 | K30 261 | PUNAKAIKI | 1ST E/2, F/2, G/2, H |
| 824 | 57 | SN8389 N36 2( | AKAROA | 1ST H/19 |
| 823 | 58 | SN8389 M35 2( | CHRISTCHURCH | 1ST 6/19 & H/24 |
| 706 | 59 | SN11640 T27 2 | TE WHARAU | 2ND I/29 |
| 822 | 60 | SN8389 M35 2( | CHRISTCHURCH | 1ST G/9 |
| 817 | 61 | SN9390 M35 2( | CHRISTCHURCH | 1ST C/18 |
| 815 | 62 | SN8380 | CHRISTCHURCH | 1ST A/20 |
| 904 | 63 | SN8733 I43 26 | WAIKOUAITI | 1ST F/20-F/21 |
| 909 | 64 | SN8479 J44 26 | DUNEDIN | 1ST F/15 |
| 9 | 65 | SN5783 Q11 2( | WAITAKERE | 2ND Q/2 AND R/1 |
| 61 | 66 | SN5091 R07 2( | BREAM HEAD | 1ST R/41 & J/42 |
| 71 | 67 | SN9211 R09 2( | WORKWORTH | 2ND J/32 |
| 66 | 68 | SN8104 R08 2( | MANGAWHAI | 2ND E/30 |
| 510 | 69 | SN5804 P19 2( | NEW PLYMOUTH | 1ST B/5 |
| 509 | 70 | SN5804 P19 2( | NEW PLYMOUTH | 1ST A/2 |
| 250 | 71 | SN11596 W15 | WHAKATANE | 2ND A/1 |
| 252 | 72 | SN11596 W15 | WHAKATANE | 2ND D/1, E/1 |
| 607 | 73 | SN12248.A I3/: | Manawatu wanganui | |

| Beach Name | Beach Type | Direction | Yr | Wr | Lr |
|---|---|---|---|---|---|
| FLAT PT STH | TBR | E-W | 180 | 26 | 99 |
| TAURANGA BAY | TBR | S-N | 135 | 30 | 102 |
| GREEN ISLAND TO KURI BUSH | TBR NONRYTH | S-N | 239 | 32 | 118 |
| KARI BUSH -NTH | TBR NONRYTH | S-N | 213 | 19 | 99 |
| SMAILLS BEACH | TBR NONRYTH | E-W | 108 | 17 | 83 |
| TWILIGHT BEACH | TBR NONRYTH | N-S | 320 | 39 | 220 |
| KANAKANA-WHARERAWA | TBR | S-N | 251 | 32 | 124 |
| WHAREKAWA TO OUTCROP | LTT | N-S | 190 | 8 | 127 |
| OUTCROP TO WHAREANA | TBR | N-S | 156 | 29 | 169 |
| HOUHORA BAY | TBR RYTH | N-S | 105 | 18 | 108 |
| HUNAHUNA STM-ROCKS | RBB | N-S | 659 | 53 | 228 |
| ROCKS-HEREKINO HARBOUR | RBB | N-S | 661 | 103 | 198 |
| OHARURU PT-NGATUTUA | TBR | S-N | 232 | 38 | 151 |
| TE HARA PT STH | TBR | N-S | 421 | 60 | 189 |
| AT WAIMAI STM | TBR | S-N | 231 | 42 | 138 |
| PAPANUI PT-MUTAWHA PT | TBR | N-S | 228 | 86 | 197 |
| PAPAMOA | RBB | W-E | 132 | 69 | 94 |
| AWANUI PT NTH | TBR OBLIQ | N-S | 381 | 75 | 394 |
| TAKAU R BEACH | TBR | S-N | 148 | 30 | 91 |
| KAITOKI BEACH | TBR NONRYTH | S-N | 237 | 38 | 182 |
| PALMERS BEACH | TBR NONRYTH | S-N | 180 | 44 | 175 |
| NEW CHUMS BEACH | TBR RYTH | E-W | 127 | 32 | 103 |
| TAIRUA BEACH | TBR | | 130 | 15 | 85 |
| TURAKINA STM NTH | RBB | S-N | 272 | 25 | 154 |
| TURAKINA STM STH | RBB | N-S | 210 | 29 | 140 |
| URUTI | RBB | W-E | 187 | 21 | 143 |
| MARAETAHA R STH | TBR | N-S | 175 | 26 | 89 |
| EAST WAIROA RV | TBR-LBT | W-E | 600 | 68 | 211 |
| OCEAN BEACH | RBB-TBR | S-N | 183 | 32 | 94 |
| ALLANS BEACH | TBR | W-E | 221 | 30 | 140 |
| PIPKARETU BEACH | TBR | N-S | 131 | 12 | 114 |
| PUKETETERAKI NTH | TBR OBLIQ | S-N | 161 | 17 | 109 |
| SHAG POINT NORTH | TBR NONRYTH | N-S | 198 | 19 | 85 |
| HALDANE BAY | TBR | E-W | 387 | 61 | 352 |
| TOMAHAWK | TBR | W-E | 88.88 | 14 | 76.25 |
| ST CLAIR | TBR | W-E | 96.429 | 14.375 | 65.625 |
| ST KILDA | TBR | W-E | 110.667 | 22.344 | 77.344 |
| CURIO BAY | TBR | S-N | 342.5 | 20 | 152.083 |
| OCEAN BEACH KIWI | TBR | S-N | 277.361 | 13.816 | 102.632 |
| RAGLAN | TBR-RBB | | 412.5 | 26.136 | 130.682 |
| PIHA | TBR | S-N | 53.571 | 20.938 | 81.25 |
| RIMMERS BEACH | TBR RYTH | S-N | 504.412 | 24.167 | 147.222 |
| MURIWAI | TBR | S-N | 266.667 | 39.423 | 157.692 |
| BENTHALS BEACH | TBR | S-N | 205.357 | 23.438 | 181.25 |
| NORTH PIHA | LBT | S-N | 108.088 | 20.139 | 84.128 |
| KARIOTAHI | RBB-R | N-S | 233.571 | 33.056 | 166.667 |
| MURIWAI | TBR OBLIQ | S-N | 643.182 | 46.875 | 368.75 |
| WAIHI BEACH | TBR | N-S | 164.063 | 21.7 | 72 |
| PAPAMOA | RBB | N-S | 90.217 | 9.583 | 52.604 |
| OMANU | RBB | N-S | 90.217 | 9.583 | 52.604 |
| HIKUWAI (HUKUWAI) | RBB-LBT | W-E | 172.024 | 22.614 | 84.091 |

| Beach Name | Beach Type | Direction | Yr | Wr | Lr |
|---|---|---|---|---|---|
| ORAKA | RBB-TBR | W-E | 312.5 | 22.083 | 108.333 |
| CASTLE POINT MAIN BEACH | RBB | N-S | 176.667 | 23.125 | 78.906 |
| PUNAKAIKI | TBR NONRYTH | S-N | 155.114 | 24.239 | 124.457 |
| SUMNER | RBB | S-N | 80.357 | 21.25 | 87.5 |
| SOUTHSHORE | TBR | N-S | 197.143 | 12.5 | 75 |
| FLAT POINT | TBR | E-W | 66.667 | 20.714 | 62.5 |
| SOUTH BRIGHTON | TBR | N-S | 305.556 | 23 | 141.25 |
| PINES BEACH | TBR | N-S | 230.208 | 20.385 | 95.192 |
| WAIKUKU BEACH | TBR OBLIQ | N-S | 409.375 | 16.389 | 72.222 |
| KARITANE | RBB | N-S | 156.731 | 16.071 | 64.286 |
| SMAILLS BEACH | TBR | | 162.5 | 7.5 | 104.167 |
| KAREKARE | TBR | S-N | 250 | 27.206 | 114.706 |
| OCEAN BEACH | LTT | N-S | 306.25 | 22.5 | 82.5 |
| LITTLE OMAHA | RBB | N-S | 110.938 | 23.056 | 50 |
| MANGAWHAI HEADS | TBR | N-S | 398.214 | 17.188 | 101.563 |
| FITZROY | TBR | S-N | 212.5 | 19.5 | 55 |
| BELLBLOCK | TBR | S-N | 246.875 | 52.778 | 138.889 |
| OHOPE | TBR RYTH | W-E | 178.571 | 13.879 | 77.155 |
| WAITAHI BEACH | RBB | W-E | 155.882 | 19.444 | 73.611 |
| HIMITANGI | TBR | S-N | 190.58 | 18.07 | 80.54 |

| Xs | Lb | Lbt | AREA | GRAPH MEAN | MOMENT MEAN | SED.FALL VELOCITY |
|---|---|---|---|---|---|---|
| 95 | 2984 | 2300 | | * | * | * |
| 127 | 1365 | 1365 | MTS | 1.8425 | 1.8131 | 0.0218 |
| 111 | 3095 | 4000 | MTS | 2.2752 | 2.2699 | 0.0288 |
| 95 | 3810 | 4000 | MTS | 2.2752 | 2.2699 | 0.0288 |
| 95 | 603 | 306 | MTS | 2.2582 | 2.2238 | 0.0242 |
| 302 | 184 | 184 | | * | * | * |
| 175 | 2032 | 2794 | | * | * | * |
| 127 | 476 | 475 | MTS | 2.0956 | 2.0555 | 0.0336 |
| 159 | 556 | 1222 | MTS | 2.0956 | 2.0555 | 0.0336 |
| 71 | 937 | 937 | | * | * | * |
| 190 | 2381 | 3281 | | * | * | * |
| 206 | 3524 | 3523 | | * | * | * |
| 190 | 2619 | 3667 | | * | * | * |
| 159 | 2063 | 2500 | | * | * | * |
| 175 | 2651 | 5158.7 | | * | * | * |
| 190 | 1746 | 1746 | | * | * | * |
| 111 | 1111 | 1111 | MTS | 1.6177 | 1.6106 | 0.0472 |
| 238 | 2222 | 2500 | | * | * | * |
| 95 | 857 | 1730 | MTS | 1.9163 | 1.8893 | 0.0338 |
| 87 | 3016 | 3016 | | * | * | * |
| 79 | 1048 | 1048 | | * | * | * |
| 79 | 1286 | 1286 | | * | * | * |
| 65 | 1937 | 2920 | | * | * | * |
| 190 | 1937 | 2921 | MTS | 2.142 | 2.1385 | 0.0407 |
| 159 | 1587 | 2778 | MTS | 2.142 | 2.1385 | 0.0407 |
| 95 | 556 | 4048 | | * | * | * |
| 127 | 2540 | 3413 | | * | * | * |
| 222 | 10159 | 10200 | MTS | * | * | * |
| 127 | 1016 | 2063 | MTS | 2.38 | 2.3507 | 0.0269 |
| 159 | 2397 | 2397 | | * | * | * |
| 175 | 587 | 587 | | * | * | * |
| 87 | 1460 | 1460 | | * | * | * |
| 111 | 3968 | 4000 | | * | * | * |
| 254 | 3968 | 3968 | | * | * | * |
| 100 | 1125 | 1500 | MTS | 2.0038 | 2.005 | 0.032 |
| 75 | 875 | 875 | MTS | 1.8342 | 1.8262 | 0.0361 |
| 75 | 2375 | 2375 | MTS | 1.4787 | 1.4858 | 0.0507 |
| 325 | 2250 | 3250 | MTS | 2.4757 | 2.4558 | 0.022 |
| 100 | 6200 | 6200 | MTS | 2.38 | 2.3507 | 0.0269 |
| 175 | 4125 | 4125 | MTS | 2.5392 | 2.5443 | 0.024 |
| 125 | 550 | 550 | HTS | 2.5877 | 2.5989 | 0.0266 |
| 200 | 1000 | 1000 | MTS | 2.5184 | 2.5186 | 0.0301 |
| 175 | 9750 | 10000 | MTS | 2.5264 | 2.5339 | 0.0309 |
| 250 | 1625 | 1625 | MTS | 2.2749 | 2.2503 | 0.0315 |
| 137.5 | 2150 | 2150 | HTS | 2.7702 | 2.7599 | 0.027 |
| 150 | 9500 | 10000 | MTS | 2.5155 | 2.4925 | 0.0285 |
| 375 | 875 | 10000 | MTS | 2.5264 | 2.5339 | 0.0309 |
| 100 | 4625 | 5000 | MTS | 2.8152 | 2.7856 | 0.0236 |
| 50 | 2250 | 5000 | MTS | 1.908 | 1.8981 | 0.0309 |
| 50 | 2250 | 5000 | MTS | 1.6177 | 1.6106 | 0.0472 |
| 75 | 4125 | 5000 | HTS | 2.1787 | 2.1748 | 0.0308 |

| Xs | Lb | Lbt | AREA | GRAPH MEAN | MOMENT MEAN | SED.FALL VELOCITY |
|---|---|---|---|---|---|---|
| 100 | 4500 | 6500 | HTS | 2.5197 | 2.4698 | 0.0202 |
| 120 | 3000 | 4875 | | * | * | * |
| 137.5 | 4250 | 5000 | MTS | 1.7785 | 1.7658 | 0.0319 |
| 137.5 | 1125 | 1125 | HTS | 2.7121 | 2.6695 | 0.0177 |
| 200 | 1750 | 2250 | HTS | 2.6284 | 2.6133 | 0.0176 |
| 75 | 550 | 550 | | * | * | * |
| 150 | 2875 | 2875 | MTS | 2.6761 | 2.6549 | 0.0171 |
| 125 | 3000 | 3000 | LTS | 2.441 | 2.4257 | 0.0195 |
| 100 | 4000 | 4000 | MTS | 2.3995 | 2.3963 | 0.0225 |
| 100 | 2375 | 4000 | HTS | 2.2587 | 2.2272 | 0.0268 |
| 112.5 | 550 | 550 | MTS | 2.2582 | 2.2238 | 0.0242 |
| 100 | 5000 | 5000 | HTS | 2.3645 | 2.3747 | 0.036 |
| 75 | 2500 | 5125 | MTS | 1.388 | 1.3766 | * |
| 62.5 | 3175 | 3175 | HTS | 2.1481 | 2.1309 | 0.0338 |
| 87.5 | 3750 | 5000 | MTS | 2.0283 | 2.0177 | 0.0351 |
| 75 | 2000 | 2000 | HTS | 2.2695 | 2.2493 | 0.0329 |
| 100 | 2875 | 4625 | HTS | 2.4237 | 2.392 | 0.0262 |
| 75 | 5950 | 6000 | MTS | 2.7441 | 2.7001 | 0.0159 |
| 100 | 3000 | 4000 | HTS | 2.1532 | 2.157 | 0.0325 |
| 137.5 | 2530 | 5000 | MTS | 2.622 | 2.5773 | 0.0202 |

| WAVE HEIGHT | WAVE PERIOD |
|---|---|
| * | * |
| 1.37 | * |
| 1.6 | * |
| 0.6 | * |
| * | * |
| * | * |
| * | * |
| * | * |
| * | * |
| * | * |
| * | * |
| * | * |
| * | * |
| * | * |
| * | * |
| 0.9857 | * |
| 0.5 | * |
| 0.6 | 10.5 |
| * | * |
| * | * |
| * | * |
| 1.3 | 9 |
| * | * |
| * | * |
| * | * |
| 1 | * |
| 0.63 | * |
| 0.75 | 7.7 |
| 0.5728 | * |
| * | * |
| * | * |
| * | * |
| * | * |
| * | * |
| 2 | * |
| 1.1263 | * |
| 1.0336 | * |
| * | * |
| 0.5728 | * |
| 0.9857 | * |
| 1.46 | * |
| 2.5 | 12.5 |
|  | 12.5 |
| 1.3125 | * |
| 1.46 | * |
| 1.3583 | * |
| 2.5 | 12.5 |
| 0.8 | 12.8 |
| 0.6127 | * |
| 0.6079 | * |
| 0.4897 | * |

| WAVE HEIGHT | WAVE PERIOD |
|---|---|
| * | * |
| * | * |
| 1.48 | 12.5 |
| 1 | 6.8 |
| 0.5 | 9 |
| * | * |
| 0.75 | 8 |
| 1.15 | 8 |
| 0.6015 | 8 |
| 0.3988 | * |
| 1.0336 | * |
| 1.1551 | * |
| 0.4595 | * |
| 1 | 8 |
| 1 | 9 |
| 1.07 | 10 |
| 0.7 | 10 |
| 0.4505 | * |
| 0.4505 | * |
| 1.04 | 7.2 |